UNIVERSITY OF AMSTERDAM

UvA-DARE (Digital Academic Repository)

Measurement of the $t\bar{t}$ production cross-section in pp collisions at $\sqrt{s}$ = 5.02 TeV with the ATLAS detector

The ATLAS collaboration

DOI
10.1007/JHEP06(2023)138

Publication date
2023

Document Version
Final published version

Published in
Journal of High Energy Physics

License
CC BY

Link to publication

Citation for published version (APA):
The ATLAS collaboration (2023). Measurement of the $t\bar{t}$ production cross-section in *pp* collisions at $\sqrt{s}$ = 5.02 TeV with the ATLAS detector. *Journal of High Energy Physics*, *2023*(6), Article 138. https://doi.org/10.1007/JHEP06(2023)138

General rights
It is not permitted to download or to forward/distribute the text or part of it without the consent of the author(s) and/or copyright holder(s), other than for strictly personal, individual use, unless the work is under an open content license (like Creative Commons).

Disclaimer/Complaints regulations
If you believe that digital publication of certain material infringes any of your rights or (privacy) interests, please let the Library know, stating your reasons. In case of a legitimate complaint, the Library will make the material inaccessible and/or remove it from the website. Please Ask the Library: https://uba.uva.nl/en/contact, or a letter to: Library of the University of Amsterdam, Secretariat, P.O. Box 19185, 1000 GD Amsterdam, The Netherlands. You will be contacted as soon as possible.

UvA-DARE is a service provided by the library of the University of Amsterdam (https://dare.uva.nl)

Download date:07 Oct 2026

Published for SISSA by Springer

Received: July 5, 2022
Revised: August 25, 2022
Accepted: September 29, 2022
Published: June 23, 2023

Measurement of the $t\bar{t}$ production cross-section in pp collisions at $\sqrt{s} = 5.02$ TeV with the ATLAS detector

The ATLAS collaboration

E-mail: atlas.publications@cern.ch

Abstract: The inclusive top-quark pair ($t\bar{t}$) production cross-section $\sigma_{t\bar{t}}$ is measured in proton–proton collisions at a centre-of-mass energy $\sqrt{s} = 5.02$ TeV, using 257 pb^{-1} of data collected in 2017 by the ATLAS experiment at the LHC. The $t\bar{t}$ cross-section is measured in both the dilepton and single-lepton final states of the $t\bar{t}$ system and then combined. The combination of the two measurements yields

$$\sigma_{t\bar{t}} = 67.5 \pm 0.9\,(\text{stat.}) \pm 2.3\,(\text{syst.}) \pm 1.1\,(\text{lumi.}) \pm 0.2\,(\text{beam})\,\text{pb},$$

where the four uncertainties reflect the limited size of the data sample, experimental and theoretical systematic effects, and imperfect knowledge of both the integrated luminosity and the LHC beam energy, giving a total uncertainty of 3.9%. The result is in agreement with theoretical quantum chromodynamic calculations at next-to-next-to-leading order in the strong coupling constant, including the resummation of next-to-next-to-leading logarithmic soft-gluon terms, and constrains the parton distribution functions of the proton at large Bjorken-x.

Keywords: Hadron-Hadron Scattering, Top Physics

ArXiv ePrint: 2207.01354

Open Access, Copyright CERN,
for the benefit of the ATLAS Collaboration.
Article funded by SCOAP^3.

https://doi.org/10.1007/JHEP06(2023)138

JHEP06(2023)138

Contents

1 Introduction **1**

2 ATLAS detector **3**

3 Event samples **3**

4 Event reconstruction **5**

5 Dilepton cross-section measurement **7**

6 Single-lepton cross-section measurement **9**

7 Systematic uncertainties **16**
7.1 Modelling uncertainties 16
7.2 Detector-related uncertainties 18

8 Results **19**

9 Combined cross-section and comparison with predictions **23**

10 Conclusion **28**

The ATLAS collaboration **35**

JHEP06(2023)138

1 Introduction

The study of top quark–antiquark ($t\bar{t}$) production in proton–proton (pp) collisions forms a central part of the physics programme of the ATLAS experiment at the Large Hadron Collider (LHC). Measurements of the inclusive $t\bar{t}$ cross-section $\sigma_{t\bar{t}}$ allow studies of quantum chromodynamics (QCD) at some of the highest accessible energy scales. Predictions for $\sigma_{t\bar{t}}$ in pp collisions are available at next-to-next-to-leading-order (NNLO) accuracy in the strong coupling constant α_s, including the resummation of next-to-next-to-leading logarithmic (NNLL) soft-gluon terms [1–6]. These predictions are in excellent agreement with measurements from the ATLAS, CMS, and LHCb collaborations at $\sqrt{s} = 7$, 8, and 13 TeV [7–16].

During the data-taking period from 2015 to 2018, known as Run 2, the LHC provided samples of pp collisions at $\sqrt{s} = 5.02$ TeV, primarily to support the heavy-ion physics programme, but also to measure Standard Model (SM) physics processes in this intermediate energy regime. For $t\bar{t}$ production, the lower $\sqrt{s}$ value increases the fraction of $q\bar{q}$-initiated events from 11% at $\sqrt{s} = 13$ TeV to about 25%, making this data complementary to

the larger samples at higher centre-of-mass energies and offering the potential for additional constraints on parton distribution functions (PDFs). Assuming a top-quark mass of $m_t = 172.5\,\text{GeV}$, the NNLO+NNLL prediction for $\sigma_{t\bar{t}}$ at $\sqrt{s} = 5.02\,\text{TeV}$ calculated with the Top++ program [17] is $68.2 \pm 4.8^{+1.9}_{-2.3}\,\text{pb}$, where the first uncertainty corresponds to PDF and α_s uncertainties and the second to QCD scale variations. The PDF and α_s uncertainties were calculated using the PDF4LHC prescription [18] with the MSTW2008 [19, 20], CT10nnlo [21, 22], and NNPDF2.3 5f FFN [23] PDF sets. The scale uncertainties were calculated from an envelope of predictions with the QCD renormalisation and factorisation scales (μ_r and μ_f) increased and decreased independently by a factor of two from their default values of $\mu_r = \mu_f = m_t$ [24, 25], while never letting the scales differ by more than a factor of two from each other. The total uncertainty corresponds to a relative precision of $^{+7.5}_{-7.7}\%$. The cross-section further varies by $^{-3.2}_{+3.3}\%$ for a $\pm 1\,\text{GeV}$ variation in m_t. The prediction agrees well with a measurement of $63.0 \pm 5.1\,\text{pb}$ from the CMS collaboration using data samples at $\sqrt{s} = 5.02$ TeV of $302\,\text{pb}^{-1}$ recorded in 2017 and $27\,\text{pb}^{-1}$ recorded in 2015 [26].

This paper reports a measurement of $\sigma_{t\bar{t}}$ at $\sqrt{s} = 5.02\,\text{TeV}$ using a $257\,\text{pb}^{-1}$ data sample recorded by the ATLAS collaboration in 2017. The measurement was performed in both the dilepton and single-lepton channels of the $t\bar{t}$ decay. The dilepton-channel final states are those where the W bosons from both top quarks decay leptonically, i.e. $t\bar{t} \to W^+bW^-\bar{b} \to \ell\ell'\nu\bar{\nu}b\bar{b}$, where ℓ and ℓ' represent an electron or muon, including those produced in leptonic decays of τ-leptons ($W \to \tau \to \ell$). Event samples with an opposite-charge pair of leptons, transverse-momentum imbalance arising from the presence of two neutrinos, and one or two jets tagged as likely to contain b-hadrons were used to measure the rate of $t\bar{t}$ production in the dilepton channel, which is characterised by high $t\bar{t}$ purity but has a relatively small number of selected events. This technique is similar to that used in measurements of $\sigma_{t\bar{t}}$ using $e\mu$ events [7, 9] but also includes the same-flavour ee and $\mu\mu$ events. The single-lepton final states are those where one W boson decays leptonically and the other decays hadronically. This results in a final state characterised by a charged lepton, transverse-momentum imbalance arising from a neutrino, two jets from the bottom quarks, and two or more jets arising from the hadronisation of the W-boson decay products. The single-lepton event samples were defined by requiring a charged lepton ℓ, missing transverse momentum indicating a neutrino, and two or more jets with at least one of the jets tagged as being likely to contain a b-hadron. The single-lepton sample was separated into subsamples with different signal-to-background ratios, increasing the precision of the measurement. The measurement also used a multivariate technique to further separate the $t\bar{t}$ signal from background events, using techniques similar to those used in $\sigma_{t\bar{t}}$ measurements at $\sqrt{s} = 13\,\text{TeV}$ [10]. This approach combined the separation power of several variables and their correlations. Finally, the dilepton and single-lepton measurements were combined, taking the correlated systematic uncertainties into account.

This paper is structured as follows. The ATLAS detector is described in section 2, followed by the data and simulation samples used in the analysis in section 3, and the event reconstruction in section 4. The dilepton measurement is described in section 5 while the single-lepton measurement is described in section 6. Systematic uncertainties associated

JHEP06(2023)138

with the measurements are described in section 7 and the results of the individual channels are reported in section 8. The combined cross-section measurement is presented in section 9, together with a comparison with predictions from various PDF sets, and an illustration of how the gluon PDF is affected by including this measurement in the ATLAS PDF fits. The conclusions of this study are summarised in section 10.

2 ATLAS detector

The ATLAS detector [27] at the LHC is centred on the pp collision point and covers nearly the whole 4π solid angle.[1] It consists of an inner tracking detector surrounded by a 2 T superconducting solenoid, electromagnetic and hadronic calorimeters, and a muon spectrometer incorporating three large superconducting toroid magnets.

The inner detector, including the insertable B-layer added as a new innermost layer in 2014 [28, 29], provides charged-particle tracking information from silicon pixel and microstrip detectors in the pseudorapidity range $|\eta| < 2.5$ and a transition radiation tracker covering $|\eta| < 2.0$.

The calorimeter system covers the pseudorapidity range $|\eta| < 4.9$ and measures the positions and energies of electrons, photons, and charged and neutral hadrons. Within the region $|\eta| < 3.2$, electromagnetic calorimetry is provided by barrel and endcap high-granularity lead and liquid-argon sampling calorimeters. The hadronic sampling calorimeter uses either scintillator tiles or liquid argon as active material and steel, copper or tungsten as absorber.

The muon spectrometer comprises separate trigger and high-precision tracking chambers measuring the tracks of muons in a magnetic field generated by superconducting air-core toroid magnets. The precision chamber system covers the region $|\eta| < 2.7$, while the muon trigger system covers the range $|\eta| < 2.4$.

A two-level trigger system is used to select which events to save for offline analysis [30]. The first level is implemented in hardware/firmware and uses a subset of the detector information to reduce the event rate from the 40 MHz proton bunch crossings to less than 100 kHz. This is followed by a software-based high-level trigger that reduces the event rate to approximately 1 kHz. An extensive software suite [31] is used in the reconstruction and analysis of real and simulated data, in detector operations, and in the trigger and data acquisition systems of the experiment.

3 Event samples

The analysis was performed on pp collision data collected at $\sqrt{s} = 5.02$ TeV in November 2017 by the ATLAS detector, with an integrated luminosity of 257 pb^{-1} after data quality

[1] ATLAS uses a right-handed coordinate system with its origin at the nominal interaction point (IP) in the centre of the detector and the z-axis along the beam line. The x-axis points from the IP to the centre of the LHC ring, and the y-axis points upwards. Cylindrical coordinates (r, ϕ) are used in the transverse plane, ϕ being the azimuthal angle around the z-axis. The pseudorapidity is defined in terms of the polar angle θ as $\eta = -\ln\tan(\theta/2)$. Angular distance is measured in units of $\Delta R \equiv \sqrt{(\Delta\eta)^2 + (\Delta\phi)^2}$.

JHEP06(2023)138

requirements [32]. Events were required to pass either a single-electron or a single-muon trigger, both of which reach the efficiency plateau region in data for leptons with an offline-reconstructed transverse momentum $p_{\mathrm{T}} > 15\,\mathrm{GeV}$ [33, 34]. The trigger efficiencies were measured using a tag-and-probe method applied to $Z \to \ell\ell$ decays (see section 7.2). Most triggered events also included signals from additional inelastic pp collisions in the same bunch crossing, referred to as pileup. The mean number of inelastic pp collisions per bunch crossing $\langle\mu\rangle$ varied between about 0.5 and 4, with an average of $\langle\mu\rangle \approx 2$ [35].

Dedicated $\sqrt{s} = 5.02\,\mathrm{TeV}$ Monte Carlo (MC) simulated event samples were used to develop the analysis procedures, evaluate signal and background contributions, and compare the predicted distributions with data. All samples were processed using the full ATLAS detector simulation [36] based on the GEANT4 framework [37]. The effects of pileup were simulated by generating additional inelastic pp collisions with the PYTHIA 8.186 event generator [38] using the A3 set of parameter values [39], a dedicated PYTHIA tune that provides a good description of inclusive pp collisions. Several of these events were overlaid on each primary simulated event, and the combined events were then processed using the same reconstruction and analysis chain as the data. As discussed in section 7.2, small corrections derived from comparisons of data and simulation at both $\sqrt{s} = 5.02\,\mathrm{TeV}$ and $\sqrt{s} = 13\,\mathrm{TeV}$ were applied as scale factors to the simulated lepton-trigger and reconstruction efficiencies, to improve agreement with the response observed in data.

The $\sqrt{s} = 5.02\,\mathrm{TeV}$ simulation samples were created using event-generator configurations similar to those developed for the analysis of $\sqrt{s} = 13\,\mathrm{TeV}$ data [9, 10]. The nominal simulated $t\bar{t}$ sample was produced using the NLO event generator POWHEG BOX v2 [40–43] with the NNPDF3.0NLO PDF set [44] and employed the PYTHIA 8.210 model with the NNPDF2.3LO PDF set and the A14 tune [45] for the parton-shower, hadronisation, and underlying-event modelling. In the POWHEG configuration, the cut-off scale for the first gluon emission (represented by the h_{damp} parameter) was set to $\frac{3}{2}m_t$ and the factorisation (μ_{f}) and renormalisation (μ_{r}) scales were set to $\mu_{\mathrm{f}} = \mu_{\mathrm{r}} = \sqrt{{m_t}^2 + p_{\mathrm{T},t}^2}$, where the top-quark transverse momentum ($p_{\mathrm{T},t}$) is evaluated before radiation [46].

Alternative $t\bar{t}$ simulation samples were generated in order to assess systematic uncertainties. One sample used the POWHEG MC generator with the HERWIG 7.1.6 parton-shower and hadronisation model [47, 48] employing the H7UE tune [48]. Another sample was generated using the MADGRAPH5_AMC@NLO 2.3.3.p1 generator (referred to hereafter as AMC@NLO) [49] with the NNPDF3.0NLO PDF set while using the PYTHIA 8 parton-shower and hadronisation model. Uncertainties in the amount of parton-shower radiation were evaluated by reweighting the nominal $t\bar{t}$ sample so as to effectively change QCD scales and shower parameters, and by generating an additional POWHEG+PYTHIA8 sample with $h_{\mathrm{damp}} = 3m_t$. The top-quark mass was set to 172.5 GeV in all top-quark samples, and the EVTGEN program [50] was used to handle the decays of b- and c-flavoured hadrons. All samples were normalised using the NNLO+NNLL $t\bar{t}$ cross-section prediction discussed in section 1.

The backgrounds in these analyses arise from single-top-quark production, W and Z bosons produced in association with hadronic jets, and diboson production. The t-channel,

JHEP06(2023)138

s-channel, and Wt associated production processes for single top quarks were simulated using the Powheg v2 [51, 52] generator with the NNPDF3.0nlo PDF set and employing Pythia 8 with the A14 tune as the parton-shower and hadronisation model. The diagram removal scheme [53] was used to handle the interference between the $t\bar{t}$ and Wt final states. The Wt sample was normalised to a cross-section of 6.05 ± 0.57 pb, obtained by extrapolating [54] the approximate NNLO calculation [55, 56] using the MSTW2008 NNLO PDF set [19, 20] to $\sqrt{s} = 5.02$ TeV, and taking into account PDF and QCD scale uncertainties. The t- and s-channel samples were normalised to the cross-section predictions from the Hathor [57] NLO MC generator, and the uncertainties were conservatively taken to be 9.5% for both processes, the same as for Wt. Two alternative Wt samples were generated: one using the Powheg+Pythia8 MC generator but with the diagram subtraction scheme [52, 58] and the other using the Powheg MC generator with the Herwig 7.1.6 parton-shower and hadronisation model employing the H7UE tune. A t-channel sample using the Powheg+Herwig7.1.6 scheme similar to the alternative Wt sample was also generated.

The $Z+$jets and $W+$jets events were simulated with the Sherpa 2.2.5 generator [59] using NLO matrix elements for up to two partons, and LO matrix elements for up to four partons, as discussed in ref. [10]. The samples were generated using the NNPDF3.0nlo PDF set and normalised using an NNLO cross-section prediction [60]. Alternative $Z+$jets samples were generated using the Powheg+Pythia8 event generator. Smaller backgrounds from diboson production (WW, WZ, and ZZ) with additional jets were simulated using the Sherpa 2.1.1 [61] generator with the CT10 PDF set [21], as discussed in ref. [62].

4 Event reconstruction

The dilepton and single-lepton measurements made use of reconstructed electrons, muons and jets, as well as the momentum imbalance in the transverse plane to infer the presence of neutrinos.

Electron candidates were reconstructed from a localised cluster of energy deposits in the electromagnetic calorimeter matched to a track in the inner detector and passing the 'Medium' likelihood-based requirements of ref. [63], giving a combined efficiency of about 80% for electrons from $Z \to ee$ decays. They were further required to have transverse momentum $p_{\mathrm{T}} > 18$ GeV and pseudorapidity $|\eta| < 2.47$. Only the dilepton measurement included electrons reconstructed in the transition region $1.37 < |\eta| < 1.52$ between the barrel and endcap electromagnetic calorimeters, to increase the reconstruction efficiencies for the final states with electrons. Electrons were also required to satisfy requirements on the transverse impact-parameter significance calculated relative to the beam line of $|d_0|/\sigma_{d_0} < 5$ and on the longitudinal impact parameter Δz_0 calculated relative to the event primary vertex of $|\Delta z_0 \sin\theta| < 0.5$ mm, where θ is the polar angle of the track. A vertex was defined as having at least two associated tracks with $p_{\mathrm{T}} > 0.5$ GeV and the primary vertex of an event was the vertex with the highest sum of p_{T}^2 of the associated tracks. To reduce background from misidentified and non-prompt electrons, the electron candidates were required to be isolated using requirements on the summed calorimeter energy within

JHEP06(2023)138

a cone of size $\Delta R = 0.2$ around the electron cluster and on the sum of track p_{T} within a cone of variable size $\Delta R = \min(0.2, 10\,\mathrm{GeV}/p_{\mathrm{T}}(e))$ around the electron track direction,[2] both divided by the electron p_{T}.

Muon candidates were reconstructed by combining matching tracks reconstructed in the inner detector and the muon spectrometer, and were required to satisfy the 'Medium' requirements of ref. [64], giving an efficiency of about 97% for muons from $Z \to \mu\mu$ decays. The muon candidates were also required to have $p_{\mathrm{T}} > 18\,\mathrm{GeV}$ and $|\eta| < 2.5$, and to be isolated using the same calorimeter isolation variable as the electrons and a track-based isolation requirement based on a cone of size $\Delta R = \min(0.3, 10\,\mathrm{GeV}/p_{\mathrm{T}}(\mu))$. Requirements on the muon-candidate track's impact parameters similar to those of the electron candidates were made for the single-lepton measurement only.

Jets were reconstructed using the anti-k_t algorithm [65, 66] with radius parameter $R = 0.4$. Particle-flow objects that combine information from topological clusters of calorimeter energy deposits and inner-detector tracks [67] were used during reconstruction, and were calibrated according to the standard calibration used for $\sqrt{s} = 13\,\mathrm{TeV}$ high-pileup data [68]. An additional calibration specific to the $\sqrt{s} = 5.02\,\mathrm{TeV}$ pp data sample was performed to account for the modified calorimeter thresholds used for this low-pileup data sample. This calibration used a sample of Z + jet events to determine a correction to the p_{T} scale for the jets as a function of jet p_{T} and η. The p_{T} of the well-measured $Z \to \ell^+\ell^-$ system was compared with the p_{T} of the jet recoiling opposite the Z boson in azimuth. The correction to the jet energy scale was typically 2%–8%. Jets were required to have $|\eta| < 2.5$, and $p_{\mathrm{T}} > 25\,\mathrm{GeV}$ for the dilepton selection and $p_{\mathrm{T}} > 20\,\mathrm{GeV}$ for the single-lepton selection, corresponding to the optimal requirements for each analysis. Jets with $p_{\mathrm{T}} < 60\,\mathrm{GeV}$ and $|\eta| < 2.4$ were subject to additional pileup rejection criteria using a multivariate jet-vertex tagger [69]. This algorithm makes use of the tracks associated to the jet and their matching to each of the reconstructed pp collision vertices.

To prevent the double-counting of electron energy deposits as jets, the closest jet to an electron candidate was removed if it was within $\Delta R_y = 0.2$ of the electron, where $\Delta R_y = \sqrt{(\Delta y)^2 + (\Delta\phi)^2}$ and Δy is the difference in rapidity between the jet and the electron. Furthermore, to reduce the contribution of leptons from heavy-flavour hadron decays inside jets, leptons within $\Delta R_y = 0.4$ of selected jets were discarded, unless the lepton was a muon and the jet had fewer than three associated tracks, in which case the jet was discarded (thus avoiding an efficiency loss for high-energy muons undergoing significant energy loss in the calorimeters that gives rise to a jet candidate).

Jets likely to contain b-hadrons were tagged using the DL1r algorithm [70], a multivariate discriminant based on deep-learning techniques making use of track impact parameters and reconstructed secondary vertices. A tagger working point with 85% efficiency for tagging b-quark jets from top-quark decays in simulated $t\bar{t}$ events was used for the dilepton-event selection, corresponding to rejection factors of about 3 against charm jets and 40 against light-quark and gluon jets. A tighter working point with 70% efficiency was

[2] I.e. a cone whose size ΔR shrinks at high electron p_{T}, e.g. to $\Delta R = 0.1$ for $p_{\mathrm{T}} = 100\,\mathrm{GeV}$, but whose size is limited to $\Delta R = 0.2$ for $p_{\mathrm{T}} < 50\,\mathrm{GeV}$.

JHEP06(2023)138

used in the single-lepton channel with rejection factors of 6 against charm jets and 200 against light-quark and gluon jets.

The missing transverse momentum was reconstructed as the negative vector sum of the transverse momenta of all identified physics objects (electrons, muons, and jets), together with a 'soft term' built from all tracks associated with the reconstructed primary vertex but not with any of the identified physics objects [71]. The magnitude of the missing transverse momentum is denoted by $E_{\mathrm{T}}^{\mathrm{miss}}$.

5 Dilepton cross-section measurement

The measurement in the dilepton channel is based on counting the numbers of events with an opposite-charge dilepton pair and one or two b-tagged jets, and fitting these event counts to predictions based on the assumed $t\bar{t}$ cross-section, leptonic selection efficiencies and estimated non-$t\bar{t}$ backgrounds. In the same-flavour channels (ee and $\mu\mu$), the dilepton invariant mass and $E_{\mathrm{T}}^{\mathrm{miss}}$ are also exploited to separate signal events from the dominant $Z+$jets background. This method allows the efficiency for reconstructing and b-tagging a b-jet from the top quark decay to be determined from the data, and also minimises uncertainties due to the modelling of additional jets from QCD radiation in the $t\bar{t}$ signal events.

Selected events in the dilepton channel were required to have exactly two opposite-charge lepton candidates with at least one lepton matched to a corresponding electron or muon trigger. Events with no reconstructed primary vertex, with an electron and muon separated in angle by $|\Delta\theta| < 0.15$ and $|\Delta\phi| < 0.15$, or where at least one jet with $p_{\mathrm{T}} > 20\,\mathrm{GeV}$ failed quality requirements [72], were rejected. In the $e\mu$ channel, $m_{\ell\ell}$ was required to satisfy $m_{\ell\ell} > 15\,\mathrm{GeV}$. In the same-flavour channels a tighter requirement of $m_{\ell\ell} > 40\,\mathrm{GeV}$ was imposed in order to match the phase space of the $Z+$jets simulation sample, and the $Z+$jets background was reduced by requiring $E_{\mathrm{T}}^{\mathrm{miss}} > 30\,\mathrm{GeV}$. In all channels, selected events were further required to have exactly one or exactly two b-tagged jets, irrespective of the number of untagged jets present.

In the $e\mu$ channel, the inclusive $t\bar{t}$ cross-section was determined from the number of opposite-charge events with one (N_1) or two (N_2) b-tagged jets using the formalism of refs. [7, 9]. The two event counts satisfy the tagging equations

$$\begin{aligned} N_1^{e\mu} &= L\sigma_{t\bar{t}}\,\epsilon_{e\mu} 2\epsilon_b^{e\mu}(1 - C_b^{e\mu}\epsilon_b^{e\mu}) + \sum_{k=\mathrm{bkg}} s_1^k\, N_1^{e\mu,k} \text{ and} \\ N_2^{e\mu} &= L\sigma_{t\bar{t}}\,\epsilon_{e\mu} C_b^{e\mu}(\epsilon_b^{e\mu})^2 \qquad\quad + \sum_{k=\mathrm{bkg}} s_2^k\, N_2^{e\mu,k}, \end{aligned} \tag{5.1}$$

where L is the integrated luminosity of the sample, $\epsilon_{e\mu}$ is the efficiency for a $t\bar{t}$ event to pass the opposite-charge $e\mu$ selection (including the $W \to \ell\nu$ branching ratios), and $C_b^{e\mu}$ is a tagging correlation coefficient close to unity. The combined probability for a jet from the quark q in the $t \to Wq$ decay to fall within the acceptance of the detector, be reconstructed as a jet with transverse momentum above the selection threshold, and be tagged as a b-jet is denoted by $\epsilon_b^{e\mu}$. The correlation coefficient $C_b^{e\mu}$ is defined by $\epsilon_{bb}^{e\mu}/(\epsilon_b^{e\mu})^2$,

JHEP06(2023)138

where $\epsilon_{b\bar{b}}^{e\mu}$ is the probability to reconstruct and tag both b-jets from the top-quark decays. In practice, it was evaluated from simulation as $C_b^{e\mu} = 4N_{e\mu}^{t\bar{t}} N_2^{t\bar{t}}/(N_1^{t\bar{t}} + 2N_2^{t\bar{t}})^2$, where $N_{e\mu}^{t\bar{t}}$ is the number of selected $e\mu$ $t\bar{t}$ events and $N_1^{t\bar{t}}$ and $N_2^{t\bar{t}}$ are the numbers of such events with one and two b-tagged jets. Evaluated in this way, it also accounts for extra b-tagged jets from mistagged light jets, and extra heavy-flavour jets in the $t\bar{t}$ event. In the baseline $t\bar{t}$ simulation, $\epsilon_{e\mu} \approx 1.35\%$, compared to the $t\bar{t} \to e\mu X$ branching ratio of 3.2% including the $W \to \tau \to e/\mu$ contributions, and $C_b^{e\mu} \approx 1.011$, indicating a small positive correlation between the reconstruction and b-tagging of the two jets produced in the top-quark decays. Background from sources other than $t\bar{t}$ events with two prompt leptons also contributes to the event counts N_1 and N_2 in eqs. (5.1). It was divided into four sources indexed by k: Wt events, $Z+$jets events, diboson events, and events with at least one misidentified lepton. The estimate of each background was scaled by a factor s_1^k or s_2^k for events with one or two b-tagged jets.

This formalism was extended to the same-flavour channels by also exploiting the invariant mass $m_{\ell\ell}$ of the lepton pair to provide discrimination against the dominant $Z+$jets background. The events were divided into six bins of $m_{\ell\ell}$ indexed by subscript m, with lower bin boundaries at 40, 71, 81, 101, 111 and 151 GeV, the last bin including all events with $m_{\ell\ell} > 151$ GeV. The numbers of opposite-charge $\ell\ell$ events in each bin m with one and two b-tagged jets, $N_{1,m}^{\ell\ell}$ and $N_{2,m}^{\ell\ell}$ can then be expressed as

$$\begin{aligned} N_{1,m}^{\ell\ell} &= L\sigma_{t\bar{t}}\,\epsilon_{\ell\ell}\,2\epsilon_b^{\ell\ell}(1 - C_b^{\ell\ell}\epsilon_b^{\ell\ell})\,f_{1,m}^{\ell\ell,t\bar{t}} + \sum_{k=\text{bkg}} s_1^k\, f_{1,m}^{\ell\ell,k} N_1^{\ell\ell,k} \text{ and} \\ N_{2,m}^{\ell\ell} &= L\sigma_{t\bar{t}}\,\epsilon_{\ell\ell}\,C_b^{\ell\ell}(\epsilon_b^{\ell\ell})^2\,f_{2,m}^{\ell\ell,t\bar{t}} + \sum_{k=\text{bkg}} s_2^k\, f_{2,m}^{\ell\ell,k} N_2^{\ell\ell,k}, \end{aligned} \tag{5.2}$$

with separate selection efficiencies $\epsilon_{\ell\ell}$ and correlation coefficients $C_b^{\ell\ell}$ for each same-flavour channel ($\ell\ell = ee$ or $\mu\mu$). The coefficients $f_{1,m}^{\ell\ell,k}$ and $f_{2,m}^{\ell\ell,k}$ represent the integrals of the $m_{\ell\ell}$ distributions, giving the fractions of events for each dilepton flavour, background source and b-tagged jet multiplicity that appear in each mass bin. The estimated total numbers of background events for each source k were scaled by s_1^k and s_2^k, whose values were taken to be common to all three dilepton channels. In the baseline $t\bar{t}$ simulation, $\epsilon_{ee} \approx 0.48\%$ and $\epsilon_{\mu\mu} \approx 0.55\%$, compared to the $t\bar{t} \to \ell\ell$ branching ratio of 1.6% for a single lepton flavour ℓ including $W \to \tau \to \ell$, and the $C_b^{\ell\ell}$ values are compatible with that of the $e\mu$ channel.

The $t\bar{t}$ cross-section was determined by comparing the observed event counts N_1 and N_2 for the $e\mu$ channel, and the observed counts in each dilepton mass bin $N_{1,m}^{\ell\ell}$ and $N_{2,m}^{\ell\ell}$ for each of the same-flavour channels, with the predictions from eqs. (5.1) and (5.2), maximising a likelihood consisting of the product of Poisson probabilities for each event count. The values of $\sigma_{t\bar{t}}$, $\epsilon_b^{\ell\ell'}$ for each dilepton flavour (with $\ell\ell' = ee$, $e\mu$, or $\mu\mu$), and s_1^k and s_2^k for the $Z+$jets background (referred to as R_1^Z and R_2^Z below) were left free in the fit. This choice allows the level of $Z+b$-tagged-jet background, which has large uncertainties when predicted from simulation, to be determined from data. The values of s_1^k and s_2^k for all other background sources were fixed to unity, as these backgrounds are either small, or in the case of Wt, well predicted by simulation. All other parameters, i.e. $\epsilon_{\ell\ell'}$ and $C_b^{\ell\ell'}$, and

JHEP06(2023)138

$N_i^{e\mu,k}$ and $N_i^{\ell\ell,k}$, $f_{i,m}^{\ell\ell,t\bar{t}}$ and $f_{i,m}^{\ell\ell,k}$ (with $\ell\ell = ee$ or $\mu\mu$), were determined from simulation, with systematic uncertainties taken into account as discussed in section 7.

This maximum-likelihood fit determines the product of b-tagging efficiencies and jet acceptance ($\epsilon_b^{\ell\ell'}$) for all three dilepton channels largely from data, minimising the dependence on the modelling of jets in the same way as in the pure $e\mu$-based analyses of refs. [7, 9]. The normalisation of the $Z+$jets background in all channels was determined from the fits to the $m_{\ell\ell}$ distribution in the same-flavour channels, minimising the dependence on the modelling of heavy-flavour jets produced in association with a Z boson. The backgrounds from Wt and diboson events were determined from simulation. Simulation was also used to predict the small background from events with misidentified leptons, which comprises up to 2% of the one b-tagged jet samples, but is significantly smaller in the two b-tagged jet samples. This background is dominated by events where one lepton candidate is a real prompt lepton from a W or Z decay, and the other is an electron from a photon conversion, a real lepton produced in the decay of a heavy-flavour hadron, or a misidentified hadron. The analysis procedure was validated using simulation-based pseudo-experiments with various input $t\bar{t}$ cross-section values. These tests verified that the fit is unbiased and gives correct uncertainty estimates.

Figure 1 shows the b-tagged-jet multiplicity in the $e\mu$ channel, and in the same-flavour channels away from the peak of the Z resonance ($|m_{\ell\ell} - m_Z| > 10\,\text{GeV}$, referred to as off-$Z$), comparing the data with the simulation prediction. In the $e\mu$ channel, the one and two b-tagged-jet samples are expected from simulation to be about 80% and 96% pure in $t\bar{t}$ events, assuming a $t\bar{t}$ cross-section of 68.2 pb, and the largest background comes from Wt events. The backgrounds from $Z+$jets are much larger in the same-flavour samples even off the Z resonance, where the average $t\bar{t}$ purities are about 60% and 94% for one and two b-tagged jet events. Near the peak of the Z resonance, the $Z+$jets contributions are even larger. The $t\bar{t}$ simulation describes the data well, except for a data excess in the zero b-tagged-jet bins of both the $e\mu$ and same-flavour channels. Qualitatively similar discrepancies have also been seen in the $e\mu$ channel at other centre-of-mass energies [7, 9], and may indicate mismodelling of the contributions of $Z+$jets or diboson events without accompanying heavy-flavour jets. However, zero b-tagged-jet events are not used in the fit, and this discrepancy has no effect on the analysis. Figure 2 shows the lepton transverse momentum, pseudorapidity, and $E_{\text{T}}^{\text{miss}}$ distributions for $e\mu$ and off-Z same-flavour events. The total prediction is normalised to the same number of selected events as in the data, to focus on shape comparisons. In general, the description of the data by the simulation is good, given the limited size of the data sample.

6 Single-lepton cross-section measurement

The single-lepton final state arising from $t\bar{t}$ decay is characterised by a charged lepton, a neutrino, and high jet multiplicity with several b-tagged jets. The primary backgrounds in this final state arise from $W+$jets production, $Z+$jets production, Wt associated single-top-quark production, misidentified and non-prompt leptons, and diboson production.

JHEP06(2023)138

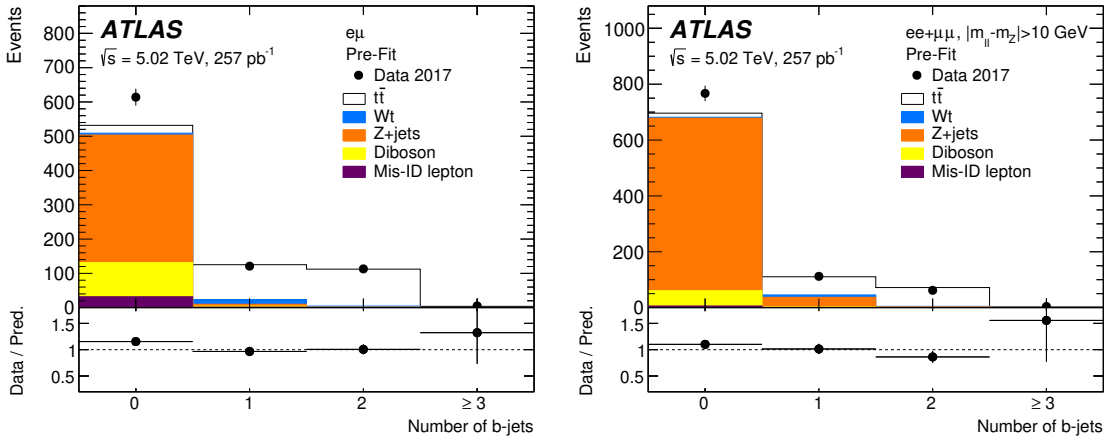

(a) (b)

Figure 1. Distributions of the number of b-tagged jets in selected opposite-charge events in (a) the $e\mu$ channel and (b) the combined ee and $\mu\mu$ same-flavour channels, additionally requiring $|m_{\ell\ell} - m_Z| > 10\,\text{GeV}$. The data are compared with the prediction from simulation normalised to the same integrated luminosity as the data. The expected contributions of $t\bar{t}$, Wt, $Z+\text{jets}$, dibosons and events with misidentified electrons or muons are shown separately. The lower panels of the figure show the ratios of data to simulation, with the error bars indicating the statistical uncertainty.

Selected events in the single-lepton channel of the $t\bar{t}$ decay were required to have exactly one electron or muon candidate with $p_{\text{T}} > 25\,\text{GeV}$, $E_{\text{T}}^{\text{miss}} > 30\,\text{GeV}$, and two or more jets with at least one of the jets being b-tagged. The minimum lepton p_{T} requirement is higher than in the dilepton analysis because of the larger background from misidentified leptons. Cuts on the transverse mass[3] of the W boson, m_{T}^{W}, and $E_{\text{T}}^{\text{miss}}$ were applied depending on the number of jets in an event in order to reduce the non-prompt lepton background. Events with two, three, or four jets were required to have $m_{\text{T}}^{W} > 30\,\text{GeV}$, as were events with five or more jets where one of the jets was b-tagged. Events with five or more jets and at least two of these being b-tagged were required to pass the looser requirement $E_{\text{T}}^{\text{miss}} + m_{\text{T}}^{W} > 60\,\text{GeV}$. Figure 3 shows the jet multiplicity and b-tagged jet multiplicity distributions of the events passing this selection. The predicted backgrounds and the expected $t\bar{t}$ contribution assuming a cross-section of 68.2 pb are also shown. The total prediction is found to be in excellent agreement with data.

The $W+\text{jets}$, $Z+\text{jets}$, single-top-quark, and diboson backgrounds were modelled using the MC samples described in section 3. The backgrounds arising from misidentified leptons were determined using a 'matrix method' technique [73]. Events were selected using looser isolation or identification requirements for the lepton and were then weighted according to the efficiencies for both the prompt and background (misidentified and non-prompt) leptons to pass the tighter baseline selection. In order to validate the method, the predictions

[3] $m_{\text{T}}^{W} = \sqrt{2p_{\text{T}}^{\ell}E_{\text{T}}^{\text{miss}}\,(1-\cos\phi)}$, where p_{T}^{ℓ} is the transverse momentum of the charged lepton and ϕ is the opening azimuthal angle between the charged lepton and the missing transverse momentum.

JHEP06(2023)138

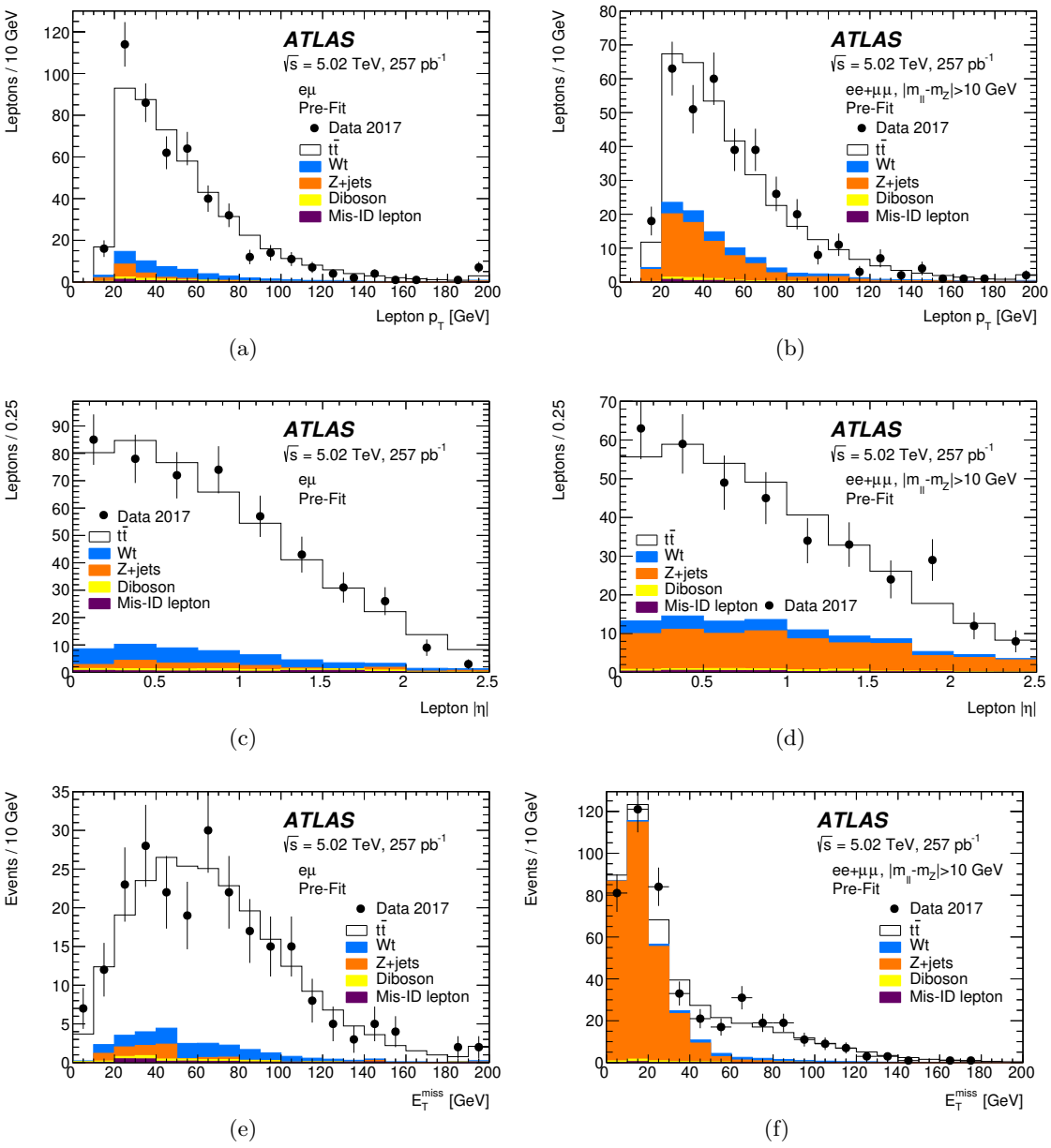

Figure 2. Distributions of (a, b) the lepton transverse momentum, (c, d) the absolute value of the lepton pseudorapidity, and (e, f) the missing transverse momentum for opposite-charge dilepton events with at least one b-tagged jet. The left column (a, c, e) shows selected $e\mu$ events and the right column (b, d, f) shows selected same-flavour events with an additional requirement of $|m_{\ell\ell} - m_Z| > 10\,\text{GeV}$. The same-flavour requirement of $E_{\text{T}}^{\text{miss}} > 30\,\text{GeV}$ is not applied in (f). The data are compared with the prediction from simulation normalised to the same number of selected events as the data, and the expected contributions from $t\bar{t}$, Wt, $Z+\text{jets}$, dibosons, and events with misidentified electrons or muons are shown separately. The last bin includes the overflows in the p_{T} and $E_{\text{T}}^{\text{miss}}$ distributions.

JHEP06(2023)138

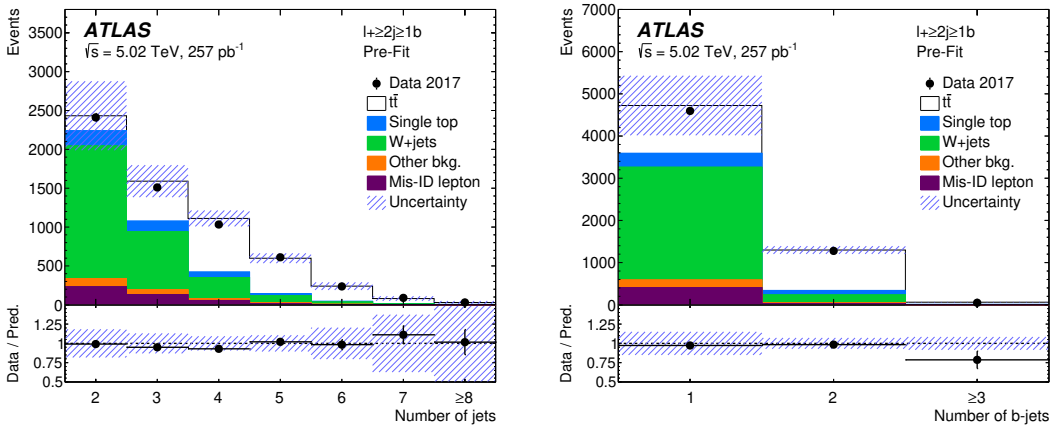

(a) (b)

Figure 3. (a) Jet multiplicity and (b) b-tagged jet multiplicity distributions in the single-lepton final state. The uncertainties are prior to the fit ('pre-fit') and the last bin contains the overflow. The 'Other bkg.' includes $Z+$jets and diboson backgrounds. The blue-hashed lines correspond to the total uncertainty of the prediction in a given bin. The lower panels show the ratio of the data to the prediction, along with the uncertainty in the ratio.

were compared with data in two dedicated validation regions with a larger fraction of misidentified-lepton candidates than expected in the analysis regions. Good agreement between data and the prediction in these validation regions was found.

Events passing the selection requirements were further split into six orthogonal regions based on the total number of jets (whether b-tagged or not) and the number of b-tagged jets: ℓ+2 jets and $\geq$1 b-tagged jet, ℓ+3 jets and 1 b-tagged jet, ℓ+3 jets and 2 b-tagged jets, $\ell+\geq$4 jets and 1 b-tagged jet, $\ell+4$ jets and 2 b-tagged jets, and $\ell+\geq$5 jets and 2 b-tagged jets. This separation created subsamples with different levels of signal and background, which provided additional constraints on the estimated backgrounds. The observed and predicted event yields in the six regions are given in table 1. The inclusion of the $\ell+3$-jet regions increased the statistical power of the measurement, while the $\ell+2$-jet region was used to improve the background modelling. In simulation, the total $t\bar{t}$ event selection efficiency integrated across all six regions is $\sim$12%.

The $H_{\mathrm{T}}^{\mathrm{had}}$ variable, defined as the scalar sum of the transverse momenta of the jets, was found to provide the single largest signal-to-background separation amongst the many kinematic variables tested. The $H_{\mathrm{T}}^{\mathrm{had}}$ distribution is shown in figure 4 for the six single-lepton regions. The predicted rates and shapes are found to be in good agreement with the observed distributions. To further increase the separation of signal from background, two boosted decision trees (BDT) using six input variables each were created using the Toolkit for Multivariate Analysis (TMVA) [74]. One BDT was trained using MC signal and background events exclusively in the two-jet and three-jet regions (ℓ+2j $\geq$1b, ℓ+3j 1b, ℓ+3j 2b) whereas the second BDT was trained in the four-jet and five-jet regions ($\ell+\geq$4j 1b, $\ell+4j$ 2b, $\ell+\geq$5j 2b). In both cases, the variables chosen were ones that were found

JHEP06(2023)138

	$\ell + 2j\ \geq 1b$	$\ell + 3j\ 1b$	$\ell + 3j\ 2b$	$\ell + \geq 4j\ 1b$	$\ell + 4j\ 2b$	$\ell + \geq 5j\ 2b$
$t\bar{t}$	194 ± 27	310 ± 33	199 ± 24	690 ± 60	318 ± 32	380 ± 60
Single top	195 ± 22	98 ± 12	38 ± 5	67 ± 9	22 ± 4	15.9 ± 2.7
$W+$jets	1700 ± 400	690 ± 210	58 ± 23	350 ± 120	30 ± 14	19 ± 10
Other bkg.	110 ± 40	55 ± 23	7.2 ± 3.0	29 ± 12	3.5 ± 1.5	3.7 ± 1.7
Misidentified leptons	250 ± 130	110 ± 60	10 ± 5	60 ± 30	6 ± 3	8 ± 5
Total	2500 ± 400	1260 ± 210	312 ± 34	1200 ± 160	380 ± 40	430 ± 70
Data	2411	1214	293	1135	375	444

Table 1. Estimated event yields in the six regions after passing the selection requirements. The 'Other bkg.' category contains the $Z+$jets and diboson contributions. The uncertainties in the signal and background yields combine the statistical and systematic uncertainties.

to individually provide good separation of signal from background and in combination provided greater separation than other choices that were considered. In the first BDT, the six input variables chosen are the $H_{\mathrm{T}}^{\mathrm{had}}$ variable, the second Fox–Wolfram moment [75] computed using all jets and the lepton (FW2 (l+j)), lepton η, the median ΔR between b-tagged jets and the lepton ($\Delta R_{b\ell}$), the median ΔR between two jets (ΔR_{jj}), and the invariant mass of two jets with the smallest ΔR ($m_{jj}^{\mathrm{min.}\Delta R}$). The second BDT uses as input the $H_{\mathrm{T}}^{\mathrm{had}}$ variable, FW2 (l+j), lepton η, $\Delta R_{b\ell}$, the median ΔR between any two untagged jets (ΔR_{uu}), and the invariant mass of two untagged jets with the smallest ΔR ($m_{\mathrm{uu}}^{\mathrm{min}\Delta R}$). The use of the median ΔR provides more rejection power than other measures of the average separation of b-tagged jets and the lepton.

The BDTs were applied to data and simulation events in the regions where they were trained and the resulting distributions of the outputs of the two BDTs used in different jet-multiplicity regions are shown in figure 5. There is good agreement between the shapes of the BDT output distributions for data and simulation in each region. Since the $t\bar{t}$ purity is already quite high in the regions with large jet and/or b-tagged jet multiplicity requirements, some of the selected $t\bar{t}$ events are kinematically similar to the bulk of the remaining background, and are thus assigned low BDT scores. The BDT output distributions were interpreted by a statistical model that employs the expected distributions for both the background and signal contributions in the six regions. This model was fitted to the observed BDT output distributions in each region to determine $\sigma_{t\bar{t}}$ as described in section 8.

JHEP06(2023)138

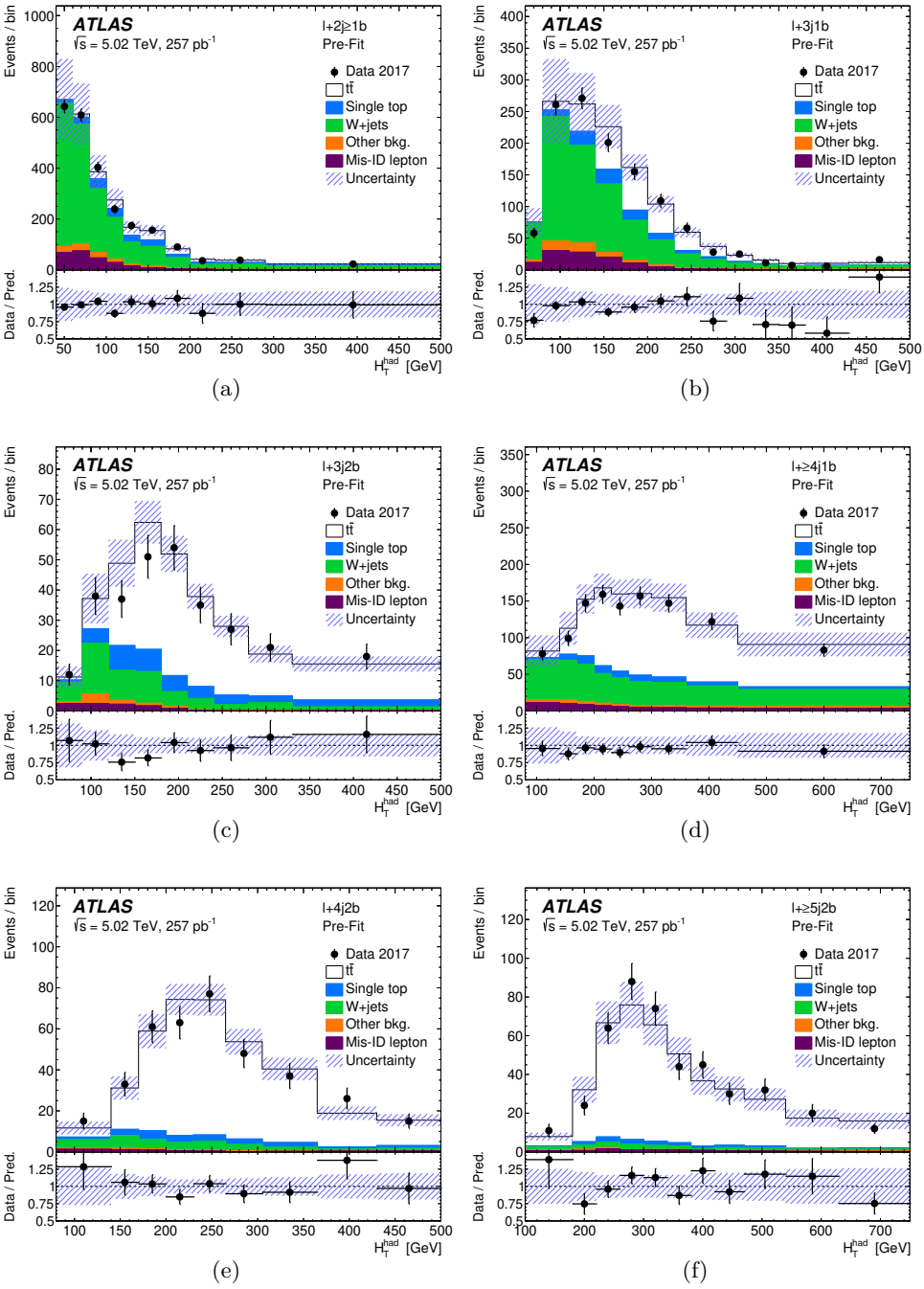

Figure 4. The observed and predicted distributions of $H_{\mathrm{T}}^{\mathrm{had}}$ in the (a) $\ell + 2j$ $\geq$1b region, (b) $\ell + 3j$ 1b region, (c) $\ell + 3j$ 2b region, (d) $\ell + \geq$4j 1b region, (e) $\ell + 4j$ 2b region, and (f) $\ell + \geq$5j 2b region. The pre-fit uncertainties are shown and the last bin contains the overflow. The 'Other bkg.' includes Z + jets and diboson backgrounds. The blue hashed lines correspond to the total uncertainty of the prediction in a given bin. The lower panels show the ratio of the data to the prediction, along with the uncertainty in the ratio.

JHEP06(2023)138

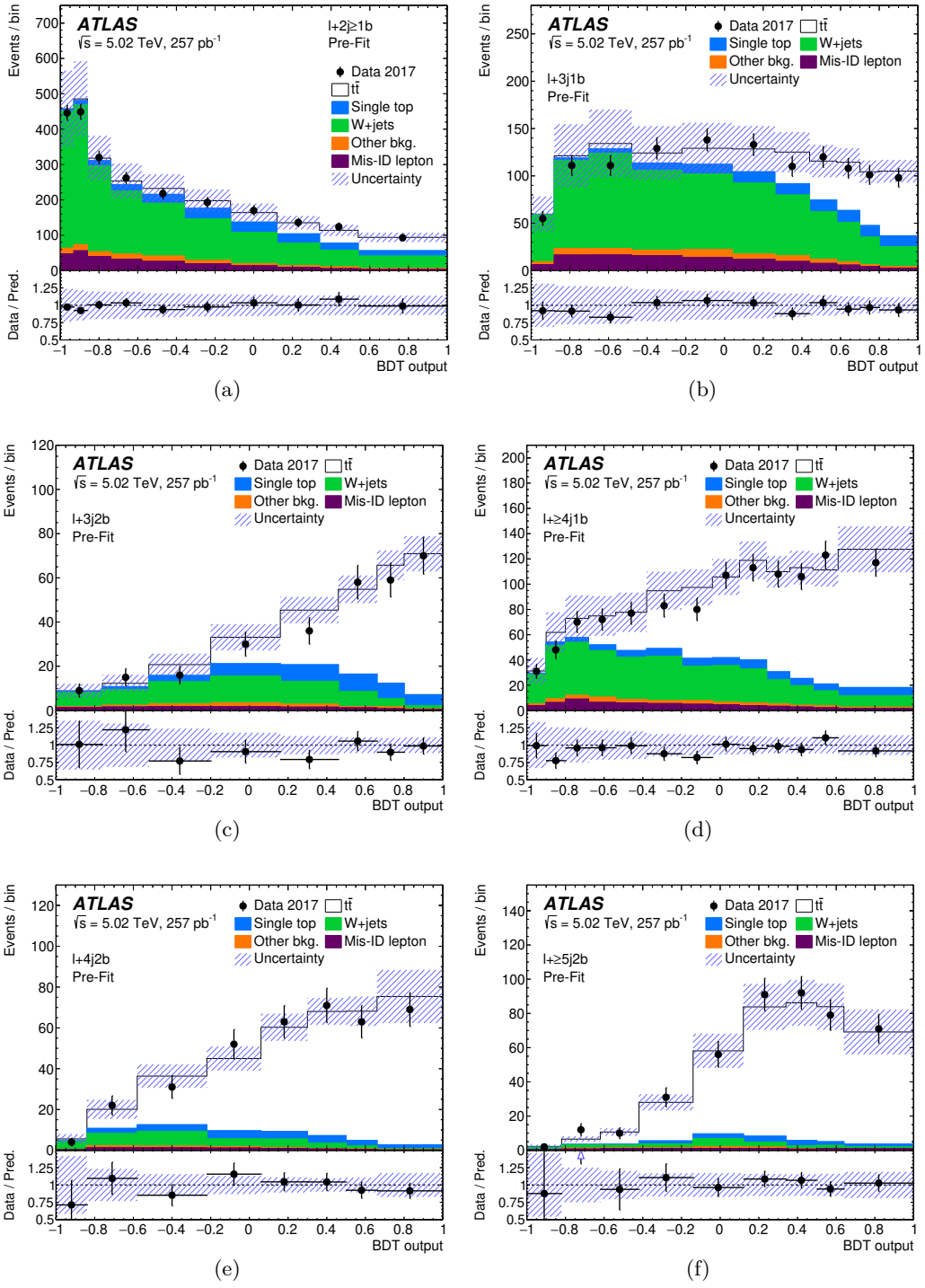

Figure 5. Comparison of the data and predicted BDT output distributions for the (a) $\ell + 2j$ $\geq 1b$ region, (b) $\ell + 3j$ $1b$ region, (c) $\ell + 3j$ $2b$ region, (d) $\ell + \geq 4j$ $1b$ region, (e) $\ell + 4j$ $2b$ region, and (f) $\ell + \geq 5j$ $2b$ region. The pre-fit uncertainties are shown. The 'Other bkg.' includes Z + jets and diboson backgrounds. The blue hashed lines correspond to the total uncertainty of the prediction in a given bin. The lower panels show the ratio of the data to the prediction, along with the uncertainty in the ratio.

JHEP06(2023)138

7 Systematic uncertainties

The systematic uncertainties in the $\sigma_{t\bar{t}}$ measurement are broken down into two categories: those arising from the modelling of signal- and background-related processes, and the detector-related uncertainties. Table 3 in section 9 gives a summary of all uncertainties for the two separate measurements and their combination.

7.1 Modelling uncertainties

Modelling uncertainties arise from the MC predictions of the $t\bar{t}$ signal and the background processes. The $t\bar{t}$ signal has uncertainties arising from the NLO generator, the parton-shower and hadronisation model, initial/final-state radiation (I/FSR), the renormalisation and factorisation scales, the value of the h_{damp} parameter, and the proton PDFs.

The uncertainty due to the choice of NLO generator was assessed by comparing the nominal Powheg+Pythia8 sample with the alternative MadGraph5_aMC@NLO+Pythia8 sample. Similarly, uncertainties in the parton-shower and hadronisation model were evaluated by comparing the nominal Powheg+Pythia8 sample with the alternative Powheg+Herwig7 sample. The uncertainty due to ISR was estimated by using the Var3c A14 tunes, which correspond to variations of α_{s} for ISR in the A14 tune [45]. Further effects on the ISR were seen when varying the renormalisation and factorisation scales μ_{r} and μ_{f}, and the h_{damp} parameter. The renormalisation and factorisation scales were varied independently by factors of 0.5 and 2.0. The uncertainty from the value of h_{damp} was evaluated by comparing the nominal $t\bar{t}$ sample with an alternative sample that has $h_{\text{damp}} = 3m_{\text{top}}$. The effect of the FSR uncertainties was evaluated by increasing and decreasing the renormalisation scale for emissions from the parton shower by factors of 0.5 and 2.0. The PDF uncertainties affecting the $t\bar{t}$ signal were evaluated by using the PDF4LHC15 Hessian uncertainties [18]. A similar procedure was used to evaluate the PDF uncertainties affecting the Wt background in the dilepton measurement only.

The predictions for $C_b^{\ell\ell'}$ in the dilepton measurement are sensitive to the fraction of $t\bar{t}$ events with extra $b\bar{b}$ or $c\bar{c}$ pairs, which was found to be underestimated by the nominal Powheg+Pythia8 samples at $\sqrt{s} = 13\,\text{TeV}$ [9, 76]. The corresponding uncertainty at $\sqrt{s} = 5.02\,\text{TeV}$ was evaluated by reweighting the nominal Powheg+Pythia8 $t\bar{t}$ sample so as to increase the rate of three-b-jet events at the generator level by 40%, the value best fitting the $\sqrt{s} = 13\,\text{TeV}$ data [9]. This variation gives an uncertainty of 0.2% in $\sigma_{t\bar{t}}$, and is included as part of the $t\bar{t}$ parton-shower/hadronisation uncertainty in table 3.

The uncertainties in the cross-sections for the Wt associated, t-channel, and s-channel single-top-quark background processes were taken to be 9.5% as discussed in section 3. The uncertainty arising from interference between the $t\bar{t}$ and Wt final states was evaluated by comparing the nominal MC sample generated using the diagram removal scheme with an alternative sample that used the diagram subtraction approach [52, 53, 58]. The uncertainties in the parton-shower and hadronisation model for Wt associated single-top-quark production were evaluated by comparing the nominal Powheg+Pythia8 samples with an alternative Powheg+Herwig7 sample. A similar comparison was performed for

JHEP06(2023)138

t-channel single-top-quark production in the single-lepton measurement (the effect is negligible in the dilepton measurement). In both measurements, the uncertainties in relevant single-top backgrounds from modelling of ISR, renormalisation and factorisation scales, and FSR were considered in a manner similar to that for $t\bar{t}$ signal.

The $W+$jets modelling uncertainties in the single-lepton measurement were evaluated by first splitting the $W+$jets background into three categories $W+\geq 1c$, $W+\geq 1b$, and $W+\geq 1q/g$ (light quarks or gluons) based on the flavour of additional jets in the event. In each category the events were further separated into categories with 2, 3, 4, or ≥ 5 jets, and a normalisation uncertainty based on Berends scaling ($4\% \oplus 24\%$ per jet) [77] was applied for each of the 12 categories. The renormalisation and factorisation scales were varied to estimate additional shape uncertainties for the three categories of $W+$jets background.

In the dilepton measurement, the normalisation of the $Z+$jets background was fitted in the same-flavour channels with a requirement of $E_{\mathrm{T}}^{\mathrm{miss}} > 30\,\mathrm{GeV}$. This normalisation factor was then propagated to the $e\mu$ channel which has no $E_{\mathrm{T}}^{\mathrm{miss}}$ requirement, implicitly assuming that the $E_{\mathrm{T}}^{\mathrm{miss}}$ distributions are well modelled in simulation. Uncertainties in this procedure were assessed by comparing the fractions of $Z \to ee/\mu\mu$ events with one and two b-tagged jets which have $E_{\mathrm{T}}^{\mathrm{miss}} > 30\,\mathrm{GeV}$ in data and simulation, probing the modelling of the $E_{\mathrm{T}}^{\mathrm{miss}}$ distributions. There were 24% more data events than predicted from the simulation sample with one b-tagged jet and 19% more events with two b-tagged jets, after averaging over same-flavour events. These values were taken as additional uncertainties of the $Z+$jets backgrounds in the $e\mu$ channel. An additional modelling uncertainty from the derivation of the $m_{\ell\ell}$ distributions (i.e. the $f_{1,m}^{\ell\ell,Z+\mathrm{jets}}$ and $f_{2,m}^{\ell\ell,Z+\mathrm{jets}}$ fractions) using the Powheg+Pythia8 MC samples rather than the Sherpa $Z+$jets samples was also applied in the dilepton measurement. In the single-lepton measurement, a 50% normalisation uncertainty in the $Z+$jets background was used to take into account the uncertainties in the cross-section, acceptance and modelling evaluated by varying the normalisation and matching scales in the Sherpa MC prediction.

The uncertainty in the diboson background was conservatively taken to be 20%. This variation accounts for uncertainties in the acceptances, and in the cross-sections calculated using the MCFM MC generator [78].

In the dilepton $\sigma_{t\bar{t}}$ measurements at $\sqrt{s} = 7$, 8, and 13 TeV, the misidentified-lepton background was found to be well modelled by simulated events. Therefore, simulation was also used to predict the misidentified-lepton background in the $\sqrt{s} = 5.02\,\mathrm{TeV}$ dilepton measurement. Variations of 50% and 100%, approximately twice the uncertainties derived at $\sqrt{s} = 13\,\mathrm{TeV}$ [9], were applied to the predicted misidentified-lepton backgrounds for the one b-jet and two b-jet samples, respectively. In the single-lepton measurement, the uncertainty in the misidentified-lepton background was first categorised according to the flavour of the misidentified lepton (e or μ) and then further split into shape and normalisation components for each of the six regions, giving 24 individual components. The shape uncertainty was estimated by comparing the nominal misidentified-lepton background sample with a sample where the electron- and muon-misidentification rates were determined using different kinematic variables and different numbers of b-tagged jets for the parameterisation. A 50% relative uncertainty was used to account for all uncertainties affecting the rate of the misidentified-lepton background [73].

JHEP06(2023)138

7.2 Detector-related uncertainties

The electron identification efficiency, energy scale, and energy resolution were measured using $Z \to ee$ events in the $\sqrt{s} = 5.02\,\text{TeV}$ data sample using techniques described in ref. [63]. Uncertainties in the identification were implemented as variations of the corresponding simulation-to-data correction factors. The $Z \to ee$ sample was also used to assess uncertainties in the modelling of electron-charge misidentification in the dilepton measurement.

The muon identification efficiencies and momentum scale calibration were taken from high-pileup $\sqrt{s} = 13\,\text{TeV}$ data [64], with additional uncertainties to account for the extrapolation to the low-pileup $\sqrt{s} = 5.02\,\text{TeV}$ data.

The efficiencies of the lepton-isolation requirements were determined using tag-and-probe techniques applied to $\sqrt{s} = 5.02\,\text{TeV}$ $Z \to ee$ and $Z \to \mu\mu$ events. The differences between the efficiencies measured in data and simulation samples were studied as functions of lepton p_{T} and η, and the activity around the lepton. Applying these shifts to leptons in simulated $t\bar{t}$ events gave per-lepton efficiency changes of up to $+0.4\%$ for electrons and -0.5% for muons. Given the small sizes of these shifts, no corrections were applied to the nominal simulation, and the largest shifts were taken as uncertainties in the efficiencies and background estimates.

The electron-trigger efficiency was measured using $Z \to ee$ events in low-pileup datasets recorded at both $\sqrt{s} = 5.02\,\text{TeV}$ and $\sqrt{s} = 13\,\text{TeV}$, using the method described in [33]. The muon-trigger efficiency was measured using $Z \to \mu\mu$ events in high-pileup $\sqrt{s} = 13\,\text{TeV}$ data recorded immediately before the low-pileup datasets [34].

The jet calibration is based on the jet-energy scale determined for $\sqrt{s} = 13\,\text{TeV}$ high-pileup data [68], with an additional correction to the jet-energy scale derived from the $Z+\text{jet}$ p_{T}-balancing technique applied to $\sqrt{s} = 5.02\,\text{TeV}$ data and simulation, as discussed in section 4. The uncertainty of 1%–2% in this correction was incorporated into the systematic uncertainties of the jet-energy scale, including the modelling uncertainty of the $Z+\text{jet}$ final state. An uncertainty from the jet-vertex tagger arises from the efficiency correction factors for this algorithm [69].

Predictions for the b-tagging efficiency (for the single-lepton measurement), $C_b^{\ell\ell'}$ (for the dilepton measurement) and background rejection were taken from $\sqrt{s} = 5.02\,\text{TeV}$ simulation samples, corrected by the standard simulation-to-data scale factors obtained from studies of $t\bar{t}$ and dijet events at $\sqrt{s} = 13\,\text{TeV}$ [70, 79, 80]. This choice is supported by the values of $\epsilon_b^{\ell\ell'}$ obtained from the dilepton measurement at $\sqrt{s} = 5.02\,\text{TeV}$ as discussed in section 8, and from simulation studies which show that the b-tagging performance is similar in the two environments.

The uncertainties in the calibrations of leptons and jets discussed above were propagated into the $E_{\text{T}}^{\text{miss}}$ calculation along with uncertainties in the modelling of the soft term [71].

The uncertainty in the integrated luminosity is 1.6%, evaluated as discussed in ref. [81] and using the LUCID-2 detector [82] for the primary luminosity measurement. The corresponding uncertainty in $\sigma_{t\bar{t}}$ is larger than 1.6% in the dilepton measurement because

JHEP06(2023)138

the luminosity uncertainty affects the evaluation of the Wt and diboson backgrounds from simulation.

The LHC beam energy is known to be within 0.1% of the nominal value based on the LHC magnetic model and comparisons of the revolution frequencies of proton and lead-ion beams [83]. A 0.1% variation in $\sqrt{s}$ corresponds to a 0.3% variation in the predicted $\sigma_{t\bar{t}}$ according to the NNLO+NNLL predictions of Top++. This uncertainty is included as a separate uncertainty in $\sigma_{t\bar{t}}$ to facilitate comparisons with theoretical predictions at exactly $\sqrt{s} = 5.02\,\text{TeV}$.

8 Results

Table 2 and figure 6 show the results of applying the fit described in section 5 to the dilepton data sample, comparing the observed event counts with the fit predictions including the $t\bar{t}$ signal component and all backgrounds. In table 2, the same-flavour channel event counts are divided into those near the peak of the $Z \to \ell\ell$ resonance ($|m_{\ell\ell} - m_Z| < 10\,\text{GeV}$ and referred to as on-Z) and those off the Z-boson resonance (off-Z), to illustrate the changing background level and composition. The fit describes the data well, with the exception of the Z-boson region in the same-flavour channels with one b-tagged jet, as noted earlier. The fitted $t\bar{t}$ production cross-section in the dilepton channel is

$$\sigma_{t\bar{t}} = 65.7 \pm 4.5\,(\text{stat.}) \pm 1.6\,(\text{syst.}) \pm 1.2\,(\text{lumi.}) \pm 0.2\,(\text{beam})\,\text{pb},$$

where the four uncertainties are due to the size of the data sample, experimental and theoretical systematic effects, and imperfect knowledge of both the integrated luminosity and the LHC beam energy. The total uncertainty of 4.9 pb corresponds to a relative uncertainty of 7.5%, of which 6.8% is the data statistical uncertainty. The 'dilepton' column of table 3 in section 9 shows a breakdown of the uncertainties. The result is quoted for a top-quark mass of 172.5 GeV, and changes by $\mp 0.2\%$ for a ± 1 GeV change in m_t.

The products of jet acceptance and b-tagging efficiencies in the three dilepton channels are $\epsilon_b^{ee} = 0.65 \pm 0.06$, $\epsilon_b^{e\mu} = 0.68 \pm 0.03$, and $\epsilon_b^{\mu\mu} = 0.59 \pm 0.06$. All three values are consistent with each other and the predictions from simulation, validating the modelling of b-tagging in the simulation. The scale factors for the $Z+\text{jets}$ background are $R_1^Z = 1.23 \pm 0.09$ and $R_2^Z = 1.68 \pm 0.52$, suggesting that the Sherpa $Z+\text{jets}$ simulation slightly underestimates this background. Consistent results were obtained from fits to the $e\mu$ and $ee + \mu\mu$ channels alone, which have total uncertainties of 8.4% and 13.5%, respectively. The result is stable against variations of the $E_{\text{T}}^{\text{miss}}$ requirement.

The potential effect of the difference between the Z-boson ee and $\mu\mu$ yields with one b-tagged jet visible in table 2 and figures 6(a) and 6(d) was addressed by fitting the two same-flavour channels separately. This gave compatible values for $\sigma_{t\bar{t}}$ and R_2^Z, but a three-standard-deviation discrepancy between the values of R_1^Z fitted in the ee and $\mu\mu$ channels. However, this discrepancy disappeared when lowering the $E_{\text{T}}^{\text{miss}}$ requirement to $E_{\text{T}}^{\text{miss}} > 20\,\text{GeV}$, which increased the $Z+\text{jets}$ background by a factor of three. The inclusive $Z \to ee$ and $Z \to \mu\mu$ yields (without requirements on additional jets) were also compared and found to be consistent within 1%, validating the modelling of the electron and muon

JHEP06(2023)138

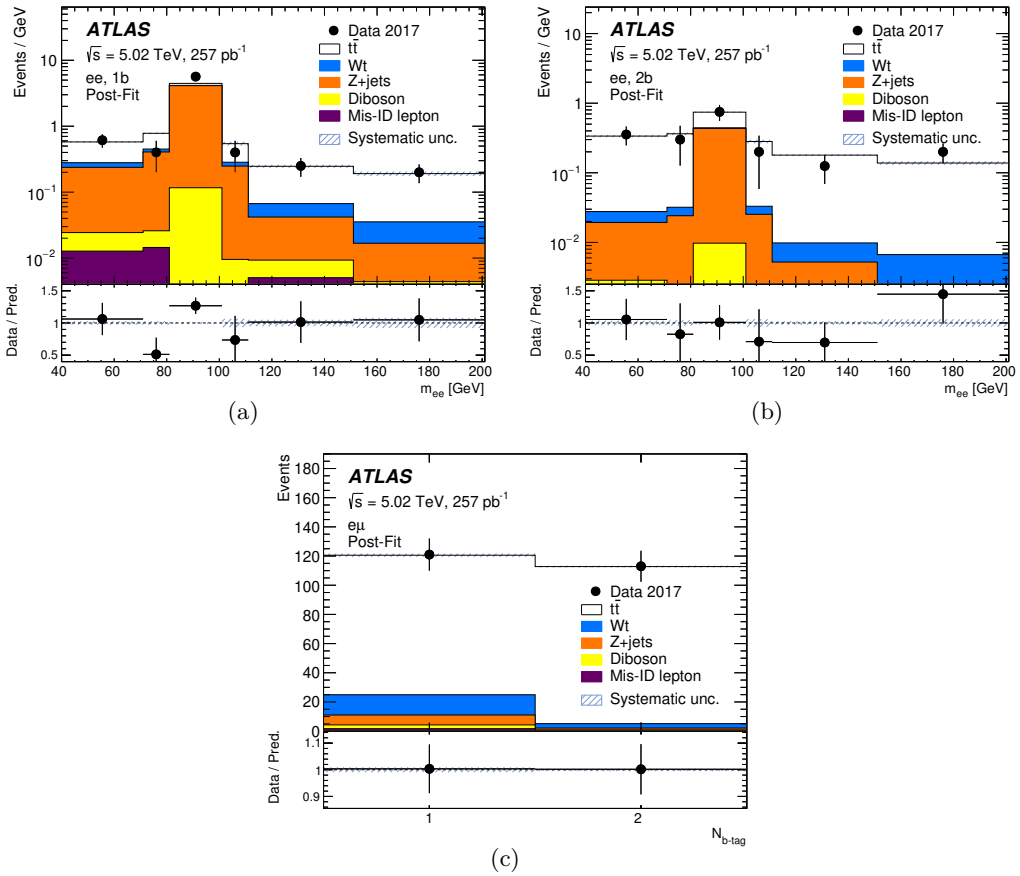

Figure 6. Results of the fit to data in the dilepton channel, showing the invariant mass distributions for the one b-tagged jet and two b-tagged jet samples in the ee (top) and $\mu\mu$ (bottom) channels, and the b-tagged jet multiplicity in the $e\mu$ channel (centre). The data are shown by the points with uncertainties, and are compared with the results of the fit, showing the scaled contributions from $t\bar{t}$, Wt, $Z+$jets, dibosons, and events with misidentified leptons. The total systematic uncertainty of the fit prediction in each bin is shown by the hatched band. The lower panels show the ratios of data to the fit predictions. In the invariant mass distributions, the last bin includes the overflow with $m_{\ell\ell} > 200\,\text{GeV}$ but is normalised to the displayed bin width.

JHEP06(2023)138

Event counts	$N^{ee}_{1,\text{off}-\text{Z}}$	$N^{ee}_{1,\text{on}-\text{Z}}$	$N^{e\mu}_{1}$	$N^{\mu\mu}_{1,\text{off}-\text{Z}}$	$N^{\mu\mu}_{1,\text{on}-\text{Z}}$
Data	47	113	121	65	106
$t\bar{t}$	30.1 ± 3.8	6.0 ± 0.7	95.6 ± 10.0	36.6 ± 3.6	7.5 ± 0.8
Wt single top	4.0 ± 0.6	0.75 ± 0.12	13.9 ± 1.5	4.5 ± 0.5	0.90 ± 0.12
$Z+$jets	14.7 ± 1.5	80.1 ± 6.0	6.8 ± 1.7	27.1 ± 3.3	111.3 ± 8.8
Diboson	0.83 ± 0.17	2.3 ± 0.5	2.6 ± 0.5	0.90 ± 0.18	2.5 ± 0.5
Misidentified leptons	0.9 ± 0.4	0.05 ± 0.03	1.7 ± 0.8	0.23 ± 0.17	0.16 ± 0.15
Total prediction	50.5 ± 3.7	89.2 ± 5.9	120.6 ± 9.7	69.4 ± 4.7	122.4 ± 8.6
Event counts	$N^{ee}_{2,\text{off}-\text{Z}}$	$N^{ee}_{2,\text{on}-\text{Z}}$	$N^{e\mu}_{2}$	$N^{\mu\mu}_{2,\text{off}-\text{Z}}$	$N^{\mu\mu}_{2,\text{on}-\text{Z}}$
Data	31	15	113	31	17
$t\bar{t}$	28.7 ± 5.3	6.0 ± 1.1	107.6 ± 10.3	26.6 ± 5.9	5.5 ± 1.2
Wt single top	0.88 ± 0.15	0.21 ± 0.07	3.0 ± 0.6	1.00 ± 0.27	0.17 ± 0.05
$Z+$jets	1.2 ± 1.0	8.5 ± 2.6	1.3 ± 0.5	2.8 ± 1.0	11.5 ± 3.8
Diboson	0.06 ± 0.01	0.16 ± 0.03	0.20 ± 0.04	0.06 ± 0.01	0.30 ± 0.06
Misidentified leptons	0.15 ± 0.15	0.04 ± 0.04	0.6 ± 0.6	0.10 ± 0.11	0.05 ± 0.06
Total prediction	31.0 ± 5.1	14.9 ± 2.6	112.8 ± 10.3	30.6 ± 5.6	17.6 ± 3.5

Table 2. Observed numbers of opposite-charge dilepton events with one (upper block) and two (lower block) b-tagged jets in data, together with the $t\bar{t}$ and background event counts from the fit prediction, including the associated statistical and systematic uncertainties. The five columns show the ee channel with $|m_{\ell\ell} - m_Z| > 10\,\text{GeV}$ (off-Z) and $|m_{\ell\ell} - m_Z| < 10\,\text{GeV}$ (on-Z), the $e\mu$ channel, and the $\mu\mu$ channel including off-Z and on-Z contributions. The uncertainty in the total prediction is in some cases smaller than the individual uncertainties due to correlations induced by the fit.

efficiencies. The difference between the observed and predicted yields seen in figure 6 was therefore attributed to a statistical fluctuation.

The $t\bar{t}$ cross-section in the single-lepton channel was determined by fitting a model consisting of the estimated background and $t\bar{t}$ signal distributions to the observed BDT distributions in the six regions simultaneously. The likelihood fit incorporated the systematic uncertainties as Gaussian nuisance parameters that modified the shape and/or normalisation of the predicted distributions as defined in section 7. Additional bin-by-bin uncertainties were included to account for the statistical uncertainties in the predicted backgrounds. The fitted background parameters in the model were found to be consistent with their central values, taking into account uncertainties. The results of the fit to the BDT distributions are shown in figure 7 and confirm that the fit gives a good description of the data distributions. The pulls and constraints of the nuisance parameters were found to be reasonable, with none of the parameters being pulled by more than half a standard deviation from their input value, or constrained to less than 50% of their input uncertainty.

The single-lepton channel fit results in

$$\sigma_{t\bar{t}} = 68.2 \pm 0.9\,(\text{stat.}) \pm 2.9\,(\text{syst.}) \pm 1.1\,(\text{lumi.}) \pm 0.2\,(\text{beam})\,\text{pb}.$$

The $t\bar{t}$ cross-sections at $\sqrt{s} = 5.02\,\text{TeV}$ measured in the single-lepton and dilepton channels are consistent.

JHEP06(2023)138

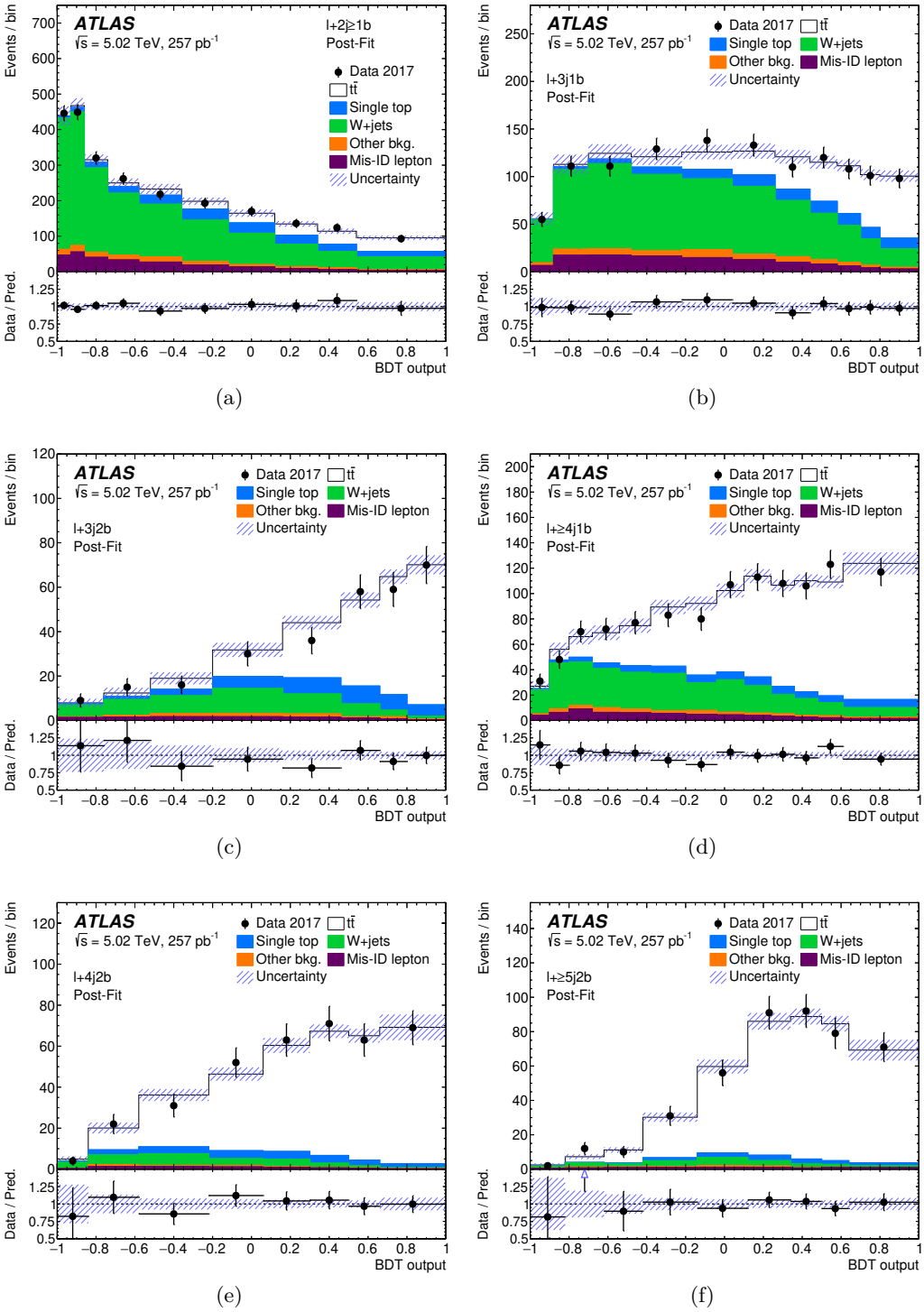

Figure 7. Comparison between data and the results of the fit to the BDT output distributions in the (a) $\ell+2j\ \geq 1b$ region, (b) $\ell+3j\ 1b$ region, (c) $\ell+3j\ 2b$ region, (d) $\ell+\geq 4j\ 1b$ region, (e) $\ell+4j\ 2b$ region, and (f) $\ell+\geq 5j\ 2b$ region. The 'Other bkg.' includes $Z+$jets and diboson backgrounds. The bottom panel displays the ratio of data to the total prediction. The hashed area represents the total uncertainty of the background.

JHEP06(2023)138

The 'single lepton' column of table 3 shows a breakdown of the individual uncertainties. The largest contributions to the total uncertainty of 3.1 pb come from modelling of the $W+$jets background, the integrated luminosity uncertainty, and the data statistical uncertainty. The result changes by $\mp 2.0\%$ for a ± 1 GeV change in m_t, a larger sensitivity than in the dilepton channel because the simulation is also used to predict the efficiencies of the jet requirements. This result is slightly more precise than the $t\bar{t}$ cross-section measurement in the single-lepton channel at $\sqrt{s} = 13$ TeV [10], despite the much smaller data sample. This arises from the use of six regions and the fit of the shapes of the BDT distributions in each region to constrain the background contributions. It also reflects the fact that both analyses are dominated by systematic uncertainties, and although the non-$t\bar{t}$ backgrounds are larger than at $\sqrt{s} = 13$ TeV, the uncertainties due to QCD radiation in $t\bar{t}$ events are less important.

9 Combined cross-section and comparison with predictions

The cross-section measurements in the dilepton and single-lepton channels were combined to provide a more precise result. The dilepton measurement used a fit of the $t\bar{t}$ signal, background contributions, and b-tagging efficiency, while the single-lepton measurement used a binned profile-likelihood fit, resulting in post-fit uncertainty correlations that must be accounted for in a combination. To combine these two measurements, taking into account their different techniques, the Convino [84] algorithm was used. It minimises a χ^2 with three terms: one encoding the results and the statistical uncertainty of each measurement, the second encoding the correlations between uncertainties in a given measurement, and the third term accounting for the prior knowledge of correlations between the uncertainties of the different measurements.

The prior probabilities (priors) for the correlations between uncertainties in the two measurements were determined by assigning each systematic uncertainty in the combination to one of three categories: unique uncertainties, one-to-one uncertainties, and one-to-many uncertainties. Unique uncertainties are ones that exist only in one of the two measurements, or which are uncorrelated between the two measurements. One-to-one uncertainties are those that affect both measurements in a similar way. Finally, one-to-many uncertainties are the set of uncertainties represented by single nuisance parameters in one measurement and multiple nuisance parameters in the other. The latter category covers most of the $t\bar{t}$ modelling uncertainties, which were represented by a single nuisance parameter in the dilepton analysis and separate nuisance parameters for each of the fit regions in the single-lepton analysis, due to the need to account for uncertainties in the shapes of the BDT input distributions.

This categorisation was used to determine the correlations between the various systematic uncertainties in the Convino minimisation procedure. By definition, unique uncertainties in one measurement are uncorrelated with all other uncertainties. One-to-one uncertainties are fully correlated between the two measurements. The one-to-many uncertainties in this combination were investigated by considering numerous correlation priors between the one nuisance parameter in one channel and the set of nuisance parameters in

JHEP06(2023)138

the other. The results of the combination were found to be insensitive to the prior employed for these one-to-many uncertainties and so the assumption of fully correlated uncertainties was employed in the fit. In the combination, the b-tagging uncertainties were treated as one-to-one uncertainties, even though different tagger working points were used in the two measurements.

The $t\bar{t}$ cross-section value at $\sqrt{s} = 5.02\,\text{TeV}$ obtained from the combination of the dilepton and single-lepton measurements is

$$\sigma_{t\bar{t}} = 67.5 \pm 0.9(\text{stat.}) \pm 2.3(\text{syst.}) \pm 1.1(\text{lumi.}) \pm 0.2(\text{beam})\,\text{pb}.$$

Table 3 shows a breakdown of uncertainties in the individual measurements and the combined result. The combination gives a lower overall uncertainty due to reductions in the signal modelling, electron reconstruction, flavour-tagging, and jet-energy-scale uncertainties. The uncertainties arising from theory and MC modelling are larger than the experimental uncertainties. The combined result changes by $\mp 2.0\%$ for a $\pm 1\,\text{GeV}$ change in m_t.

The combined result is consistent with the NNLO+NNLL QCD prediction of $\sigma_{t\bar{t}} = 68.2^{+5.2}_{-5.3}\,\text{pb}$ discussed in section 1, and with the CMS collaboration measurement [26]. The individual and combined ATLAS collaboration results are compared in figure 8 with measurements in the $e\mu$ and single-lepton channels at other $\sqrt{s}$ values. Predictions using the CT10 [21], NNPDF2.3 [23], MSTW2008 [19, 20], CT14 [85], and NNPDF3.1_NOTOP [86] PDF sets are also shown. The first three PDF sets do not incorporate any constraints from LHC data, while the last two are PDF sets that use some LHC data but no $t\bar{t}$ cross-section measurements.

Figure 9(a) compares the measured cross-section at $\sqrt{s} = 5.02\,\text{TeV}$ with the predictions from the aforementioned PDF sets, as well as the MSHT20 [88], NNPDF4.0 [89], ABMP16 [90], CT18 [91] and CT18A [91] PDFs, and the combination of the CT10, MSTW2008, and NNPDF2.3 PDFs using the PDF4LHC recipe. The result is also compared with the recent ATLASPDF21 PDF fit [92], which includes a diverse set of ATLAS collaboration measurements at $\sqrt{s} = 7$, 8 and 13 TeV (including $t\bar{t}$ differential cross-section measurements at $\sqrt{s} = 8$ and 13 TeV), together with deep-inelastic scattering data from ep collisions at the HERA collider [93]. The measured value is compatible with the predictions from all the PDF sets considered, except for ABMP16, which has a softer gluon distribution and predicts a $\sigma_{t\bar{t}}$ value 2.2 standard deviations lower than measured.

Figure 9(b) shows the effect of adding the combined $\sqrt{s} = 5.02\,\text{TeV}$ $t\bar{t}$ cross-section measurement to the ATLASPDF21 PDF fit. The combination was performed using the xFitter framework [94] as described in ref. [92]. At a squared-momentum-transfer value of $Q^2 = 10^4\,\text{GeV}^2$, the addition of the new data reduces the gluon PDF uncertainty in the region of Bjorken-x (the fraction of the proton momentum carried by the parton participating in the initial interaction) above $x \approx 0.05$, and gives e.g. a 5% reduction at $x = 0.1$. The uncertainties in the valance and sea quark PDFs are unaffected.

JHEP06(2023)138

Category	$\delta\sigma_{t\bar{t}}$ [%]		
	Dilepton	Single lepton	Combination
$t\bar{t}$ generator†	1.2	1.0	0.8
$t\bar{t}$ parton-shower/hadronisation*,†	0.3	0.9	0.7
$t\bar{t}$ h_{damp} and scale variations†	1.0	1.1	0.8
$t\bar{t}$ parton distribution functions†	0.2	0.2	0.2
Single-top background	1.1	0.8	0.6
$W/Z+$jets background*	0.8	2.4	1.8
Diboson background	0.3	0.1	< 0.1
Misidentified leptons*	0.7	0.3	0.3
Electron identification/isolation	0.8	1.2	0.8
Electron energy scale/resolution	0.1	0.1	< 0.1
Muon identification/isolation	0.6	0.2	0.3
Muon momentum scale/resolution	0.1	0.1	0.1
Lepton-trigger efficiency	0.2	0.9	0.7
Jet-energy scale/resolution	0.1	1.1	0.8
$\sqrt{s} = 5.02\,\text{TeV}$ JES correction	0.1	0.6	0.5
Jet-vertex tagging	< 0.1	0.2	0.2
Flavour tagging	0.1	1.1	0.8
$E_{\text{T}}^{\text{miss}}$	0.1	0.4	0.3
Simulation statistical uncertainty*	0.2	0.6	0.5
Data statistical uncertainty*	6.8	1.3	1.3
Total systematic uncertainty	2.5	4.2	3.4
Integrated luminosity	1.8	1.6	1.6
Beam energy	0.3	0.3	0.3
Total uncertainty	7.5	4.5	3.9

Table 3. Breakdown of uncertainties in the dilepton, single-lepton, and combined measurements of the inclusive $t\bar{t}$ cross-section at $\sqrt{s} = 5.02\,\text{TeV}$. For each category, the dilepton uncertainties are calculated by summing all the contributing uncertainties in quadrature. The single-lepton and combination uncertainties are calculated by fixing the set of nuisance parameters corresponding to a category, repeating the fit, and subtracting in quadrature the resulting uncertainty from the total uncertainty of the nominal fit. Categories that include unique uncertainties, uncorrelated between dilepton and single-lepton measurements, are denoted by *, and those with one-to-many uncertainties by † (see text). Other categories include only one-to-one uncertainty sources, correlated between channels. The total uncertainty is the sum in quadrature of the total systematic uncertainty, the statistical uncertainty, and the effects of the uncertainties in the integrated luminosity and beam energy. The systematic uncertainties for the single-lepton and combination measurements do not add up in quadrature to the total systematic uncertainty because of their correlations in the fit.

JHEP06(2023)138

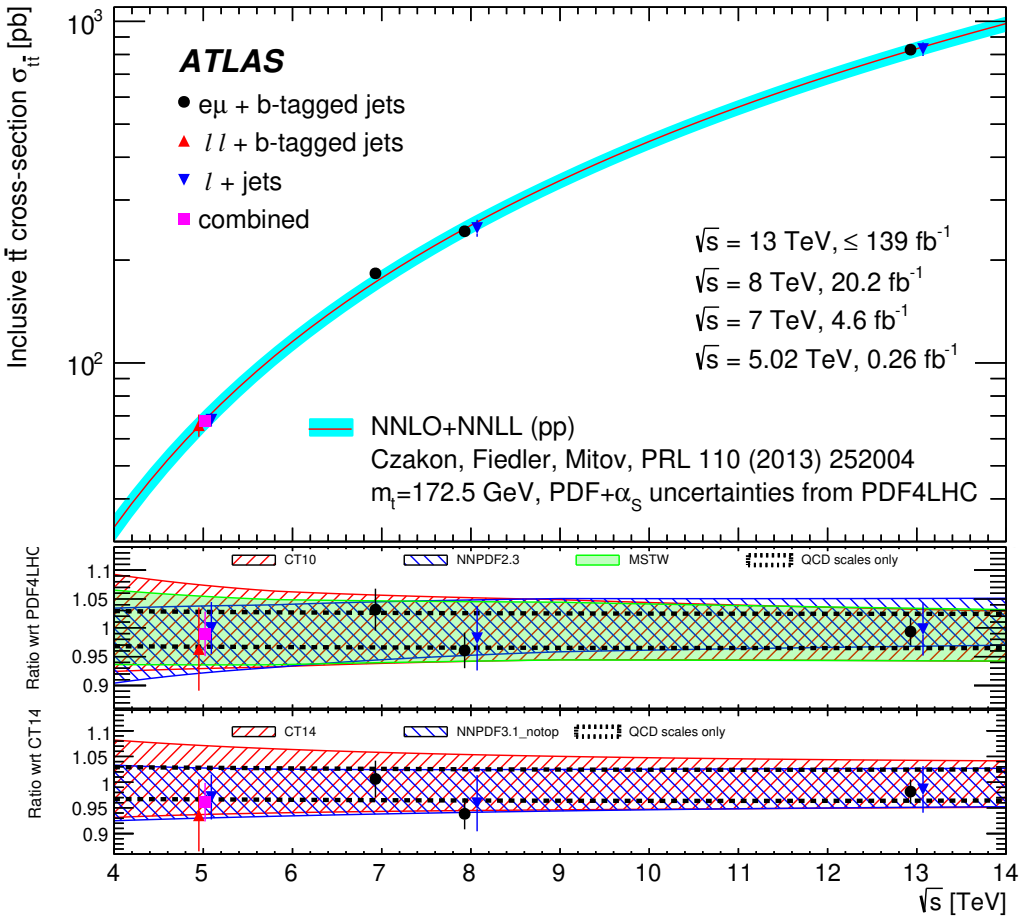

Figure 8. The upper panel shows the inclusive $t\bar{t}$ cross-section $\sigma_{t\bar{t}}$ as a function of centre-of-mass energy $\sqrt{s}$, comparing ATLAS collaboration measurements from this analysis, from the $e\mu$ plus b-tagged-jets final state at $\sqrt{s} = 7$, 8, and 13 TeV, and from the single-lepton final state at $\sqrt{s} = 8$ and 13 TeV with NNLO+NNLL theoretical predictions [5] calculated using Top++ [17] with the PDF4LHC prescription for PDF and α_s uncertainties [87], and $m_t = 172.5$ GeV. The middle panel shows the ratios of the measurements and predictions to the central value of the prediction using PDF4LHC PDFs. The total uncertainties when using the individual NNPDF2.3, MSTW2008 and CT10 PDFs are shown as overlapping hatched or coloured bands, and the dotted lines show the QCD scale uncertainties alone. The lower panel shows the ratios of the measurements and predictions from the CT14 and NNPDF3.1_notop PDFs to the central value from CT14. Measurements made at the same $\sqrt{s}$ are slightly offset for clarity. The $\sqrt{s} = 7$ and 8 TeV results are taken from refs. [7, 8], with the LHC beam energy uncertainties reduced according to ref. [83]. The $\sqrt{s} = 13$ TeV results are taken from refs. [9, 10].

JHEP06(2023)138

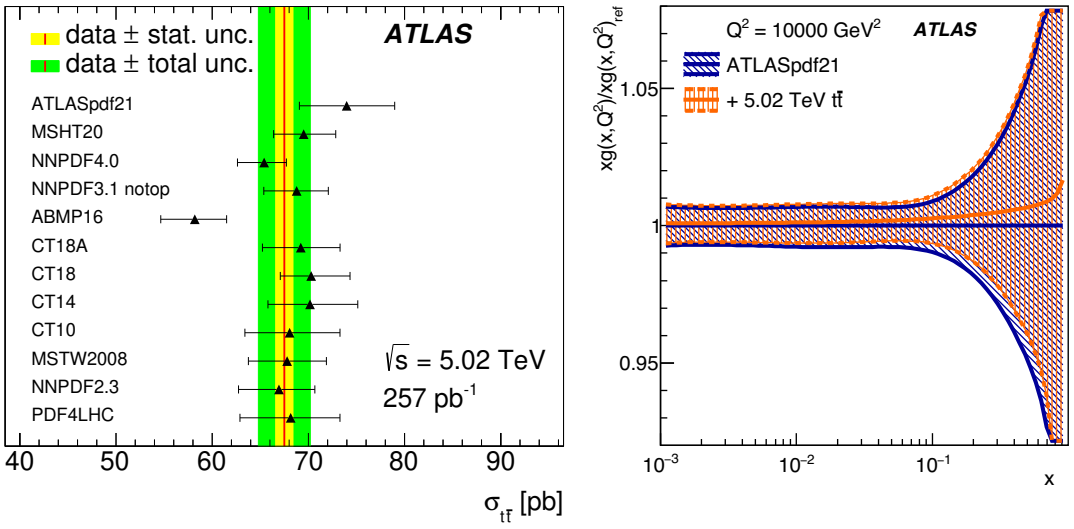

(a) (b)

Figure 9. (a) Measurement of the $t\bar{t}$ production cross-section at $\sqrt{s} = 5.02\,\text{TeV}$ in the combined dilepton and single-lepton channels compared with the predictions from various NNLO PDF sets. The bands show the experimental measurement, with the statistical (inner yellow band) and total (outer green band) uncertainties shown separately. The last entry shows the prediction using the PDF4LHC recipe, encompassing the predictions from the CT10, MSTW2008 and NNPDF2.3 PDF sets. (b) Ratio of the gluon PDF determined using the data of the ATLASpdf21 PDF fit plus the constraint from the combined $t\bar{t}$ cross-section measurement compared with the ATLASpdf21 fit alone, as a function of Bjorken-x. The hatched bands show the uncertainties in the combined fit (orange) and ATLASpdf21 fit (blue), and the orange line shows the shift in central value when adding the $\sqrt{s} = 5.02\,\text{TeV}$ cross-section measurement.

JHEP06(2023)138

10 Conclusion

The inclusive $t\bar{t}$ production cross-section $\sigma_{t\bar{t}}$ has been measured in pp collisions at $\sqrt{s} = 5.02\,\text{TeV}$ using $257\,\text{pb}^{-1}$ of data recorded by the ATLAS experiment at the LHC in 2017 using events from both the dilepton and single-lepton channels. The combined result is

$$\sigma_{t\bar{t}} = 67.5 \pm 0.9\,(\text{stat.}) \pm 2.3\,(\text{syst.}) \pm 1.1\,(\text{lumi.}) \pm 0.2\,(\text{beam})\,\text{pb},$$

where the four uncertainties are due to the size of the data sample, experimental and theoretical systematic effects, and imperfect knowledge of both the integrated luminosity and the LHC beam energy. The total uncertainty is 2.7 pb, or 3.9%. The result is consistent with the NNLO+NNLL QCD prediction of $68.2^{+5.2}_{-5.3}\,\text{pb}$ and with a previous measurement by the CMS collaboration, but has a total uncertainty that is almost a factor of two smaller. This measurement provides additional constraints on the gluon distribution of the proton PDF for Bjorken-$x > 0.05$.

Acknowledgments

We thank CERN for the very successful operation of the LHC, as well as the support staff from our institutions without whom ATLAS could not be operated efficiently.

We acknowledge the support of ANPCyT, Argentina; YerPhI, Armenia; ARC, Australia; BMWFW and FWF, Austria; ANAS, Azerbaijan; CNPq and FAPESP, Brazil; NSERC, NRC and CFI, Canada; CERN; ANID, Chile; CAS, MOST and NSFC, China; Minciencias, Colombia; MEYS CR, Czech Republic; DNRF and DNSRC, Denmark; IN2P3-CNRS and CEA-DRF/IRFU, France; SRNSFG, Georgia; BMBF, HGF and MPG, Germany; GSRI, Greece; RGC and Hong Kong SAR, China; ISF and Benoziyo Center, Israel; INFN, Italy; MEXT and JSPS, Japan; CNRST, Morocco; NWO, Netherlands; RCN, Norway; MEiN, Poland; FCT, Portugal; MNE/IFA, Romania; MESTD, Serbia; MSSR, Slovakia; ARRS and MIZŠ, Slovenia; DSI/NRF, South Africa; MICINN, Spain; SRC and Wallenberg Foundation, Sweden; SERI, SNSF and Cantons of Bern and Geneva, Switzerland; MOST, Taiwan; TENMAK, Türkiye; STFC, United Kingdom; DOE and NSF, United States of America. In addition, individual groups and members have received support from BCKDF, CANARIE, Compute Canada and CRC, Canada; PRIMUS 21/SCI/017 and UNCE SCI/013, Czech Republic; COST, ERC, ERDF, Horizon 2020 and Marie Skłodowska-Curie Actions, European Union; Investissements d'Avenir Labex, Investissements d'Avenir Idex and ANR, France; DFG and AvH Foundation, Germany; Herakleitos, Thales and Aristeia programmes co-financed by EU-ESF and the Greek NSRF, Greece; BSF-NSF and MINERVA, Israel; Norwegian Financial Mechanism 2014-2021, Norway; NCN and NAWA, Poland; La Caixa Banking Foundation, CERCA Programme Generalitat de Catalunya and PROMETEO and GenT Programmes Generalitat Valenciana, Spain; Göran Gustafssons Stiftelse, Sweden; The Royal Society and Leverhulme Trust, United Kingdom.

The crucial computing support from all WLCG partners is acknowledged gratefully, in particular from CERN, the ATLAS Tier-1 facilities at TRIUMF (Canada), NDGF

JHEP06(2023)138

(Denmark, Norway, Sweden), CC-IN2P3 (France), KIT/GridKA (Germany), INFN-CNAF (Italy), NL-T1 (Netherlands), PIC (Spain), ASGC (Taiwan), RAL (UK) and BNL (USA), the Tier-2 facilities worldwide and large non-WLCG resource providers. Major contributors of computing resources are listed in ref. [95].

Open Access. This article is distributed under the terms of the Creative Commons Attribution License (CC-BY 4.0), which permits any use, distribution and reproduction in any medium, provided the original author(s) and source are credited. SCOAP^3 supports the goals of the International Year of Basic Sciences for Sustainable Development.

References

[1] M. Cacciari et al., *Top-pair production at hadron colliders with next-to-next-to-leading logarithmic soft-gluon resummation*, *Phys. Lett. B* **710** (2012) 612 [arXiv:1111.5869] [INSPIRE].

[2] P. Bärnreuther, M. Czakon and A. Mitov, *Percent Level Precision Physics at the Tevatron: First Genuine NNLO QCD Corrections to $q\bar{q} \to t\bar{t} + X$*, *Phys. Rev. Lett.* **109** (2012) 132001 [arXiv:1204.5201] [INSPIRE].

[3] M. Czakon and A. Mitov, *NNLO corrections to top-pair production at hadron colliders: the all-fermionic scattering channels*, *JHEP* **12** (2012) 054 [arXiv:1207.0236] [INSPIRE].

[4] M. Czakon and A. Mitov, *NNLO corrections to top pair production at hadron colliders: the quark-gluon reaction*, *JHEP* **01** (2013) 080 [arXiv:1210.6832] [INSPIRE].

[5] M. Czakon, P. Fiedler and A. Mitov, *Total top-quark pair-production cross section at hadron colliders through $O(\alpha_s^4)$*, *Phys. Rev. Lett.* **110** (2013) 252004 [arXiv:1303.6254] [INSPIRE].

[6] S. Catani et al., *Top-quark pair hadroproduction at next-to-next-to-leading order in QCD*, *Phys. Rev. D* **99** (2019) 051501 [arXiv:1901.04005] [INSPIRE].

[7] ATLAS collaboration, *Measurement of the $t\bar{t}$ production cross-section using $e\mu$ events with b-tagged jets in pp collisions at $\sqrt{s} = 7$ and 8 TeV with the ATLAS detector*, *Eur. Phys. J. C* **74** (2014) 3109 [*Addendum ibid.* **76** (2016) 642] [arXiv:1406.5375] [INSPIRE].

[8] ATLAS collaboration, *Measurement of the inclusive and fiducial $t\bar{t}$ production cross-sections in the lepton+jets channel in pp collisions at $\sqrt{s} = 8$ TeV with the ATLAS detector*, *Eur. Phys. J. C* **78** (2018) 487 [arXiv:1712.06857] [INSPIRE].

[9] ATLAS collaboration, *Measurement of the $t\bar{t}$ production cross-section and lepton differential distributions in $e\mu$ dilepton events from pp collisions at $\sqrt{s} = 13$ TeV with the ATLAS detector*, *Eur. Phys. J. C* **80** (2020) 528 [arXiv:1910.08819] [INSPIRE].

[10] ATLAS collaboration, *Measurement of the $t\bar{t}$ production cross-section in the lepton+jets channel at $\sqrt{s} = 13$ TeV with the ATLAS experiment*, *Phys. Lett. B* **810** (2020) 135797 [arXiv:2006.13076] [INSPIRE].

[11] CMS collaboration, *Measurement of the t-tbar production cross section in the e-mu channel in proton-proton collisions at sqrt(s) = 7 and 8 TeV*, *JHEP* **08** (2016) 029 [arXiv:1603.02303] [INSPIRE].

[12] CMS collaboration, *Measurements of the $t\bar{t}$ production cross section in lepton+jets final states in pp collisions at 8 TeV and ratio of 8 to 7 TeV cross sections*, *Eur. Phys. J. C* **77** (2017) 15 [arXiv:1602.09024] [INSPIRE].

JHEP06(2023)138

[13] CMS collaboration, *Measurement of the $t\bar{t}$ production cross section using events with one lepton and at least one jet in pp collisions at $\sqrt{s} = 13$ TeV*, *JHEP* **09** (2017) 051 [arXiv:1701.06228] [INSPIRE].

[14] CMS collaboration, *Measurement of the $t\bar{t}$ production cross section, the top quark mass, and the strong coupling constant using dilepton events in pp collisions at $\sqrt{s} = 13$ TeV*, *Eur. Phys. J. C* **79** (2019) 368 [arXiv:1812.10505] [INSPIRE].

[15] LHCb collaboration, *First observation of top quark production in the forward region*, *Phys. Rev. Lett.* **115** (2015) 112001 [arXiv:1506.00903] [INSPIRE].

[16] LHCb collaboration, *Measurement of forward top pair production in the dilepton channel in pp collisions at $\sqrt{s} = 13$ TeV*, *JHEP* **08** (2018) 174 [arXiv:1803.05188] [INSPIRE].

[17] M. Czakon and A. Mitov, *Top++: a program for the calculation of the top-pair cross-section at hadron colliders*, *Comput. Phys. Commun.* **185** (2014) 2930 [arXiv:1112.5675] [INSPIRE].

[18] J. Butterworth et al., *PDF4LHC recommendations for LHC Run II*, *J. Phys. G* **43** (2016) 023001 [arXiv:1510.03865] [INSPIRE].

[19] A.D. Martin, W.J. Stirling, R.S. Thorne and G. Watt, *Parton distributions for the LHC*, *Eur. Phys. J. C* **63** (2009) 189 [arXiv:0901.0002] [INSPIRE].

[20] A.D. Martin, W.J. Stirling, R.S. Thorne and G. Watt, *Uncertainties on α_s in global PDF analyses and implications for predicted hadronic cross sections*, *Eur. Phys. J. C* **64** (2009) 653 [arXiv:0905.3531] [INSPIRE].

[21] H.-L. Lai et al., *New parton distributions for collider physics*, *Phys. Rev. D* **82** (2010) 074024 [arXiv:1007.2241] [INSPIRE].

[22] J. Gao et al., *CT10 next-to-next-to-leading order global analysis of QCD*, *Phys. Rev. D* **89** (2014) 033009 [arXiv:1302.6246] [INSPIRE].

[23] R.D. Ball et al., *Parton distributions with LHC data*, *Nucl. Phys. B* **867** (2013) 244 [arXiv:1207.1303] [INSPIRE].

[24] M. Cacciari et al., *The $t\bar{t}$ cross-section at 1.8 TeV and 1.96 TeV: a study of the systematics due to parton densities and scale dependence*, *JHEP* **04** (2004) 068 [hep-ph/0303085] [INSPIRE].

[25] S. Catani, D. de Florian, M. Grazzini and P. Nason, *Soft gluon resummation for Higgs boson production at hadron colliders*, *JHEP* **07** (2003) 028 [hep-ph/0306211] [INSPIRE].

[26] CMS collaboration, *Measurement of the inclusive $t\bar{t}$ production cross section in proton-proton collisions at $\sqrt{s} = 5.02$ TeV*, *JHEP* **04** (2022) 144 [arXiv:2112.09114] [INSPIRE].

[27] ATLAS collaboration, *The ATLAS Experiment at the CERN Large Hadron Collider*, 2008 *JINST* **3** S08003 [INSPIRE].

[28] ATLAS collaboration, *ATLAS Insertable B-Layer: Technical Design Report*, CERN-LHCC-2010-013 (2010).

[29] ATLAS IBL collaboration, *Production and integration of the ATLAS insertable B-layer*, 2018 *JINST* **13** T05008 [arXiv:1803.00844] [INSPIRE].

[30] ATLAS collaboration, *Performance of the ATLAS Trigger System in 2015*, *Eur. Phys. J. C* **77** (2017) 317 [arXiv:1611.09661] [INSPIRE].

[31] ATLAS collaboration, *The ATLAS collaboration software and firmware*, ATL-SOFT-PUB-2021-001 (2021).

JHEP06(2023)138

[32] ATLAS collaboration, *ATLAS data quality operations and performance for 2015–2018 data-taking*, 2020 *JINST* **15** P04003 [arXiv:1911.04632] [INSPIRE].

[33] ATLAS collaboration, *Performance of electron and photon triggers in ATLAS during LHC Run 2*, *Eur. Phys. J. C* **80** (2020) 47 [arXiv:1909.00761] [INSPIRE].

[34] ATLAS collaboration, *Performance of the ATLAS muon triggers in Run 2*, 2020 *JINST* **15** P09015 [arXiv:2004.13447] [INSPIRE].

[35] ATLAS collaboration, *Luminosity determination for low-pileup datasets at* $\sqrt{s} = 5$ *and* 13 *TeV using the ATLAS detector at the LHC*, ATLAS-CONF-2020-023 (2020).

[36] ATLAS collaboration, *The ATLAS Simulation Infrastructure*, *Eur. Phys. J. C* **70** (2010) 823 [arXiv:1005.4568] [INSPIRE].

[37] GEANT4 collaboration, *GEANT4 — a simulation toolkit*, *Nucl. Instrum. Meth. A* **506** (2003) 250 [INSPIRE].

[38] T. Sjöstrand, S. Mrenna and P.Z. Skands, *A brief introduction to PYTHIA 8.1*, *Comput. Phys. Commun.* **178** (2008) 852 [arXiv:0710.3820] [INSPIRE].

[39] ATLAS collaboration, *The Pythia 8 A3 tune description of ATLAS minimum bias and inelastic measurements incorporating the Donnachie–Landshoff diffractive model*, ATL-PHYS-PUB-2016-017 (2016).

[40] S. Frixione, P. Nason and G. Ridolfi, *A positive-weight next-to-leading-order Monte Carlo for heavy flavour hadroproduction*, *JHEP* **09** (2007) 126 [arXiv:0707.3088] [INSPIRE].

[41] P. Nason, *A new method for combining NLO QCD with shower Monte Carlo algorithms*, *JHEP* **11** (2004) 040 [hep-ph/0409146] [INSPIRE].

[42] S. Frixione, P. Nason and C. Oleari, *Matching NLO QCD computations with Parton Shower simulations: the POWHEG method*, *JHEP* **11** (2007) 070 [arXiv:0709.2092] [INSPIRE].

[43] S. Alioli, P. Nason, C. Oleari and E. Re, *A general framework for implementing NLO calculations in shower Monte Carlo programs: the POWHEG BOX*, *JHEP* **06** (2010) 043 [arXiv:1002.2581] [INSPIRE].

[44] NNPDF collaboration, *Parton distributions for the LHC Run II*, *JHEP* **04** (2015) 040 [arXiv:1410.8849] [INSPIRE].

[45] ATLAS collaboration, *ATLAS Pythia 8 tunes to* 7 *TeV data*, ATL-PHYS-PUB-2014-021 (2014).

[46] ATLAS collaboration, *Studies on top-quark Monte Carlo modelling for Top2016*, ATL-PHYS-PUB-2016-020 (2016).

[47] M. Bähr et al., *Herwig++ physics and manual*, *Eur. Phys. J. C* **58** (2008) 639 [arXiv:0803.0883] [INSPIRE].

[48] J. Bellm et al., *Herwig 7.0/Herwig++ 3.0 release note*, *Eur. Phys. J. C* **76** (2016) 196 [arXiv:1512.01178] [INSPIRE].

[49] J. Alwall et al., *The automated computation of tree-level and next-to-leading order differential cross sections, and their matching to parton shower simulations*, *JHEP* **07** (2014) 079 [arXiv:1405.0301] [INSPIRE].

[50] D.J. Lange, *The EvtGen particle decay simulation package*, *Nucl. Instrum. Meth. A* **462** (2001) 152 [INSPIRE].

JHEP06(2023)138

[51] R. Frederix, E. Re and P. Torrielli, *Single-top t-channel hadroproduction in the four-flavour scheme with POWHEG and aMC@NLO*, *JHEP* **09** (2012) 130 [arXiv:1207.5391] [INSPIRE].

[52] E. Re, *Single-top Wt-channel production matched with parton showers using the POWHEG method*, *Eur. Phys. J. C* **71** (2011) 1547 [arXiv:1009.2450] [INSPIRE].

[53] S. Frixione et al., *Single-top hadroproduction in association with a W boson*, *JHEP* **07** (2008) 029 [arXiv:0805.3067] [INSPIRE].

[54] LHC top working group, NLO single-top channel cross-sections, https://twiki.cern.ch/twiki/bin/view/LHCPhysics/SingleTopRefXsec.

[55] N. Kidonakis, *Two-loop soft anomalous dimensions for single top quark associated production with a W^- or H^-*, *Phys. Rev. D* **82** (2010) 054018 [arXiv:1005.4451] [INSPIRE].

[56] N. Kidonakis, *Top Quark Production*, in the proceedings of the *Helmholtz international summer school on physics of heavy quarks and hadrons*, Dubna, Russia, July 15–28 (2013) DOI:10.3204/DESY-PROC-2013-03/Kidonakis [arXiv:1311.0283] [INSPIRE].

[57] M. Aliev et al., *HATHOR: HAdronic Top and Heavy quarks crOss section calculatoR*, *Comput. Phys. Commun.* **182** (2011) 1034 [arXiv:1007.1327] [INSPIRE].

[58] C.D. White, S. Frixione, E. Laenen and F. Maltoni, *Isolating Wt production at the LHC*, *JHEP* **11** (2009) 074 [arXiv:0908.0631] [INSPIRE].

[59] SHERPA collaboration, *Event Generation with Sherpa 2.2*, *SciPost Phys.* **7** (2019) 034 [arXiv:1905.09127] [INSPIRE].

[60] C. Anastasiou, L.J. Dixon, K. Melnikov and F. Petriello, *High precision QCD at hadron colliders: Electroweak gauge boson rapidity distributions at NNLO*, *Phys. Rev. D* **69** (2004) 094008 [hep-ph/0312266] [INSPIRE].

[61] T. Gleisberg et al., *Event generation with SHERPA 1.1*, *JHEP* **02** (2009) 007 [arXiv:0811.4622] [INSPIRE].

[62] ATLAS collaboration, *Measurement of the $t\bar{t}Z$ and $t\bar{t}W$ cross sections in proton-proton collisions at $\sqrt{s} = 13$ TeV with the ATLAS detector*, *Phys. Rev. D* **99** (2019) 072009 [arXiv:1901.03584] [INSPIRE].

[63] ATLAS collaboration, *Electron and photon performance measurements with the ATLAS detector using the 2015–2017 LHC proton-proton collision data*, 2019 *JINST* **14** P12006 [arXiv:1908.00005] [INSPIRE].

[64] ATLAS collaboration, *Muon reconstruction and identification efficiency in ATLAS using the full Run 2 pp collision data set at $\sqrt{s} = 13$ TeV*, *Eur. Phys. J. C* **81** (2021) 578 [arXiv:2012.00578] [INSPIRE].

[65] M. Cacciari, G.P. Salam and G. Soyez, *The anti-k_t jet clustering algorithm*, *JHEP* **04** (2008) 063 [arXiv:0802.1189] [INSPIRE].

[66] M. Cacciari, G.P. Salam and G. Soyez, *FastJet user manual*, *Eur. Phys. J. C* **72** (2012) 1896 [arXiv:1111.6097] [INSPIRE].

[67] ATLAS collaboration, *Jet reconstruction and performance using particle flow with the ATLAS Detector*, *Eur. Phys. J. C* **77** (2017) 466 [arXiv:1703.10485] [INSPIRE].

[68] ATLAS collaboration, *Jet energy scale and resolution measured in proton–proton collisions at $\sqrt{s} = 13$ TeV with the ATLAS detector*, *Eur. Phys. J. C* **81** (2021) 689 [arXiv:2007.02645] [INSPIRE].

JHEP06(2023)138

[69] ATLAS collaboration, *Performance of pile-up mitigation techniques for jets in pp collisions at $\sqrt{s} = 8$ TeV using the ATLAS detector*, *Eur. Phys. J. C* **76** (2016) 581 [arXiv:1510.03823] [INSPIRE].

[70] ATLAS collaboration, *ATLAS b-jet identification performance and efficiency measurement with $t\bar{t}$ events in pp collisions at $\sqrt{s} = 13$ TeV*, *Eur. Phys. J. C* **79** (2019) 970 [arXiv:1907.05120] [INSPIRE].

[71] ATLAS collaboration, *Performance of missing transverse momentum reconstruction with the ATLAS detector using proton-proton collisions at $\sqrt{s} = 13$ TeV*, *Eur. Phys. J. C* **78** (2018) 903 [arXiv:1802.08168] [INSPIRE].

[72] ATLAS collaboration, *Selection of jets produced in 13 TeV proton–proton collisions with the ATLAS detector*, ATLAS-CONF-2015-029 (2015).

[73] ATLAS collaboration, *Estimation of non-prompt and fake lepton backgrounds in final states with top quarks produced in proton–proton collisions at $\sqrt{s} = 8$ TeV with the ATLAS Detector*, ATLAS-CONF-2014-058 (2014)

[74] A. Hoecker et al., *TMVA — Toolkit for Multivariate Data Analysis*, physics/0703039.

[75] G.C. Fox and S. Wolfram, *Observables for the analysis of event shapes in e^+e^- annihilation and other processes*, *Phys. Rev. Lett.* **41** (1978) 1581 [INSPIRE].

[76] ATLAS collaboration, *Measurements of inclusive and differential fiducial cross-sections of $t\bar{t}$ production with additional heavy-flavour jets in proton-proton collisions at $\sqrt{s} = 13$ TeV with the ATLAS detector*, *JHEP* **04** (2019) 046 [arXiv:1811.12113] [INSPIRE].

[77] C.F. Berger et al., *Precise Predictions for W + 4 Jet Production at the Large Hadron Collider*, *Phys. Rev. Lett.* **106** (2011) 092001 [arXiv:1009.2338] [INSPIRE].

[78] J.M. Campbell and R.K. Ellis, *MCFM for the Tevatron and the LHC*, *Nucl. Phys. B Proc. Suppl.* **205-206** (2010) 10 [arXiv:1007.3492] [INSPIRE].

[79] ATLAS collaboration, *Measurement of b-tagging efficiency of c-jets in $t\bar{t}$ events using a likelihood approach with the ATLAS detector*, ATLAS-CONF-2018-001 (2018).

[80] ATLAS collaboration, *Calibration of light-flavour b-jet mistagging rates using ATLAS proton–proton collision data at $\sqrt{s} = 13$ TeV*, ATLAS-CONF-2018-006 (2018).

[81] ATLAS collaboration, *Luminosity determination in pp collisions at $\sqrt{s} = 13$ TeV using the ATLAS detector at the LHC*, arXiv:2212.09379.

[82] G. Avoni et al., *The new LUCID-2 detector for luminosity measurement and monitoring in ATLAS*, 2018 *JINST* **13** P07017 [INSPIRE].

[83] E. Todesco and J. Wenninger, *Large Hadron Collider momentum calibration and accuracy*, *Phys. Rev. Accel. Beams* **20** (2017) 081003 [INSPIRE].

[84] J. Kieseler, *A method and tool for combining differential or inclusive measurements obtained with simultaneously constrained uncertainties*, *Eur. Phys. J. C* **77** (2017) 792 [arXiv:1706.01681] [INSPIRE].

[85] S. Dulat et al., *New parton distribution functions from a global analysis of quantum chromodynamics*, *Phys. Rev. D* **93** (2016) 033006 [arXiv:1506.07443] [INSPIRE].

[86] NNPDF collaboration, *Parton distributions from high-precision collider data*, *Eur. Phys. J. C* **77** (2017) 663 [arXiv:1706.00428] [INSPIRE].

JHEP06(2023)138

[87] M. Botje et al., *The PDF4LHC Working Group Interim Recommendations*, arXiv:1101.0538 [INSPIRE].

[88] S. Bailey et al., *Parton distributions from LHC, HERA, Tevatron and fixed target data: MSHT20 PDFs*, *Eur. Phys. J. C* **81** (2021) 341 [arXiv:2012.04684] [INSPIRE].

[89] NNPDF collaboration, *The path to proton structure at 1% accuracy*, *Eur. Phys. J. C* **82** (2022) 428 [arXiv:2109.02653] [INSPIRE].

[90] S. Alekhin, J. Blümlein, S. Moch and R. Placakyte, *Parton distribution functions, α_s, and heavy-quark masses for LHC Run II*, *Phys. Rev. D* **96** (2017) 014011 [arXiv:1701.05838] [INSPIRE].

[91] T.-J. Hou et al., *New CTEQ global analysis of quantum chromodynamics with high-precision data from the LHC*, *Phys. Rev. D* **103** (2021) 014013 [arXiv:1912.10053] [INSPIRE].

[92] ATLAS collaboration, *Determination of the parton distribution functions of the proton using diverse ATLAS data from pp collisions at $\sqrt{s} = 7$, 8 and 13 TeV*, *Eur. Phys. J. C* **82** (2022) 438 [arXiv:2112.11266] [INSPIRE].

[93] H1 and ZEUS collaborations, *Combination of measurements of inclusive deep inelastic $e^{\pm}p$ scattering cross sections and QCD analysis of HERA data*, *Eur. Phys. J. C* **75** (2015) 580 [arXiv:1506.06042] [INSPIRE].

[94] S. Alekhin et al., *HERAFitter*, *Eur. Phys. J. C* **75** (2015) 304 [arXiv:1410.4412] [INSPIRE].

[95] ATLAS collaboration, *ATLAS Computing Acknowledgements*, ATL-SOFT-PUB-2021-003 (2021).

JHEP06(2023)138

The ATLAS collaboration

G. Aad[101], B. Abbott[119], D.C. Abbott[102], K. Abeling[55], S.H. Abidi[29], A. Aboulhorma[35e], H. Abramowicz[150], H. Abreu[149], Y. Abulaiti[116], A.C. Abusleme Hoffman[136a], B.S. Acharya[68a,68b,o], B. Achkar[55], C. Adam Bourdarios[4], L. Adamczyk[84a], L. Adamek[154], S.V. Addepalli[26], J. Adelman[114], A. Adiguzel[21c], S. Adorni[56], T. Adye[133], A.A. Affolder[135], Y. Afik[36], M.N. Agaras[13], J. Agarwala[72a,72b], A. Aggarwal[99], C. Agheorghiesei[27c], J.A. Aguilar-Saavedra[129f], A. Ahmad[36], F. Ahmadov[38,w], W.S. Ahmed[103], S. Ahuja[94], X. Ai[48], G. Aielli[75a,75b], I. Aizenberg[167], M. Akbiyik[99], T.P.A. Åkesson[97], A.V. Akimov[37], K. Al Khoury[41], G.L. Alberghi[23b], J. Albert[163], P. Albicocco[53], M.J. Alconada Verzini[89], S. Alderweireldt[52], M. Aleksa[36], I.N. Aleksandrov[38], C. Alexa[27b], T. Alexopoulos[10], A. Alfonsi[113], F. Alfonsi[23b], M. Alhroob[119], B. Ali[131], S. Ali[147], M. Aliev[37], G. Alimonti[70a], W. Alkakhi[55], C. Allaire[36], B.M.M. Allbrooke[145], P.P. Allport[20], A. Aloisio[71a,71b], F. Alonso[89], C. Alpigiani[137], E. Alunno Camelia[75a,75b], M. Alvarez Estevez[98], M.G. Alviggi[71a,71b], Y. Amaral Coutinho[81b], A. Ambler[103], C. Amelung[36], C.G. Ames[108], D. Amidei[105], S.P. Amor Dos Santos[129a], S. Amoroso[48], K.R. Amos[161], C.S. Amrouche[56], V. Ananiev[124], C. Anastopoulos[138], T. Andeen[11], J.K. Anders[19], S.Y. Andrean[47a,47b], A. Andreazza[70a,70b], S. Angelidakis[9], A. Angerami[41,y], A.V. Anisenkov[37], A. Annovi[73a], C. Antel[56], M.T. Anthony[138], E. Antipov[120], M. Antonelli[53], D.J.A. Antrim[17a], F. Anulli[74a], M. Aoki[82], T. Aoki[152], J.A. Aparisi Pozo[161], M.A. Aparo[145], L. Aperio Bella[48], C. Appelt[18], N. Aranzabal[36], V. Araujo Ferraz[81a], C. Arcangeletti[53], A.T.H. Arce[51], E. Arena[91], J-F. Arguin[107], S. Argyropoulos[54], J.-H. Arling[48], A.J. Armbruster[36], O. Arnaez[154], H. Arnold[113], Z.P. Arrubarrena Tame[108], G. Artoni[74a,74b], H. Asada[110], K. Asai[117], S. Asai[152], N.A. Asbah[61], J. Assahsah[35d], K. Assamagan[29], R. Astalos[28a], R.J. Atkin[33a], M. Atkinson[160], N.B. Atlay[18], H. Atmani[62b], P.A. Atmasiddha[105], K. Augsten[131], S. Auricchio[71a,71b], A.D. Auriol[20], V.A. Austrup[169], G. Avner[149], G. Avolio[36], K. Axiotis[56], M.K. Ayoub[14c], G. Azuelos[107,aa], D. Babal[28a], H. Bachacou[134], K. Bachas[151,q], A. Bachiu[34], F. Backman[47a,47b], A. Badea[61], P. Bagnaia[74a,74b], M. Bahmani[18], A.J. Bailey[161], V.R. Bailey[160], J.T. Baines[133], C. Bakalis[10], O.K. Baker[170], P.J. Bakker[113], E. Bakos[15], D. Bakshi Gupta[8], S. Balaji[146], R. Balasubramanian[113], E.M. Baldin[37], P. Balek[132], E. Ballabene[70a,70b], F. Balli[134], L.M. Baltes[63a], W.K. Balunas[32], J. Balz[99], E. Banas[85], M. Bandieramonte[128], A. Bandyopadhyay[24], S. Bansal[24], L. Barak[150], E.L. Barberio[104], D. Barberis[57b,57a], M. Barbero[101], G. Barbour[95], K.N. Barends[33a], T. Barillari[109], M-S. Barisits[36], T. Barklow[142], R.M. Barnett[17a], P. Baron[121], D.A. Baron Moreno[100], A. Baroncelli[62a], G. Barone[29], A.J. Barr[125], L. Barranco Navarro[47a,47b], F. Barreiro[98], J. Barreiro Guimarães da Costa[14a], U. Barron[150], M.G. Barros Teixeira[129a], S. Barsov[37], F. Bartels[63a], R. Bartoldus[142], A.E. Barton[90], P. Bartos[28a], A. Basalaev[48], A. Basan[99], M. Baselga[49], I. Bashta[76a,76b], A. Bassalat[66,ag], M.J. Basso[154], C.R. Basson[100], R.L. Bates[59], S. Batlamous[35e], J.R. Batley[32], B. Batool[140], M. Battaglia[135], D. Battulga[18], M. Bauce[74a,74b], P. Bauer[24], A. Bayirli[21a],

JHEP06(2023)138

J.B. Beacham[51], T. Beau[126], P.H. Beauchemin[157], F. Becherer[54], P. Bechtle[24], H.P. Beck[19,p], K. Becker[165], C. Becot[48], A.J. Beddall[21d], V.A. Bednyakov[38], C.P. Bee[144], L.J. Beemster[15], T.A. Beermann[36], M. Begalli[81d,81d], M. Begel[29], A. Behera[144], J.K. Behr[48], C. Beirao Da Cruz E Silva[36], J.F. Beirer[55,36], F. Beisiegel[24], M. Belfkir[115b], G. Bella[150], L. Bellagamba[23b], A. Bellerive[34], P. Bellos[20], K. Beloborodov[37], K. Belotskiy[37], N.L. Belyaev[37], D. Benchekroun[35a], F. Bendebba[35a], Y. Benhammou[150], D.P. Benjamin[29], M. Benoit[29], J.R. Bensinger[26], S. Bentvelsen[113], L. Beresford[36], M. Beretta[53], D. Berge[18], E. Bergeaas Kuutmann[159], N. Berger[4], B. Bergmann[131], J. Beringer[17a], S. Berlendis[7], G. Bernardi[5], C. Bernius[142], F.U. Bernlochner[24], T. Berry[94], P. Berta[132], A. Berthold[50], I.A. Bertram[90], S. Bethke[109], A. Betti[74a,74b], A.J. Bevan[93], M. Bhamjee[33c], S. Bhatta[144], D.S. Bhattacharya[164], P. Bhattarai[26], V.S. Bhopatkar[120], R. Bi[29,ad], R.M. Bianchi[128], O. Biebel[108], R. Bielski[122], M. Biglietti[76a], T.R.V. Billoud[131], M. Bindi[55], A. Bingul[21b], C. Bini[74a,74b], S. Biondi[23b,23a], A. Biondini[91], C.J. Birch-sykes[100], G.A. Bird[20,133], M. Birman[167], T. Bisanz[36], E. Bisceglie[43b,43a], D. Biswas[168,k], A. Bitadze[100], K. Bjørke[124], I. Bloch[48], C. Blocker[26], A. Blue[59], U. Blumenschein[93], J. Blumenthal[99], G.J. Bobbink[113], V.S. Bobrovnikov[37], M. Boehler[54], D. Bogavac[36], A.G. Bogdanchikov[37], C. Bohm[47a], V. Boisvert[94], P. Bokan[48], T. Bold[84a], M. Bomben[5], M. Bona[93], M. Boonekamp[134], C.D. Booth[94], A.G. Borbély[59], H.M. Borecka-Bielska[107], L.S. Borgna[95], G. Borissov[90], D. Bortoletto[125], D. Boscherini[23b], M. Bosman[13], J.D. Bossio Sola[36], K. Bouaouda[35a], J. Boudreau[128], E.V. Bouhova-Thacker[90], D. Boumediene[40], R. Bouquet[5], A. Boveia[118], J. Boyd[36], D. Boye[29], I.R. Boyko[38], J. Bracinik[20], N. Brahimi[62d], G. Brandt[169], O. Brandt[32], F. Braren[48], B. Brau[102], J.E. Brau[122], K. Brendlinger[48], R. Brener[167], L. Brenner[36], R. Brenner[159], S. Bressler[167], B. Brickwedde[99], D. Britton[59], D. Britzger[109], I. Brock[24], G. Brooijmans[41], W.K. Brooks[136f], E. Brost[29], T.L. Bruckler[125], P.A. Bruckman de Renstrom[85], B. Brüers[48], D. Bruncko[28b,*], A. Bruni[23b], G. Bruni[23b], M. Bruschi[23b], N. Bruscino[74a,74b], L. Bryngemark[142], T. Buanes[16], Q. Buat[137], P. Buchholz[140], A.G. Buckley[59], I.A. Budagov[38,*], M.K. Bugge[124], O. Bulekov[37], B.A. Bullard[61], S. Burdin[91], C.D. Burgard[48], A.M. Burger[40], B. Burghgrave[8], J.T.P. Burr[32], C.D. Burton[11], J.C. Burzynski[141], E.L. Busch[41], V. Büscher[99], P.J. Bussey[59], J.M. Butler[25], C.M. Buttar[59], J.M. Butterworth[95], W. Buttinger[133], C.J. Buxo Vazquez[106], A.R. Buzykaev[37], G. Cabras[23b], S. Cabrera Urbán[161], D. Caforio[58], H. Cai[128], Y. Cai[14a,14d], V.M.M. Cairo[36], O. Cakir[3a], N. Calace[36], P. Calafiura[17a], G. Calderini[126], P. Calfayan[67], G. Callea[59], L.P. Caloba[81b], D. Calvet[40], S. Calvet[40], T.P. Calvet[101], M. Calvetti[73a,73b], R. Camacho Toro[126], S. Camarda[36], D. Camarero Munoz[26], P. Camarri[75a,75b], M.T. Camerlingo[76a,76b], D. Cameron[124], C. Camincher[163], M. Campanelli[95], A. Camplani[42], V. Canale[71a,71b], A. Canesse[103], M. Cano Bret[79], J. Cantero[161], Y. Cao[160], F. Capocasa[26], M. Capua[43b,43a], A. Carbone[70a,70b], R. Cardarelli[75a], J.C.J. Cardenas[8], F. Cardillo[161], T. Carli[36], G. Carlino[71a], B.T. Carlson[128,r], E.M. Carlson[163,155a], L. Carminati[70a,70b], M. Carnesale[74a,74b], S. Caron[112], E. Carquin[136f], S. Carrá[70a,70b], G. Carratta[23b,23a], F. Carrio Argos[33g], J.W.S. Carter[154], T.M. Carter[52], M.P. Casado[13,h], A.F. Casha[154],

JHEP06(2023)138

E.G. Castiglia[170], F.L. Castillo[63a], L. Castillo Garcia[13], V. Castillo Gimenez[161], N.F. Castro[129a,129e], A. Catinaccio[36], J.R. Catmore[124], V. Cavaliere[29], N. Cavalli[23b,23a], V. Cavasinni[73a,73b], E. Celebi[21a], F. Celli[125], M.S. Centonze[69a,69b], K. Cerny[121], A.S. Cerqueira[81a], A. Cerri[145], L. Cerrito[75a,75b], F. Cerutti[17a], A. Cervelli[23b], S.A. Cetin[21d], Z. Chadi[35a], D. Chakraborty[114], M. Chala[129f], J. Chan[168], W.Y. Chan[152], J.D. Chapman[32], B. Chargeishvili[148b], D.G. Charlton[20], T.P. Charman[93], M. Chatterjee[19], S. Chekanov[6], S.V. Chekulaev[155a], G.A. Chelkov[38,a], A. Chen[105], B. Chen[150], B. Chen[163], C. Chen[62a], H. Chen[14c], H. Chen[29], J. Chen[62c], J. Chen[26], S. Chen[152], S.J. Chen[14c], X. Chen[62c], X. Chen[14b,z], Y. Chen[62a], C.L. Cheng[168], H.C. Cheng[64a], A. Cheplakov[38], E. Cheremushkina[48], E. Cherepanova[113], R. Cherkaoui El Moursli[35e], E. Cheu[7], K. Cheung[65], L. Chevalier[134], V. Chiarella[53], G. Chiarelli[73a], N. Chiedde[101], G. Chiodini[69a], A.S. Chisholm[20], A. Chitan[27b], M. Chitishvili[161], Y.H. Chiu[163], M.V. Chizhov[38], K. Choi[11], A.R. Chomont[74a,74b], Y. Chou[102], E.Y.S. Chow[113], T. Chowdhury[33g], L.D. Christopher[33g], K.L. Chu[64a], M.C. Chu[64a], X. Chu[14a,14d], J. Chudoba[130], J.J. Chwastowski[85], D. Cieri[109], K.M. Ciesla[84a], V. Cindro[92], A. Ciocio[17a], F. Cirotto[71a,71b], Z.H. Citron[167,l], M. Citterio[70a], D.A. Ciubotaru[27b], B.M. Ciungu[154], A. Clark[56], P.J. Clark[52], J.M. Clavijo Columbie[48], S.E. Clawson[100], C. Clement[47a,47b], J. Clercx[48], L. Clissa[23b,23a], Y. Coadou[101], M. Cobal[68a,68c], A. Coccaro[57b], R.F. Coelho Barrue[129a], R. Coelho Lopes De Sa[102], S. Coelli[70a], H. Cohen[150], A.E.C. Coimbra[70a,70b], B. Cole[41], J. Collot[60], P. Conde Muiño[129a,129g], M.P. Connell[33c], S.H. Connell[33c], I.A. Connelly[59], E.I. Conroy[125], F. Conventi[71a,ab], H.G. Cooke[20], A.M. Cooper-Sarkar[125], F. Cormier[162], L.D. Corpe[36], M. Corradi[74a,74b], E.E. Corrigan[97], F. Corriveau[103,v], A. Cortes-Gonzalez[18], M.J. Costa[161], F. Costanza[4], D. Costanzo[138], B.M. Cote[118], G. Cowan[94], J.W. Cowley[32], K. Cranmer[116], S. Crépé-Renaudin[60], F. Crescioli[126], M. Cristinziani[140], M. Cristoforetti[77a,77b,c], V. Croft[157], G. Crosetti[43b,43a], A. Cueto[36], T. Cuhadar Donszelmann[158], H. Cui[14a,14d], Z. Cui[7], A.R. Cukierman[142], W.R. Cunningham[59], F. Curcio[43b,43a], P. Czodrowski[36], M.M. Czurylo[63b], M.J. Da Cunha Sargedas De Sousa[62a], J.V. Da Fonseca Pinto[81b], C. Da Via[100], W. Dabrowski[84a], T. Dado[49], S. Dahbi[33g], T. Dai[105], C. Dallapiccola[102], M. Dam[42], G. D'amen[29], V. D'Amico[108], J. Damp[99], J.R. Dandoy[127], M.F. Daneri[30], M. Danninger[141], V. Dao[36], G. Darbo[57b], S. Darmora[6], S.J. Das[29], S. D'Auria[70a,70b], C. David[155b], T. Davidek[132], D.R. Davis[51], B. Davis-Purcell[34], I. Dawson[93], K. De[8], R. De Asmundis[71a], M. De Beurs[113], N. De Biase[48], S. De Castro[23b,23a], N. De Groot[112], P. de Jong[113], H. De la Torre[106], A. De Maria[14c], A. De Salvo[74a], U. De Sanctis[75a,75b], A. De Santo[145], J.B. De Vivie De Regie[60], D.V. Dedovich[38], J. Degens[113], A.M. Deiana[44], F. Del Corso[23b,23a], J. Del Peso[98], F. Del Rio[63a], F. Deliot[134], C.M. Delitzsch[49], M. Della Pietra[71a,71b], D. Della Volpe[56], A. Dell'Acqua[36], L. Dell'Asta[70a,70b], M. Delmastro[4], P.A. Delsart[60], S. Demers[170], M. Demichev[38], S.P. Denisov[37], L. D'Eramo[114], D. Derendarz[85], F. Derue[126], P. Dervan[91], K. Desch[24], K. Dette[154], C. Deutsch[24], P.O. Deviveiros[36], F.A. Di Bello[74a,74b], A. Di Ciaccio[75a,75b], L. Di Ciaccio[4], A. Di Domenico[74a,74b], C. Di Donato[71a,71b], A. Di Girolamo[36],

JHEP06(2023)138

G. Di Gregorio[73a,73b], A. Di Luca[77a,77b], B. Di Micco[76a,76b], R. Di Nardo[76a,76b], C. Diaconu[101], F.A. Dias[113], T. Dias Do Vale[141], M.A. Diaz[136a,136b], F.G. Diaz Capriles[24], M. Didenko[161], E.B. Diehl[105], L. Diehl[54], S. Díez Cornell[48], C. Diez Pardos[140], C. Dimitriadi[24,159], A. Dimitrievska[17a], W. Ding[14b], J. Dingfelder[24], I-M. Dinu[27b], S.J. Dittmeier[63b], F. Dittus[36], F. Djama[101], T. Djobava[148b], J.I. Djuvsland[16], C. Doglioni[100,97], J. Dolejsi[132], Z. Dolezal[132], M. Donadelli[81c], B. Dong[62c], J. Donini[40], A. D'Onofrio[14c], M. D'Onofrio[91], J. Dopke[133], A. Doria[71a], M.T. Dova[89], A.T. Doyle[59], M.A. Draguet[125], E. Drechsler[141], E. Dreyer[167], I. Drivas-koulouris[10], A.S. Drobac[157], M. Drozdova[56], D. Du[62a], T.A. du Pree[113], F. Dubinin[37], M. Dubovsky[28a], E. Duchovni[167], G. Duckeck[108], O.A. Ducu[27b], D. Duda[109], A. Dudarev[36], M. D'uffizi[100], L. Duflot[66], M. Dührssen[36], C. Dülsen[169], A.E. Dumitriu[27b], M. Dunford[63a], S. Dungs[49], K. Dunne[47a,47b], A. Duperrin[101], H. Duran Yildiz[3a], M. Düren[58], A. Durglishvili[148b], B.L. Dwyer[114], G.I. Dyckes[17a], M. Dyndal[84a], S. Dysch[100], B.S. Dziedzic[85], Z.O. Earnshaw[145], B. Eckerova[28a], M.G. Eggleston[51], E. Egidio Purcino De Souza[81b], L.F. Ehrke[56], G. Eigen[16], K. Einsweiler[17a], T. Ekelof[159], P.A. Ekman[97], Y. El Ghazali[35b], H. El Jarrari[35e,147], A. El Moussaouy[35a], V. Ellajosyula[159], M. Ellert[159], F. Ellinghaus[169], A.A. Elliot[93], N. Ellis[36], J. Elmsheuser[29], M. Elsing[36], D. Emeliyanov[133], A. Emerman[41], Y. Enari[152], I. Ene[17a], S. Epari[13], J. Erdmann[49], A. Ereditato[19], P.A. Erland[85], M. Errenst[169], M. Escalier[66], C. Escobar[161], E. Etzion[150], G. Evans[129a], H. Evans[67], M.O. Evans[145], A. Ezhilov[37], S. Ezzarqtouni[35a], F. Fabbri[59], L. Fabbri[23b,23a], G. Facini[95], V. Fadeyev[135], R.M. Fakhrutdinov[37], S. Falciano[74a], P.J. Falke[24], S. Falke[36], J. Faltova[132], Y. Fan[14a], Y. Fang[14a,14d], G. Fanourakis[46], M. Fanti[70a,70b], M. Faraj[68a,68b], A. Farbin[8], A. Farilla[76a], T. Farooque[106], S.M. Farrington[52], F. Fassi[35e], D. Fassouliotis[9], M. Faucci Giannelli[75a,75b], W.J. Fawcett[32], L. Fayard[66], P. Federicova[130], O.L. Fedin[37,a], G. Fedotov[37], M. Feickert[160], L. Feligioni[101], A. Fell[138], D.E. Fellers[122], C. Feng[62b], M. Feng[14b], Z. Feng[113], M.J. Fenton[158], A.B. Fenyuk[37], L. Ferencz[48], S.W. Ferguson[45], J.A. Pretel[54], J. Ferrando[48], A. Ferrari[159], P. Ferrari[113], R. Ferrari[72a], D. Ferrere[56], C. Ferretti[105], F. Fiedler[99], A. Filipčič[92], E.K. Filmer[1], F. Filthaut[112], M.C.N. Fiolhais[129a,129c,b], L. Fiorini[161], F. Fischer[140], W.C. Fisher[106], T. Fitschen[20], I. Fleck[140], P. Fleischmann[105], T. Flick[169], L. Flores[127], M. Flores[33d], L.R. Flores Castillo[64a], F.M. Follega[77a,77b], N. Fomin[16], J.H. Foo[154], B.C. Forland[67], A. Formica[134], A.C. Forti[100], E. Fortin[101], A.W. Fortman[61], M.G. Foti[17a], L. Fountas[9], D. Fournier[66], H. Fox[90], P. Francavilla[73a,73b], S. Francescato[61], M. Franchini[23b,23a], S. Franchino[63a], D. Francis[36], L. Franco[112], L. Franconi[19], M. Franklin[61], G. Frattari[26], A.C. Freegard[93], P.M. Freeman[20], W.S. Freund[81b], N. Fritzsche[50], A. Froch[54], D. Froidevaux[36], J.A. Frost[125], Y. Fu[62a], M. Fujimoto[117], E. Fullana Torregrosa[161,*], J. Fuster[161], A. Gabrielli[23b,23a], A. Gabrielli[154], P. Gadow[48], G. Gagliardi[57b,57a], L.G. Gagnon[17a], G.E. Gallardo[125], E.J. Gallas[125], B.J. Gallop[133], R. Gamboa Goni[93], K.K. Gan[118], S. Ganguly[152], J. Gao[62a], Y. Gao[52], F.M. Garay Walls[136a,136b], B. Garcia[29,ad], C. García[161], J.E. García Navarro[161], J.A. García Pascual[14a], M. Garcia-Sciveres[17a], R.W. Gardner[39], D. Garg[79], R.B. Garg[142], S. Gargiulo[54], C.A. Garner[154],

JHEP06(2023)138

V. Garonne[29], S.J. Gasiorowski[137], P. Gaspar[81b], G. Gaudio[72a], V. Gautam[13], P. Gauzzi[74a,74b], I.L. Gavrilenko[37], A. Gavrilyuk[37], C. Gay[162], G. Gaycken[48], E.N. Gazis[10], A.A. Geanta[27b,27e], C.M. Gee[135], J. Geisen[97], M. Geisen[99], C. Gemme[57b], M.H. Genest[60], S. Gentile[74a,74b], S. George[94], W.F. George[20], T. Geralis[46], L.O. Gerlach[55], P. Gessinger-Befurt[36], M. Ghasemi Bostanabad[163], M. Ghneimat[140], A. Ghosal[140], A. Ghosh[158], A. Ghosh[7], B. Giacobbe[23b], S. Giagu[74a,74b], N. Giangiacomi[154], P. Giannetti[73a], A. Giannini[62a], S.M. Gibson[94], M. Gignac[135], D.T. Gil[84b], A.K. Gilbert[84a], B.J. Gilbert[41], D. Gillberg[34], G. Gilles[113], N.E.K. Gillwald[48], L. Ginabat[126], D.M. Gingrich[2,aa], M.P. Giordani[68a,68c], P.F. Giraud[134], G. Giugliarelli[68a,68c], D. Giugni[70a], F. Giuli[36], I. Gkialas[9,i], L.K. Gladilin[37], C. Glasman[98], G.R. Gledhill[122], M. Glisic[122], I. Gnesi[43b,e], Y. Go[29,ad], M. Goblirsch-Kolb[26], D. Godin[107], S. Goldfarb[104], T. Golling[56], M.G.D. Gololo[33g], D. Golubkov[37], J.P. Gombas[106], A. Gomes[129a,129b], G. Gomes Da Silva[140], A.J. Gomez Delegido[161], R. Goncalves Gama[55], R. Gonçalo[129a,129c], G. Gonella[122], L. Gonella[20], A. Gongadze[38], F. Gonnella[20], J.L. Gonski[41], S. González de la Hoz[161], S. Gonzalez Fernandez[13], R. Gonzalez Lopez[91], C. Gonzalez Renteria[17a], R. Gonzalez Suarez[159], S. Gonzalez-Sevilla[56], G.R. Gonzalvo Rodriguez[161], R.Y. González Andana[52], L. Goossens[36], N.A. Gorasia[20], P.A. Gorbounov[37], B. Gorini[36], E. Gorini[69a,69b], A. Gorišek[92], A.T. Goshaw[51], M.I. Gostkin[38], C.A. Gottardo[36], M. Gouighri[35b], V. Goumarre[48], A.G. Goussiou[137], N. Govender[33c], C. Goy[4], I. Grabowska-Bold[84a], K. Graham[34], E. Gramstad[124], S. Grancagnolo[18], M. Grandi[145], V. Gratchev[37,*], P.M. Gravila[27f], F.G. Gravili[69a,69b], H.M. Gray[17a], M. Greco[69a,69b], C. Grefe[24], I.M. Gregor[48], P. Grenier[142], C. Grieco[13], A.A. Grillo[135], K. Grimm[31,m], S. Grinstein[13,t], J.-F. Grivaz[66], E. Gross[167], J. Grosse-Knetter[55], C. Grud[105], A. Grummer[111], J.C. Grundy[125], L. Guan[105], W. Guan[168], C. Gubbels[162], J.G.R. Guerrero Rojas[161], G. Guerrieri[68a,68b], F. Guescini[109], R. Gugel[99], J.A.M. Guhit[105], A. Guida[48], T. Guillemin[4], E. Guilloton[165,133], S. Guindon[36], F. Guo[14a,14d], J. Guo[62c], L. Guo[66], Y. Guo[105], R. Gupta[48], S. Gurbuz[24], S.S. Gurdasani[54], G. Gustavino[36], M. Guth[56], P. Gutierrez[119], L.F. Gutierrez Zagazeta[127], C. Gutschow[95], C. Guyot[134], C. Gwenlan[125], C.B. Gwilliam[91], E.S. Haaland[124], A. Haas[116], M. Habedank[48], C. Haber[17a], H.K. Hadavand[8], A. Hadef[99], S. Hadzic[109], M. Haleem[164], J. Haley[120], J.J. Hall[138], G.D. Hallewell[101], L. Halser[19], K. Hamano[163], H. Hamdaoui[35e], M. Hamer[24], G.N. Hamity[52], J. Han[62b], K. Han[62a], L. Han[14c], L. Han[62a], S. Han[17a], Y.F. Han[154], K. Hanagaki[82], M. Hance[135], D.A. Hangal[41,y], H. Hanif[141], M.D. Hank[39], R. Hankache[100], J.B. Hansen[42], J.D. Hansen[42], P.H. Hansen[42], K. Hara[156], D. Harada[56], T. Harenberg[169], S. Harkusha[37], Y.T. Harris[125], N.M. Harrison[118], P.F. Harrison[165], N.M. Hartman[142], N.M. Hartmann[108], Y. Hasegawa[139], A. Hasib[52], S. Haug[19], R. Hauser[106], M. Havranek[131], C.M. Hawkes[20], R.J. Hawkings[36], S. Hayashida[110], D. Hayden[106], C. Hayes[105], R.L. Hayes[162], C.P. Hays[125], J.M. Hays[93], H.S. Hayward[91], F. He[62a], Y. He[153], Y. He[126], M.P. Heath[52], V. Hedberg[97], A.L. Heggelund[124], N.D. Hehir[93], C. Heidegger[54], K.K. Heidegger[54], W.D. Heidorn[80], J. Heilman[34], S. Heim[48],

JHEP06(2023)138

T. Heim[17a], J.G. Heinlein[127], J.J. Heinrich[122], L. Heinrich[109], J. Hejbal[130], L. Helary[48], A. Held[168], S. Hellesund[124], C.M. Helling[162], S. Hellman[47a,47b], C. Helsens[36], R.C.W. Henderson[90], L. Henkelmann[32], A.M. Henriques Correia[36], H. Herde[142], Y. Hernández Jiménez[144], M.G. Herrmann[108], T. Herrmann[50], G. Herten[54], R. Hertenberger[108], L. Hervas[36], N.P. Hessey[155a], H. Hibi[83], E. Higón-Rodriguez[161], S.J. Hillier[20], I. Hinchliffe[17a], F. Hinterkeuser[24], M. Hirose[123], S. Hirose[156], D. Hirschbuehl[169], T.G. Hitchings[100], B. Hiti[92], J. Hobbs[144], R. Hobincu[27e], N. Hod[167], M.C. Hodgkinson[138], B.H. Hodkinson[32], A. Hoecker[36], J. Hofer[48], D. Hohn[54], T. Holm[24], M. Holzbock[109], L.B.A.H. Hommels[32], B.P. Honan[100], J. Hong[62c], T.M. Hong[128], Y. Hong[55], J.C. Honig[54], A. Hönle[109], B.H. Hooberman[160], W.H. Hopkins[6], Y. Horii[110], S. Hou[147], A.S. Howard[92], J. Howarth[59], J. Hoya[6], M. Hrabovsky[121], A. Hrynevich[37], T. Hryn'ova[4], P.J. Hsu[65], S.-C. Hsu[137], Q. Hu[41,y], Y.F. Hu[14a,14d,ac], D.P. Huang[95], S. Huang[64b], X. Huang[14c], Y. Huang[62a], Y. Huang[14a], Z. Huang[100], Z. Hubacek[131], M. Huebner[24], F. Huegging[24], T.B. Huffman[125], M. Huhtinen[36], S.K. Huiberts[16], R. Hulsken[103], N. Huseynov[12,a], J. Huston[106], J. Huth[61], R. Hyneman[142], S. Hyrych[28a], G. Iacobucci[56], G. Iakovidis[29], I. Ibragimov[140], L. Iconomidou-Fayard[66], P. Iengo[71a,71b], R. Iguchi[152], T. Iizawa[56], Y. Ikegami[82], A. Ilg[19], N. Ilic[154], H. Imam[35a], T. Ingebretsen Carlson[47a,47b], G. Introzzi[72a,72b], M. Iodice[76a], V. Ippolito[74a,74b], M. Ishino[152], W. Islam[168], C. Issever[18,48], S. Istin[21a,af], H. Ito[166], J.M. Iturbe Ponce[64a], R. Iuppa[77a,77b], A. Ivina[167], J.M. Izen[45], V. Izzo[71a], P. Jacka[130,131], P. Jackson[1], R.M. Jacobs[48], B.P. Jaeger[141], C.S. Jagfeld[108], G. Jäkel[169], K. Jakobs[54], T. Jakoubek[167], J. Jamieson[59], K.W. Janas[84a], G. Jarlskog[97], A.E. Jaspan[91], M. Javurkova[102], F. Jeanneau[134], L. Jeanty[122], J. Jejelava[148a,x], P. Jenni[54,f], C.E. Jessiman[34], S. Jézéquel[4], J. Jia[144], X. Jia[61], X. Jia[14a,14d], Z. Jia[14c], Y. Jiang[62a], S. Jiggins[52], J. Jimenez Pena[109], S. Jin[14c], A. Jinaru[27b], O. Jinnouchi[153], P. Johansson[138], K.A. Johns[7], D.M. Jones[32], E. Jones[165], P. Jones[32], R.W.L. Jones[90], T.J. Jones[91], R. Joshi[118], J. Jovicevic[15], X. Ju[17a], J.J. Junggeburth[36], A. Juste Rozas[13,t], S. Kabana[136e], A. Kaczmarska[85], M. Kado[74a,74b], H. Kagan[118], M. Kagan[142], A. Kahn[41], A. Kahn[127], C. Kahra[99], T. Kaji[166], E. Kajomovitz[149], N. Kakati[167], C.W. Kalderon[29], A. Kamenshchikov[154], S. Kanayama[153], N.J. Kang[135], Y. Kano[110], D. Kar[33g], K. Karava[125], M.J. Kareem[155b], E. Karentzos[54], I. Karkanias[151], S.N. Karpov[38], Z.M. Karpova[38], V. Kartvelishvili[90], A.N. Karyukhin[37], E. Kasimi[151], C. Kato[62d], J. Katzy[48], S. Kaur[34], K. Kawade[139], K. Kawagoe[88], T. Kawamoto[134], G. Kawamura[55], E.F. Kay[163], F.I. Kaya[157], S. Kazakos[13], V.F. Kazanin[37], Y. Ke[144], J.M. Keaveney[33a], R. Keeler[163], G.V. Kehris[61], J.S. Keller[34], A.S. Kelly[95], D. Kelsey[145], J.J. Kempster[20], K.E. Kennedy[41], O. Kepka[130], B.P. Kerridge[165], S. Kersten[169], B.P. Kerševan[92], S. Keshri[66], L. Keszeghova[28a], S. Ketabchi Haghighat[154], M. Khandoga[126], A. Khanov[120], A.G. Kharlamov[37], T. Kharlamova[37], E.E. Khoda[137], T.J. Khoo[18], G. Khoriauli[164], J. Khubua[148b], Y.A.R. Khwaira[66], M. Kiehn[36], A. Kilgallon[122], D.W. Kim[47a,47b], E. Kim[153], Y.K. Kim[39], N. Kimura[95], A. Kirchhoff[55], D. Kirchmeier[50], C. Kirfel[24], J. Kirk[133],

JHEP06(2023)138

A.E. Kiryunin[109], T. Kishimoto[152], D.P. Kisliuk[154], C. Kitsaki[10], O. Kivernyk[24], M. Klassen[63a], C. Klein[34], L. Klein[164], M.H. Klein[105], M. Klein[91], S.B. Klein[56], U. Klein[91], P. Klimek[36], A. Klimentov[29], F. Klimpel[109], T. Klingl[24], T. Klioutchnikova[36], F.F. Klitzner[108], P. Kluit[113], S. Kluth[109], E. Kneringer[78], T.M. Knight[154], A. Knue[54], D. Kobayashi[88], R. Kobayashi[86], M. Kocian[142], P. Kodyš[132], D.M. Koeck[145], P.T. Koenig[24], T. Koffas[34], N.M. Köhler[36], M. Kolb[134], I. Koletsou[4], T. Komarek[121], K. Köneke[54], A.X.Y. Kong[1], T. Kono[117], N. Konstantinidis[95], B. Konya[97], R. Kopeliansky[67], S. Koperny[84a], K. Korcyl[85], K. Kordas[151], G. Koren[150], A. Korn[95], S. Korn[55], I. Korolkov[13], N. Korotkova[37], B. Kortman[113], O. Kortner[109], S. Kortner[109], W.H. Kostecka[114], V.V. Kostyukhin[140], A. Kotsokechagia[134], A. Kotwal[51], A. Koulouris[36], A. Kourkoumeli-Charalampidi[72a,72b], C. Kourkoumelis[9], E. Kourlitis[6], O. Kovanda[145], R. Kowalewski[163], W. Kozanecki[134], A.S. Kozhin[37], V.A. Kramarenko[37], G. Kramberger[92], P. Kramer[99], M.W. Krasny[126], A. Krasznahorkay[36], J.A. Kremer[99], T. Kresse[50], J. Kretzschmar[91], K. Kreul[18], P. Krieger[154], F. Krieter[108], S. Krishnamurthy[102], A. Krishnan[63b], M. Krivos[132], K. Krizka[17a], K. Kroeninger[49], H. Kroha[109], J. Kroll[130], J. Kroll[127], K.S. Krowpman[106], U. Kruchonak[38], H. Krüger[24], N. Krumnack[80], M.C. Kruse[51], J.A. Krzysiak[85], A. Kubota[153], O. Kuchinskaia[37], S. Kuday[3a], D. Kuechler[48], J.T. Kuechler[48], S. Kuehn[36], T. Kuhl[48], V. Kukhtin[38], Y. Kulchitsky[37,a], S. Kuleshov[136d,136b], M. Kumar[33g], N. Kumari[101], M. Kuna[60], A. Kupco[130], T. Kupfer[49], A. Kupich[37], O. Kuprash[54], H. Kurashige[83], L.L. Kurchaninov[155a], Y.A. Kurochkin[37], A. Kurova[37], E.S. Kuwertz[36], M. Kuze[153], A.K. Kvam[102], J. Kvita[121], T. Kwan[103], K.W. Kwok[64a], N.G. Kyriacou[105], L.A.O. Laatu[101], C. Lacasta[161], F. Lacava[74a,74b], H. Lacker[18], D. Lacour[126], N.N. Lad[95], E. Ladygin[38], B. Laforge[126], T. Lagouri[136e], S. Lai[55], I.K. Lakomiec[84a], N. Lalloue[60], J.E. Lambert[119], S. Lammers[67], W. Lampl[7], C. Lampoudis[151], A.N. Lancaster[114], E. Lançon[29], U. Landgraf[54], M.P.J. Landon[93], V.S. Lang[54], R.J. Langenberg[102], A.J. Lankford[158], F. Lanni[36], K. Lantzsch[24], A. Lanza[72a], A. Lapertosa[57b,57a], J.F. Laporte[134], T. Lari[70a], F. Lasagni Manghi[23b], M. Lassnig[36], V. Latonova[130], T.S. Lau[64a], A. Laudrain[99], A. Laurier[34], S.D. Lawlor[94], Z. Lawrence[100], M. Lazzaroni[70a,70b], B. Le[100], B. Leban[92], A. Lebedev[80], M. LeBlanc[36], T. LeCompte[6], F. Ledroit-Guillon[60], A.C.A. Lee[95], G.R. Lee[16], L. Lee[61], S.C. Lee[147], S. Lee[47a,47b], T.F. Lee[91], L.L. Leeuw[33c], H.P. Lefebvre[94], M. Lefebvre[163], C. Leggett[17a], K. Lehmann[141], G. Lehmann Miotto[36], M. Leigh[56], W.A. Leight[102], A. Leisos[151,s], M.A.L. Leite[81c], C.E. Leitgeb[48], R. Leitner[132], K.J.C. Leney[44], T. Lenz[24], S. Leone[73a], C. Leonidopoulos[52], A. Leopold[143], C. Leroy[107], R. Les[106], C.G. Lester[32], M. Levchenko[37], J. Levêque[4], D. Levin[105], L.J. Levinson[167], M.P. Lewicki[85], D.J. Lewis[20], B. Li[14b], B. Li[62b], C. Li[62a], C-Q. Li[62c,62d], H. Li[62a], H. Li[62b], H. Li[14c], H. Li[62b], J. Li[62c], K. Li[137], L. Li[62c], M. Li[14a,14d], Q.Y. Li[62a], S. Li[62d,62c,d], T. Li[62b], X. Li[103], Z. Li[62b], Z. Li[125], Z. Li[103], Z. Li[91], Z. Liang[14a], M. Liberatore[48], B. Liberti[75a], K. Lie[64c], J. Lieber Marin[81b], K. Lin[106], R.A. Linck[67], R.E. Lindley[7], J.H. Lindon[2], A. Linss[48], E. Lipeles[127], A. Lipniacka[16], A. Lister[162], J.D. Little[4], B. Liu[14a], B.X. Liu[141], D. Liu[62d,62c], J.B. Liu[62a],

JHEP06(2023)138

J.K.K. Liu[32], K. Liu[62d,62c], M. Liu[62a], M.Y. Liu[62a], P. Liu[14a], Q. Liu[62d,137,62c], X. Liu[62a], Y. Liu[48], Y. Liu[14c,14d], Y.L. Liu[105], Y.W. Liu[62a], M. Livan[72a,72b], J. Llorente Merino[141], S.L. Lloyd[93], E.M. Lobodzinska[48], P. Loch[7], S. Loffredo[75a,75b], T. Lohse[18], K. Lohwasser[138], M. Lokajicek[130], J.D. Long[160], I. Longarini[74a,74b], L. Longo[69a,69b], R. Longo[160], I. Lopez Paz[36], A. Lopez Solis[48], J. Lorenz[108], N. Lorenzo Martinez[4], A.M. Lory[108], A. Lösle[54], X. Lou[47a,47b], X. Lou[14a,14d], A. Lounis[66], J. Love[6], P.A. Love[90], J.J. Lozano Bahilo[161], G. Lu[14a,14d], M. Lu[79], S. Lu[127], Y.J. Lu[65], H.J. Lubatti[137], C. Luci[74a,74b], F.L. Lucio Alves[14c], A. Lucotte[60], F. Luehring[67], I. Luise[144], O. Lukianchuk[66], O. Lundberg[143], B. Lund-Jensen[143], N.A. Luongo[122], M.S. Lutz[150], D. Lynn[29], H. Lyons[91], R. Lysak[130], E. Lytken[97], F. Lyu[14a], V. Lyubushkin[38], T. Lyubushkina[38], H. Ma[29], L.L. Ma[62b], Y. Ma[95], D.M. Mac Donell[163], G. Maccarrone[53], J.C. MacDonald[138], R. Madar[40], W.F. Mader[50], J. Maeda[83], T. Maeno[29], M. Maerker[50], V. Magerl[54], J. Magro[68a,68c], H. Maguire[138], D.J. Mahon[41], C. Maidantchik[81b], A. Maio[129a,129b,129d], K. Maj[84a], O. Majersky[28a], S. Majewski[122], N. Makovec[66], V. Maksimovic[15], B. Malaescu[126], Pa. Malecki[85], V.P. Maleev[37], F. Malek[60], D. Malito[43b,43a], U. Mallik[79], C. Malone[32], S. Maltezos[10], S. Malyukov[38], J. Mamuzic[13], G. Mancini[53], G. Manco[72a,72b], J.P. Mandalia[93], I. Mandić[92], L. Manhaes de Andrade Filho[81a], I.M. Maniatis[151], M. Manisha[134], J. Manjarres Ramos[50], D.C. Mankad[167], A. Mann[108], B. Mansoulie[134], S. Manzoni[36], A. Marantis[151], G. Marchiori[5], M. Marcisovsky[130], L. Marcoccia[75a,75b], C. Marcon[70a,70b], M. Marinescu[20], M. Marjanovic[119], Z. Marshall[17a], S. Marti-Garcia[161], T.A. Martin[165], V.J. Martin[52], B. Martin dit Latour[16], L. Martinelli[74a,74b], M. Martinez[13,t], P. Martinez Agullo[161], V.I. Martinez Outschoorn[102], P. Martinez Suarez[13], S. Martin-Haugh[133], V.S. Martoiu[27b], A.C. Martyniuk[95], A. Marzin[36], S.R. Maschek[109], L. Masetti[99], T. Mashimo[152], J. Masik[100], A.L. Maslennikov[37], L. Massa[23b], P. Massarotti[71a,71b], P. Mastrandrea[73a,73b], A. Mastroberardino[43b,43a], T. Masubuchi[152], T. Mathisen[159], N. Matsuzawa[152], J. Maurer[27b], B. Maček[92], D.A. Maximov[37], R. Mazini[147], I. Maznas[151], M. Mazza[106], S.M. Mazza[135], C. Mc Ginn[29,ad], J.P. Mc Gowan[103], S.P. Mc Kee[105], T.G. McCarthy[109], W.P. McCormack[17a], E.F. McDonald[104], A.E. McDougall[113], J.A. Mcfayden[145], G. Mchedlidze[148b], R.P. Mckenzie[33g], T.C. Mclachlan[48], D.J. Mclaughlin[95], K.D. McLean[163], S.J. McMahon[133], P.C. McNamara[104], C.M. Mcpartland[91], R.A. McPherson[163,v], T. Megy[40], S. Mehlhase[108], A. Mehta[91], B. Meirose[45], D. Melini[149], B.R. Mellado Garcia[33g], A.H. Melo[55], F. Meloni[48], E.D. Mendes Gouveia[129a], A.M. Mendes Jacques Da Costa[20], H.Y. Meng[154], L. Meng[90], S. Menke[109], M. Mentink[36], E. Meoni[43b,43a], C. Merlassino[125], L. Merola[71a,71b], C. Meroni[70a], G. Merz[105], O. Meshkov[37], J.K.R. Meshreki[140], J. Metcalfe[6], A.S. Mete[6], C. Meyer[67], J-P. Meyer[134], M. Michetti[18], R.P. Middleton[133], L. Mijović[52], G. Mikenberg[167], M. Mikestikova[130], M. Mikuž[92], H. Mildner[138], A. Milic[154], C.D. Milke[44], D.W. Miller[39], L.S. Miller[34], A. Milov[167], D.A. Milstead[47a,47b], T. Min[14c], A.A. Minaenko[37], I.A. Minashvili[148b], L. Mince[59], A.I. Mincer[116], B. Mindur[84a], M. Mineev[38], Y. Mino[86], L.M. Mir[13], M. Miralles Lopez[161], M. Mironova[125], T. Mitani[166], A. Mitra[165], V.A. Mitsou[161],

JHEP06(2023)138

O. Miu[154], P.S. Miyagawa[93], Y. Miyazaki[88], A. Mizukami[82], J.U. Mjörnmark[97], T. Mkrtchyan[63a], T. Mlinarevic[95], M. Mlynarikova[36], T. Moa[47a,47b], S. Mobius[55], K. Mochizuki[107], P. Moder[48], P. Mogg[108], A.F. Mohammed[14a,14d], S. Mohapatra[41], G. Mokgatitswane[33g], B. Mondal[140], S. Mondal[131], K. Mönig[48], E. Monnier[101], L. Monsonis Romero[161], J. Montejo Berlingen[36], M. Montella[118], F. Monticelli[89], N. Morange[66], A.L. Moreira De Carvalho[129a], M. Moreno Llácer[161], C. Moreno Martinez[13], P. Morettini[57b], S. Morgenstern[165], M. Morii[61], M. Morinaga[152], V. Morisbak[124], A.K. Morley[36], F. Morodei[74a,74b], L. Morvaj[36], P. Moschovakos[36], B. Moser[36], M. Mosidze[148b], T. Moskalets[54], P. Moskvitina[112], J. Moss[31,n], E.J.W. Moyse[102], S. Muanza[101], J. Mueller[128], D. Muenstermann[90], R. Müller[19], G.A. Mullier[97], J.J. Mullin[127], D.P. Mungo[70a,70b], J.L. Munoz Martinez[13], D. Munoz Perez[161], F.J. Munoz Sanchez[100], M. Murin[100], W.J. Murray[165,133], A. Murrone[70a,70b], J.M. Muse[119], M. Muškinja[17a], C. Mwewa[29], A.G. Myagkov[37,a], A.J. Myers[8], A.A. Myers[128], G. Myers[67], M. Myska[131], B.P. Nachman[17a], O. Nackenhorst[49], A. Nag[50], K. Nagai[125], K. Nagano[82], J.L. Nagle[29,ad], E. Nagy[101], A.M. Nairz[36], Y. Nakahama[82], K. Nakamura[82], H. Nanjo[123], R. Narayan[44], E.A. Narayanan[111], I. Naryshkin[37], M. Naseri[34], C. Nass[24], G. Navarro[22a], J. Navarro-Gonzalez[161], R. Nayak[150], A. Nayaz[18], P.Y. Nechaeva[37], F. Nechansky[48], L. Nedic[125], T.J. Neep[20], A. Negri[72a,72b], M. Negrini[23b], C. Nellist[112], C. Nelson[103], K. Nelson[105], S. Nemecek[130], M. Nessi[36,g], M.S. Neubauer[160], F. Neuhaus[99], J. Neundorf[48], R. Newhouse[162], P.R. Newman[20], C.W. Ng[128], Y.S. Ng[18], Y.W.Y. Ng[158], B. Ngair[35e], H.D.N. Nguyen[107], R.B. Nickerson[125], R. Nicolaidou[134], J. Nielsen[135], M. Niemeyer[55], N. Nikiforou[36], V. Nikolaenko[37,a], I. Nikolic-Audit[126], K. Nikolopoulos[20], P. Nilsson[29], H.R. Nindhito[56], A. Nisati[74a], N. Nishu[2], R. Nisius[109], J-E. Nitschke[50], E.K. Nkadimeng[33g], S.J. Noacco Rosende[89], T. Nobe[152], D.L. Noel[32], Y. Noguchi[86], T. Nommensen[146], M.A. Nomura[29], M.B. Norfolk[138], R.R.B. Norisam[95], B.J. Norman[34], J. Novak[92], T. Novak[48], O. Novgorodova[50], L. Novotny[131], R. Novotny[111], L. Nozka[121], K. Ntekas[158], E. Nurse[95], F.G. Oakham[34,aa], J. Ocariz[126], A. Ochi[83], I. Ochoa[129a], S. Oerdek[159], A. Ogrodnik[84a], A. Oh[100], C.C. Ohm[143], H. Oide[153], R. Oishi[152], M.L. Ojeda[48], Y. Okazaki[86], M.W. O'Keefe[91], Y. Okumura[152], A. Olariu[27b], L.F. Oleiro Seabra[129a], S.A. Olivares Pino[136e], D. Oliveira Damazio[29], D. Oliveira Goncalves[81a], J.L. Oliver[158], M.J.R. Olsson[158], A. Olszewski[85], J. Olszowska[85,*], Ö.O. Öncel[54], D.C. O'Neil[141], A.P. O'Neill[19], A. Onofre[129a,129e], P.U.E. Onyisi[11], M.J. Oreglia[39], G.E. Orellana[89], D. Orestano[76a,76b], N. Orlando[13], R.S. Orr[154], V. O'Shea[59], R. Ospanov[62a], G. Otero y Garzon[30], H. Otono[88], P.S. Ott[63a], G.J. Ottino[17a], M. Ouchrif[35d], J. Ouellette[29,ad], F. Ould-Saada[124], M. Owen[59], R.E. Owen[133], K.Y. Oyulmaz[21a], V.E. Ozcan[21a], N. Ozturk[8], S. Ozturk[21d], J. Pacalt[121], H.A. Pacey[32], K. Pachal[51], A. Pacheco Pages[13], C. Padilla Aranda[13], G. Padovano[74a,74b], S. Pagan Griso[17a], G. Palacino[67], A. Palazzo[69a,69b], S. Palazzo[52], S. Palestini[36], M. Palka[84b], J. Pan[170], T. Pan[64a], D.K. Panchal[11], C.E. Pandini[113], J.G. Panduro Vazquez[94], H. Pang[14b], P. Pani[48], G. Panizzo[68a,68c], L. Paolozzi[56], C. Papadatos[107], S. Parajuli[44], A. Paramonov[6], C. Paraskevopoulos[10], D. Paredes Hernandez[64b], T.H. Park[154],

JHEP06(2023)138

M.A. Parker[32], F. Parodi[57b,57a], E.W. Parrish[114], V.A. Parrish[52], J.A. Parsons[41], U. Parzefall[54], B. Pascual Dias[107], L. Pascual Dominguez[150], V.R. Pascuzzi[17a], F. Pasquali[113], E. Pasqualucci[74a], S. Passaggio[57b], F. Pastore[94], P. Pasuwan[47a,47b], P. Patel[85], J.R. Pater[100], J. Patton[91], T. Pauly[36], J. Pearkes[142], M. Pedersen[124], R. Pedro[129a], S.V. Peleganchuk[37], O. Penc[36], E.A. Pender[52], C. Peng[64b], H. Peng[62a], K.E. Penski[108], M. Penzin[37], B.S. Peralva[81d,81d], A.P. Pereira Peixoto[60], L. Pereira Sanchez[47a,47b], D.V. Perepelitsa[29,ad], E. Perez Codina[155a], M. Perganti[10], L. Perini[70a,70b,*], H. Pernegger[36], S. Perrella[36], A. Perrevoort[112], O. Perrin[40], K. Peters[48], R.F.Y. Peters[100], B.A. Petersen[36], T.C. Petersen[42], E. Petit[101], V. Petousis[131], C. Petridou[151], A. Petrukhin[140], M. Pettee[17a], N.E. Pettersson[36], A. Petukhov[37], K. Petukhova[132], A. Peyaud[134], R. Pezoa[136f], L. Pezzotti[36], G. Pezzullo[170], T.M. Pham[168], T. Pham[104], P.W. Phillips[133], M.W. Phipps[160], G. Piacquadio[144], E. Pianori[17a], F. Piazza[70a,70b], R. Piegaia[30], D. Pietreanu[27b], A.D. Pilkington[100], M. Pinamonti[68a,68c], J.L. Pinfold[2], B.C. Pinheiro Pereira[129a], C. Pitman Donaldson[95], D.A. Pizzi[34], L. Pizzimento[75a,75b], A. Pizzini[113], M.-A. Pleier[29], V. Plesanovs[54], V. Pleskot[132], E. Plotnikova[38], G. Poddar[4], R. Poettgen[97], L. Poggioli[126], I. Pogrebnyak[106], D. Pohl[24], I. Pokharel[55], S. Polacek[132], G. Polesello[72a], A. Poley[141,155a], R. Polifka[131], A. Polini[23b], C.S. Pollard[125], Z.B. Pollock[118], V. Polychronakos[29], E. Pompa Pacchi[74a,74b], D. Ponomarenko[37], L. Pontecorvo[36], S. Popa[27a], G.A. Popeneciu[27d], D.M. Portillo Quintero[155a], S. Pospisil[131], P. Postolache[27c], K. Potamianos[125], I.N. Potrap[38], C.J. Potter[32], H. Potti[1], T. Poulsen[48], J. Poveda[161], M.E. Pozo Astigarraga[36], A. Prades Ibanez[161], M.M. Prapa[46], D. Price[100], M. Primavera[69a], M.A. Principe Martin[98], M.L. Proffitt[137], N. Proklova[127], K. Prokofiev[64c], G. Proto[75a,75b], S. Protopopescu[29], J. Proudfoot[6], M. Przybycien[84a], J.E. Puddefoot[138], D. Pudzha[37], P. Puzo[66], D. Pyatiizbyantseva[37], J. Qian[105], Y. Qin[100], T. Qiu[93], A. Quadt[55], M. Queitsch-Maitland[100], G. Quetant[56], G. Rabanal Bolanos[61], D. Rafanoharana[54], F. Ragusa[70a,70b], J.L. Rainbolt[39], J.A. Raine[56], S. Rajagopalan[29], E. Ramakoti[37], K. Ran[48,14d], V. Raskina[126], D.F. Rassloff[63a], S. Rave[99], B. Ravina[55], I. Ravinovich[167], M. Raymond[36], A.L. Read[124], N.P. Readioff[138], D.M. Rebuzzi[72a,72b], G. Redlinger[29], K. Reeves[45], J.A. Reidelsturz[169], D. Reikher[150], A. Reiss[99], A. Rej[140], C. Rembser[36], A. Renardi[48], M. Renda[27b], M.B. Rendel[109], A.G. Rennie[59], S. Resconi[70a], M. Ressegotti[57b,57a], E.D. Resseguie[17a], S. Rettie[95], B. Reynolds[118], E. Reynolds[17a], M. Rezaei Estabragh[169], O.L. Rezanova[37], P. Reznicek[132], E. Ricci[77a,77b], R. Richter[109], S. Richter[47a,47b], E. Richter-Was[84b], M. Ridel[126], P. Rieck[116], P. Riedler[36], M. Rijssenbeek[144], A. Rimoldi[72a,72b], M. Rimoldi[48], L. Rinaldi[23b,23a], T.T. Rinn[29], M.P. Rinnagel[108], G. Ripellino[143], I. Riu[13], P. Rivadeneira[48], J.C. Rivera Vergara[163], F. Rizatdinova[120], E. Rizvi[93], C. Rizzi[56], B.A. Roberts[165], B.R. Roberts[17a], S.H. Robertson[103,v], M. Robin[48], D. Robinson[32], C.M. Robles Gajardo[136f], M. Robles Manzano[99], A. Robson[59], A. Rocchi[75a,75b], C. Roda[73a,73b], S. Rodriguez Bosca[63a], Y. Rodriguez Garcia[22a], A. Rodriguez Rodriguez[54], A.M. Rodríguez Vera[155b], S. Roe[36], J.T. Roemer[158], A.R. Roepe-Gier[119], J. Roggel[169], O. Røhne[124], R.A. Rojas[163], B. Roland[54], C.P.A. Roland[67], J. Roloff[29], A. Romaniouk[37], E. Romano[72a,72b],

JHEP06(2023)138

M. Romano[23b], A.C. Romero Hernandez[160], N. Rompotis[91], L. Roos[126], S. Rosati[74a], B.J. Rosser[39], E. Rossi[4], E. Rossi[71a,71b], L.P. Rossi[57b], L. Rossini[48], R. Rosten[118], M. Rotaru[27b], B. Rottler[54], D. Rousseau[66], D. Rousso[32], G. Rovelli[72a,72b], A. Roy[160], A. Rozanov[101], Y. Rozen[149], X. Ruan[33g], A. Rubio Jimenez[161], A.J. Ruby[91], V.H. Ruelas Rivera[18], T.A. Ruggeri[1], F. Rühr[54], A. Ruiz-Martinez[161], A. Rummler[36], Z. Rurikova[54], N.A. Rusakovich[38], H.L. Russell[163], J.P. Rutherfoord[7], K. Rybacki[90], M. Rybar[132], E.B. Rye[124], A. Ryzhov[37], J.A. Sabater Iglesias[56], P. Sabatini[161], L. Sabetta[74a,74b], H.F-W. Sadrozinski[135], F. Safai Tehrani[74a], B. Safarzadeh Samani[145], M. Safdari[142], S. Saha[103], M. Sahinsoy[109], M. Saimpert[134], M. Saito[152], T. Saito[152], D. Salamani[36], G. Salamanna[76a,76b], A. Salnikov[142], J. Salt[161], A. Salvador Salas[13], D. Salvatore[43b,43a], F. Salvatore[145], A. Salzburger[36], D. Sammel[54], D. Sampsonidis[151], D. Sampsonidou[62d,62c], J. Sánchez[161], A. Sanchez Pineda[4], V. Sanchez Sebastian[161], H. Sandaker[124], C.O. Sander[48], J.A. Sandesara[102], M. Sandhoff[169], C. Sandoval[22b], D.P.C. Sankey[133], A. Sansoni[53], L. Santi[74a,74b], C. Santoni[40], H. Santos[129a,129b], S.N. Santpur[17a], A. Santra[167], K.A. Saoucha[138], J.G. Saraiva[129a,129d], J. Sardain[7], O. Sasaki[82], K. Sato[156], C. Sauer[63b], F. Sauerburger[54], E. Sauvan[4], P. Savard[154,aa], R. Sawada[152], C. Sawyer[133], L. Sawyer[96], I. Sayago Galvan[161], C. Sbarra[23b], A. Sbrizzi[23b,23a], T. Scanlon[95], J. Schaarschmidt[137], P. Schacht[109], D. Schaefer[39], U. Schäfer[99], A.C. Schaffer[66], D. Schaile[108], R.D. Schamberger[144], E. Schanet[108], C. Scharf[18], V.A. Schegelsky[37], D. Scheirich[132], F. Schenck[18], M. Schernau[158], C. Scheulen[55], C. Schiavi[57b,57a], Z.M. Schillaci[26], E.J. Schioppa[69a,69b], M. Schioppa[43b,43a], B. Schlag[99], K.E. Schleicher[54], S. Schlenker[36], K. Schmieden[99], C. Schmitt[99], S. Schmitt[48], L. Schoeffel[134], A. Schoening[63b], P.G. Scholer[54], E. Schopf[125], M. Schott[99], J. Schovancova[36], S. Schramm[56], F. Schroeder[169], H-C. Schultz-Coulon[63a], M. Schumacher[54], B.A. Schumm[135], Ph. Schune[134], A. Schwartzman[142], T.A. Schwarz[105], Ph. Schwemling[134], R. Schwienhorst[106], A. Sciandra[135], G. Sciolla[26], F. Scuri[73a], F. Scutti[104], C.D. Sebastiani[91], K. Sedlaczek[49], P. Seema[18], S.C. Seidel[111], A. Seiden[135], B.D. Seidlitz[41], T. Seiss[39], C. Seitz[48], J.M. Seixas[81b], G. Sekhniaidze[71a], S.J. Sekula[44], L. Selem[4], N. Semprini-Cesari[23b,23a], S. Sen[51], D. Sengupta[56], V. Senthilkumar[161], L. Serin[66], L. Serkin[68a,68b], M. Sessa[76a,76b], H. Severini[119], S. Sevova[142], F. Sforza[57b,57a], A. Sfyrla[56], E. Shabalina[55], R. Shaheen[143], J.D. Shahinian[127], N.W. Shaikh[47a,47b], D. Shaked Renous[167], L.Y. Shan[14a], M. Shapiro[17a], A. Sharma[36], A.S. Sharma[162], P. Sharma[79], S. Sharma[48], P.B. Shatalov[37], K. Shaw[145], S.M. Shaw[100], Q. Shen[62c,5], P. Sherwood[95], L. Shi[95], C.O. Shimmin[170], Y. Shimogama[166], J.D. Shinner[94], I.P.J. Shipsey[125], S. Shirabe[60], M. Shiyakova[38], J. Shlomi[167], M.J. Shochet[39], J. Shojaii[104], D.R. Shope[124], S. Shrestha[118,ae], E.M. Shrif[33g], M.J. Shroff[163], P. Sicho[130], A.M. Sickles[160], E. Sideras Haddad[33g], A. Sidoti[23b], F. Siegert[50], Dj. Sijacki[15], R. Sikora[84a], F. Sili[89], J.M. Silva[20], M.V. Silva Oliveira[36], S.B. Silverstein[47a], S. Simion[66], R. Simoniello[36], E.L. Simpson[59], N.D. Simpson[97], S. Simsek[21d], S. Sindhu[55], P. Sinervo[154], V. Sinetckii[37], S. Singh[141], S. Singh[154], S. Sinha[48], S. Sinha[33g], M. Sioli[23b,23a], I. Siral[122], S.Yu. Sivoklokov[37,*], J. Sjölin[47a,47b], A. Skaf[55], E. Skorda[97], P. Skubic[119], M. Slawinska[85], V. Smakhtin[167],

JHEP06(2023)138

B.H. Smart[133], J. Smiesko[36], S.Yu. Smirnov[37], Y. Smirnov[37], L.N. Smirnova[37,a], O. Smirnova[97], A.C. Smith[41], E.A. Smith[39], H.A. Smith[125], J.L. Smith[91], R. Smith[142], M. Smizanska[90], K. Smolek[131], A. Smykiewicz[85], A.A. Snesarev[37], H.L. Snoek[113], S. Snyder[29], R. Sobie[163,v], A. Soffer[150], C.A. Solans Sanchez[36], E.Yu. Soldatov[37], U. Soldevila[161], A.A. Solodkov[37], S. Solomon[54], A. Soloshenko[38], K. Solovieva[54], O.V. Solovyanov[37], V. Solovyev[37], P. Sommer[36], A. Sonay[13], W.Y. Song[155b], A. Sopczak[131], A.L. Sopio[95], F. Sopkova[28b], V. Sothilingam[63a], S. Sottocornola[72a,72b], R. Soualah[115c], Z. Soumaimi[35e], D. South[48], S. Spagnolo[69a,69b], M. Spalla[109], F. Spanò[94], D. Sperlich[54], G. Spigo[36], M. Spina[145], S. Spinali[90], D.P. Spiteri[59], M. Spousta[132], E.J. Staats[34], A. Stabile[70a,70b], R. Stamen[63a], M. Stamenkovic[113], A. Stampekis[20], M. Standke[24], E. Stanecka[85], M.V. Stange[50], B. Stanislaus[17a], M.M. Stanitzki[48], M. Stankaityte[125], B. Stapf[48], E.A. Starchenko[37], G.H. Stark[135], J. Stark[101], D.M. Starko[155b], P. Staroba[130], P. Starovoitov[63a], S. Stärz[103], R. Staszewski[85], G. Stavropoulos[46], J. Steentoft[159], P. Steinberg[29], A.L. Steinhebel[122], B. Stelzer[141,155a], H.J. Stelzer[128], O. Stelzer-Chilton[155a], H. Stenzel[58], T.J. Stevenson[145], G.A. Stewart[36], M.C. Stockton[36], G. Stoicea[27b], M. Stolarski[129a], S. Stonjek[109], A. Straessner[50], J. Strandberg[143], S. Strandberg[47a,47b], M. Strauss[119], T. Strebler[101], P. Strizenec[28b], R. Ströhmer[164], D.M. Strom[122], L.R. Strom[48], R. Stroynowski[44], A. Strubig[47a,47b], S.A. Stucci[29], B. Stugu[16], J. Stupak[119], N.A. Styles[48], D. Su[142], S. Su[62a], W. Su[62d,137,62c], X. Su[62a,66], K. Sugizaki[152], V.V. Sulin[37], M.J. Sullivan[91], D.M.S. Sultan[77a,77b], L. Sultanaliyeva[37], S. Sultansoy[3b], T. Sumida[86], S. Sun[105], S. Sun[168], O. Sunneborn Gudnadottir[159], M.R. Sutton[145], M. Svatos[130], M. Swiatlowski[155a], T. Swirski[164], I. Sykora[28a], M. Sykora[132], T. Sykora[132], D. Ta[99], K. Tackmann[48,u], A. Taffard[158], R. Tafirout[155a], J.S. Tafoya Vargas[66], R.H.M. Taibah[126], R. Takashima[87], K. Takeda[83], E.P. Takeva[52], Y. Takubo[82], M. Talby[101], A.A. Talyshev[37], K.C. Tam[64b], N.M. Tamir[150], A. Tanaka[152], J. Tanaka[152], R. Tanaka[66], M. Tanasini[57b,57a], J. Tang[62c], Z. Tao[162], S. Tapia Araya[80], S. Tapprogge[99], A. Tarek Abouelfadl Mohamed[106], S. Tarem[149], K. Tariq[62b], G. Tarna[27b], G.F. Tartarelli[70a], P. Tas[132], M. Tasevsky[130], E. Tassi[43b,43a], A.C. Tate[160], G. Tateno[152], Y. Tayalati[35e], G.N. Taylor[104], W. Taylor[155b], H. Teagle[91], A.S. Tee[168], R. Teixeira De Lima[142], P. Teixeira-Dias[94], J.J. Teoh[154], K. Terashi[152], J. Terron[98], S. Terzo[13], M. Testa[53], R.J. Teuscher[154,v], A. Thaler[78], O. Theiner[56], N. Themistokleous[52], T. Theveneaux-Pelzer[18], O. Thielmann[169], D.W. Thomas[94], J.P. Thomas[20], E.A. Thompson[48], P.D. Thompson[20], E. Thomson[127], E.J. Thorpe[93], Y. Tian[55], V. Tikhomirov[37,a], Yu.A. Tikhonov[37], S. Timoshenko[37], E.X.L. Ting[1], P. Tipton[170], S. Tisserant[101], S.H. Tlou[33g], A. Tnourji[40], K. Todome[23b,23a], S. Todorova-Nova[132], S. Todt[50], M. Togawa[82], J. Tojo[88], S. Tokár[28a], K. Tokushuku[82], R. Tombs[32], M. Tomoto[82,110], L. Tompkins[142], K.W. Topolnicki[84b], P. Tornambe[102], E. Torrence[122], H. Torres[50], E. Torró Pastor[161], M. Toscani[30], C. Tosciri[39], D.R. Tovey[138], A. Traeet[16], I.S. Trandafir[27b], T. Trefzger[164], A. Tricoli[29], I.M. Trigger[155a], S. Trincaz-Duvoid[126], D.A. Trischuk[26], B. Trocmé[60], A. Trofymov[66], C. Troncon[70a], L. Truong[33c], M. Trzebinski[85], A. Trzupek[85], F. Tsai[144], M. Tsai[105], A. Tsiamis[151],

JHEP06(2023)138

P.V. Tsiareshka[37], S. Tsigaridas[155a], A. Tsirigotis[151,s], V. Tsiskaridze[144], E.G. Tskhadadze[148a], M. Tsopoulou[151], Y. Tsujikawa[86], I.I. Tsukerman[37], V. Tsulaia[17a], S. Tsuno[82], O. Tsur[149], D. Tsybychev[144], Y. Tu[64b], A. Tudorache[27b], V. Tudorache[27b], A.N. Tuna[36], S. Turchikhin[38], I. Turk Cakir[3a], R. Turra[70a], T. Turtuvshin[38], P.M. Tuts[41], S. Tzamarias[151], P. Tzanis[10], E. Tzovara[99], K. Uchida[152], F. Ukegawa[156], P.A. Ulloa Poblete[136c], G. Unal[36], M. Unal[11], A. Undrus[29], G. Unel[158], J. Urban[28b], P. Urquijo[104], G. Usai[8], R. Ushioda[153], M. Usman[107], Z. Uysal[21b], V. Vacek[131], B. Vachon[103], K.O.H. Vadla[124], T. Vafeiadis[36], C. Valderanis[108], E. Valdes Santurio[47a,47b], M. Valente[155a], S. Valentinetti[23b,23a], A. Valero[161], A. Vallier[101], J.A. Valls Ferrer[161], T.R. Van Daalen[137], P. Van Gemmeren[6], M. Van Rijnbach[124,36], S. Van Stroud[95], I. Van Vulpen[113], M. Vanadia[75a,75b], W. Vandelli[36], M. Vandenbroucke[134], E.R. Vandewall[120], D. Vannicola[150], L. Vannoli[57b,57a], R. Vari[74a], E.W. Varnes[7], C. Varni[17a], T. Varol[147], D. Varouchas[66], L. Varriale[161], K.E. Varvell[146], M.E. Vasile[27b], L. Vaslin[40], G.A. Vasquez[163], F. Vazeille[40], T. Vazquez Schroeder[36], J. Veatch[31], V. Vecchio[100], M.J. Veen[102], I. Veliscek[125], L.M. Veloce[154], F. Veloso[129a,129c], S. Veneziano[74a], A. Ventura[69a,69b], A. Verbytskyi[109], M. Verducci[73a,73b], C. Vergis[24], M. Verissimo De Araujo[81b], W. Verkerke[113], J.C. Vermeulen[113], C. Vernieri[142], P.J. Verschuuren[94], M. Vessella[102], M.C. Vetterli[141,aa], A. Vgenopoulos[151], N. Viaux Maira[136f], T. Vickey[138], O.E. Vickey Boeriu[138], G.H.A. Viehhauser[125], L. Vigani[63b], M. Villa[23b,23a], M. Villaplana Perez[161], E.M. Villhauer[52], E. Vilucchi[53], M.G. Vincter[34], G.S. Virdee[20], A. Vishwakarma[52], C. Vittori[23b,23a], I. Vivarelli[145], V. Vladimirov[165], E. Voevodina[109], F. Vogel[108], P. Vokac[131], J. Von Ahnen[48], E. Von Toerne[24], B. Vormwald[36], V. Vorobel[132], K. Vorobev[37], M. Vos[161], J.H. Vossebeld[91], M. Vozak[113], L. Vozdecky[93], N. Vranjes[15], M. Vranjes Milosavljevic[15], M. Vreeswijk[113], R. Vuillermet[36], O. Vujinovic[99], I. Vukotic[39], S. Wada[156], C. Wagner[102], W. Wagner[169], S. Wahdan[169], H. Wahlberg[89], R. Wakasa[156], M. Wakida[110], V.M. Walbrecht[109], J. Walder[133], R. Walker[108], W. Walkowiak[140], A.M. Wang[61], A.Z. Wang[168], C. Wang[62a], C. Wang[62c], H. Wang[17a], J. Wang[64a], P. Wang[44], R.-J. Wang[99], R. Wang[61], R. Wang[6], S.M. Wang[147], S. Wang[62b], T. Wang[62a], W.T. Wang[79], W.X. Wang[62a], X. Wang[14c], X. Wang[160], X. Wang[62c], Y. Wang[62d], Y. Wang[14c], Z. Wang[105], Z. Wang[62d,51,62c], Z. Wang[105], A. Warburton[103], R.J. Ward[20], N. Warrack[59], A.T. Watson[20], M.F. Watson[20], G. Watts[137], B.M. Waugh[95], A.F. Webb[11], C. Weber[29], M.S. Weber[19], S.M. Weber[63a], C. Wei[62a], Y. Wei[125], A.R. Weidberg[125], J. Weingarten[49], M. Weirich[99], C. Weiser[54], C.J. Wells[48], T. Wenaus[29], B. Wendland[49], T. Wengler[36], N.S. Wenke[109], N. Wermes[24], M. Wessels[63a], K. Whalen[122], A.M. Wharton[90], A.S. White[61], A. White[8], M.J. White[1], D. Whiteson[158], L. Wickremasinghe[123], W. Wiedenmann[168], C. Wiel[50], M. Wielers[133], N. Wieseotte[99], C. Wiglesworth[42], L.A.M. Wiik-Fuchs[54], D.J. Wilbern[119], H.G. Wilkens[36], D.M. Williams[41], H.H. Williams[127], S. Williams[32], S. Willocq[102], P.J. Windischhofer[125], F. Winklmeier[122], B.T. Winter[54], M. Wittgen[142], M. Wobisch[96], R. Wölker[125], J. Wollrath[158], M.W. Wolter[85], H. Wolters[129a,129c], V.W.S. Wong[162], A.F. Wongel[48], S.D. Worm[48], B.K. Wosiek[85], K.W. Woźniak[85],

JHEP06(2023)138

K. Wraight[59], J. Wu[14a,14d], M. Wu[64a], M. Wu[112], S.L. Wu[168], X. Wu[56], Y. Wu[62a], Z. Wu[134,62a], J. Wuerzinger[125], T.R. Wyatt[100], B.M. Wynne[52], S. Xella[42], L. Xia[14c], M. Xia[14b], J. Xiang[64c], X. Xiao[105], M. Xie[62a], X. Xie[62a], J. Xiong[17a], I. Xiotidis[145], D. Xu[14a], H. Xu[62a], H. Xu[62a], L. Xu[62a], R. Xu[127], T. Xu[105], W. Xu[105], Y. Xu[14b], Z. Xu[62b], Z. Xu[142], B. Yabsley[146], S. Yacoob[33a], N. Yamaguchi[88], Y. Yamaguchi[153], H. Yamauchi[156], T. Yamazaki[17a], Y. Yamazaki[83], J. Yan[62c], S. Yan[125], Z. Yan[25], H.J. Yang[62c,62d], H.T. Yang[17a], S. Yang[62a], T. Yang[64c], X. Yang[62a], X. Yang[14a], Y. Yang[44], Z. Yang[62a,105], W-M. Yao[17a], Y.C. Yap[48], H. Ye[14c], J. Ye[44], S. Ye[29], X. Ye[62a], Y. Yeh[95], I. Yeletskikh[38], M.R. Yexley[90], P. Yin[41], K. Yorita[166], C.J.S. Young[54], C. Young[142], M. Yuan[105], R. Yuan[62b,j], L. Yue[95], X. Yue[63a], M. Zaazoua[35e], B. Zabinski[85], E. Zaid[52], T. Zakareishvili[148b], N. Zakharchuk[34], S. Zambito[56], J.A. Zamora Saa[136d], J. Zang[152], D. Zanzi[54], O. Zaplatilek[131], S.V. Zeißner[49], C. Zeitnitz[169], J.C. Zeng[160], D.T. Zenger Jr[26], O. Zenin[37], T. Ženiš[28a], S. Zenz[93], S. Zerradi[35a], D. Zerwas[66], B. Zhang[14c], D.F. Zhang[138], G. Zhang[14b], J. Zhang[62b], J. Zhang[6], K. Zhang[14a,14d], L. Zhang[14c], P. Zhang[14a,14d], R. Zhang[168], S. Zhang[105], T. Zhang[152], X. Zhang[62c], X. Zhang[62b], Z. Zhang[17a], Z. Zhang[66], H. Zhao[137], P. Zhao[51], T. Zhao[62b], Y. Zhao[135], Z. Zhao[62a], A. Zhemchugov[38], X. Zheng[62a], Z. Zheng[142], D. Zhong[160], B. Zhou[105], C. Zhou[168], H. Zhou[7], N. Zhou[62c], Y. Zhou[7], C.G. Zhu[62b], C. Zhu[14a,14d], H.L. Zhu[62a], H. Zhu[14a], J. Zhu[105], Y. Zhu[62c], Y. Zhu[62a], X. Zhuang[14a], K. Zhukov[37], V. Zhulanov[37], N.I. Zimine[38], J. Zinsser[63b], M. Ziolkowski[140], L. Živković[15], A. Zoccoli[23b,23a], K. Zoch[56], T.G. Zorbas[138], O. Zormpa[46], W. Zou[41], L. Zwalinski[36]

[1] *Department of Physics, University of Adelaide, Adelaide; Australia*
[2] *Department of Physics, University of Alberta, Edmonton AB; Canada*
[3] [(a)] *Department of Physics, Ankara University, Ankara;* [(b)] *Division of Physics, TOBB University of Economics and Technology, Ankara; Türkiye*
[4] *LAPP, Univ. Savoie Mont Blanc, CNRS/IN2P3, Annecy; France*
[5] *APC, Université Paris Cité, CNRS/IN2P3, Paris; France*
[6] *High Energy Physics Division, Argonne National Laboratory, Argonne IL; United States of America*
[7] *Department of Physics, University of Arizona, Tucson AZ; United States of America*
[8] *Department of Physics, University of Texas at Arlington, Arlington TX; United States of America*
[9] *Physics Department, National and Kapodistrian University of Athens, Athens; Greece*
[10] *Physics Department, National Technical University of Athens, Zografou; Greece*
[11] *Department of Physics, University of Texas at Austin, Austin TX; United States of America*
[12] *Institute of Physics, Azerbaijan Academy of Sciences, Baku; Azerbaijan*
[13] *Institut de Física d'Altes Energies (IFAE), Barcelona Institute of Science and Technology, Barcelona; Spain*
[14] [(a)] *Institute of High Energy Physics, Chinese Academy of Sciences, Beijing;* [(b)] *Physics Department, Tsinghua University, Beijing;* [(c)] *Department of Physics, Nanjing University, Nanjing;* [(d)] *University of Chinese Academy of Science (UCAS), Beijing; China*
[15] *Institute of Physics, University of Belgrade, Belgrade; Serbia*
[16] *Department for Physics and Technology, University of Bergen, Bergen; Norway*
[17] [(a)] *Physics Division, Lawrence Berkeley National Laboratory, Berkeley CA;* [(b)] *University of California, Berkeley CA; United States of America*
[18] *Institut für Physik, Humboldt Universität zu Berlin, Berlin; Germany*
[19] *Albert Einstein Center for Fundamental Physics and Laboratory for High Energy Physics, University of Bern, Bern; Switzerland*

JHEP06(2023)138

[20] School of Physics and Astronomy, University of Birmingham, Birmingham; United Kingdom
[21] [(a)] Department of Physics, Bogazici University, Istanbul; [(b)] Department of Physics Engineering, Gaziantep University, Gaziantep; [(c)] Department of Physics, Istanbul University, Istanbul; [(d)] Istinye University, Sariyer, Istanbul; Türkiye
[22] [(a)] Facultad de Ciencias y Centro de Investigaciónes, Universidad Antonio Nariño, Bogotá; [(b)] Departamento de Física, Universidad Nacional de Colombia, Bogotá; Colombia
[23] [(a)] Dipartimento di Fisica e Astronomia A. Righi, Università di Bologna, Bologna; [(b)] INFN Sezione di Bologna; Italy
[24] Physikalisches Institut, Universität Bonn, Bonn; Germany
[25] Department of Physics, Boston University, Boston MA; United States of America
[26] Department of Physics, Brandeis University, Waltham MA; United States of America
[27] [(a)] Transilvania University of Brasov, Brasov; [(b)] Horia Hulubei National Institute of Physics and Nuclear Engineering, Bucharest; [(c)] Department of Physics, Alexandru Ioan Cuza University of Iasi, Iasi; [(d)] National Institute for Research and Development of Isotopic and Molecular Technologies, Physics Department, Cluj-Napoca; [(e)] University Politehnica Bucharest, Bucharest; [(f)] West University in Timisoara, Timisoara; [(g)] Faculty of Physics, University of Bucharest, Bucharest; Romania
[28] [(a)] Faculty of Mathematics, Physics and Informatics, Comenius University, Bratislava; [(b)] Department of Subnuclear Physics, Institute of Experimental Physics of the Slovak Academy of Sciences, Kosice; Slovak Republic
[29] Physics Department, Brookhaven National Laboratory, Upton NY; United States of America
[30] Universidad de Buenos Aires, Facultad de Ciencias Exactas y Naturales, Departamento de Física, y CONICET, Instituto de Física de Buenos Aires (IFIBA), Buenos Aires; Argentina
[31] California State University, CA; United States of America
[32] Cavendish Laboratory, University of Cambridge, Cambridge; United Kingdom
[33] [(a)] Department of Physics, University of Cape Town, Cape Town; [(b)] iThemba Labs, Western Cape; [(c)] Department of Mechanical Engineering Science, University of Johannesburg, Johannesburg; [(d)] National Institute of Physics, University of the Philippines Diliman (Philippines); [(e)] University of South Africa, Department of Physics, Pretoria; [(f)] University of Zululand, KwaDlangezwa; [(g)] School of Physics, University of the Witwatersrand, Johannesburg; South Africa
[34] Department of Physics, Carleton University, Ottawa ON; Canada
[35] [(a)] Faculté des Sciences Ain Chock, Réseau Universitaire de Physique des Hautes Energies — Université Hassan II, Casablanca; [(b)] Faculté des Sciences, Université Ibn-Tofail, Kénitra; [(c)] Faculté des Sciences Semlalia, Université Cadi Ayyad, LPHEA-Marrakech; [(d)] LPMR, Faculté des Sciences, Université Mohamed Premier, Oujda; [(e)] Faculté des sciences, Université Mohammed V, Rabat; [(f)] Institute of Applied Physics, Mohammed VI Polytechnic University, Ben Guerir; Morocco
[36] CERN, Geneva; Switzerland
[37] Affiliated with an institute covered by a cooperation agreement with CERN
[38] Affiliated with an international laboratory covered by a cooperation agreement with CERN
[39] Enrico Fermi Institute, University of Chicago, Chicago IL; United States of America
[40] LPC, Université Clermont Auvergne, CNRS/IN2P3, Clermont-Ferrand; France
[41] Nevis Laboratory, Columbia University, Irvington NY; United States of America
[42] Niels Bohr Institute, University of Copenhagen, Copenhagen; Denmark
[43] [(a)] Dipartimento di Fisica, Università della Calabria, Rende; [(b)] INFN Gruppo Collegato di Cosenza, Laboratori Nazionali di Frascati; Italy
[44] Physics Department, Southern Methodist University, Dallas TX; United States of America
[45] Physics Department, University of Texas at Dallas, Richardson TX; United States of America
[46] National Centre for Scientific Research "Demokritos", Agia Paraskevi; Greece
[47] [(a)] Department of Physics, Stockholm University; [(b)] Oskar Klein Centre, Stockholm; Sweden
[48] Deutsches Elektronen-Synchrotron DESY, Hamburg and Zeuthen; Germany
[49] Fakultät Physik, Technische Universität Dortmund, Dortmund; Germany
[50] Institut für Kern- und Teilchenphysik, Technische Universität Dresden, Dresden; Germany
[51] Department of Physics, Duke University, Durham NC; United States of America

JHEP06(2023)138

[52] SUPA — School of Physics and Astronomy, University of Edinburgh, Edinburgh; United Kingdom
[53] INFN e Laboratori Nazionali di Frascati, Frascati; Italy
[54] Physikalisches Institut, Albert-Ludwigs-Universität Freiburg, Freiburg; Germany
[55] II. Physikalisches Institut, Georg-August-Universität Göttingen, Göttingen; Germany
[56] Département de Physique Nucléaire et Corpusculaire, Université de Genève, Genève; Switzerland
[57] [(a)] Dipartimento di Fisica, Università di Genova, Genova; [(b)] INFN Sezione di Genova; Italy
[58] II. Physikalisches Institut, Justus-Liebig-Universität Giessen, Giessen; Germany
[59] SUPA — School of Physics and Astronomy, University of Glasgow, Glasgow; United Kingdom
[60] LPSC, Université Grenoble Alpes, CNRS/IN2P3, Grenoble INP, Grenoble; France
[61] Laboratory for Particle Physics and Cosmology, Harvard University, Cambridge MA; United States of America
[62] [(a)] Department of Modern Physics and State Key Laboratory of Particle Detection and Electronics, University of Science and Technology of China, Hefei; [(b)] Institute of Frontier and Interdisciplinary Science and Key Laboratory of Particle Physics and Particle Irradiation (MOE), Shandong University, Qingdao; [(c)] School of Physics and Astronomy, Shanghai Jiao Tong University, Key Laboratory for Particle Astrophysics and Cosmology (MOE), SKLPPC, Shanghai; [(d)] Tsung-Dao Lee Institute, Shanghai; China
[63] [(a)] Kirchhoff-Institut für Physik, Ruprecht-Karls-Universität Heidelberg, Heidelberg; [(b)] Physikalisches Institut, Ruprecht-Karls-Universität Heidelberg, Heidelberg; Germany
[64] [(a)] Department of Physics, Chinese University of Hong Kong, Shatin, N.T., Hong Kong; [(b)] Department of Physics, University of Hong Kong, Hong Kong; [(c)] Department of Physics and Institute for Advanced Study, Hong Kong University of Science and Technology, Clear Water Bay, Kowloon, Hong Kong; China
[65] Department of Physics, National Tsing Hua University, Hsinchu; Taiwan
[66] IJCLab, Université Paris-Saclay, CNRS/IN2P3, 91405, Orsay; France
[67] Department of Physics, Indiana University, Bloomington IN; United States of America
[68] [(a)] INFN Gruppo Collegato di Udine, Sezione di Trieste, Udine; [(b)] ICTP, Trieste; [(c)] Dipartimento Politecnico di Ingegneria e Architettura, Università di Udine, Udine; Italy
[69] [(a)] INFN Sezione di Lecce; [(b)] Dipartimento di Matematica e Fisica, Università del Salento, Lecce; Italy
[70] [(a)] INFN Sezione di Milano; [(b)] Dipartimento di Fisica, Università di Milano, Milano; Italy
[71] [(a)] INFN Sezione di Napoli; [(b)] Dipartimento di Fisica, Università di Napoli, Napoli; Italy
[72] [(a)] INFN Sezione di Pavia; [(b)] Dipartimento di Fisica, Università di Pavia, Pavia; Italy
[73] [(a)] INFN Sezione di Pisa; [(b)] Dipartimento di Fisica E. Fermi, Università di Pisa, Pisa; Italy
[74] [(a)] INFN Sezione di Roma; [(b)] Dipartimento di Fisica, Sapienza Università di Roma, Roma; Italy
[75] [(a)] INFN Sezione di Roma Tor Vergata; [(b)] Dipartimento di Fisica, Università di Roma Tor Vergata, Roma; Italy
[76] [(a)] INFN Sezione di Roma Tre; [(b)] Dipartimento di Matematica e Fisica, Università Roma Tre, Roma; Italy
[77] [(a)] INFN-TIFPA; [(b)] Università degli Studi di Trento, Trento; Italy
[78] Universität Innsbruck, Department of Astro and Particle Physics, Innsbruck; Austria
[79] University of Iowa, Iowa City IA; United States of America
[80] Department of Physics and Astronomy, Iowa State University, Ames IA; United States of America
[81] [(a)] Departamento de Engenharia Elétrica, Universidade Federal de Juiz de Fora (UFJF), Juiz de Fora; [(b)] Universidade Federal do Rio De Janeiro COPPE/EE/IF, Rio de Janeiro; [(c)] Instituto de Física, Universidade de São Paulo, São Paulo; [(d)] Rio de Janeiro State University, Rio de Janeiro; Brazil
[82] KEK, High Energy Accelerator Research Organization, Tsukuba; Japan
[83] Graduate School of Science, Kobe University, Kobe; Japan
[84] [(a)] AGH University of Science and Technology, Faculty of Physics and Applied Computer Science, Krakow; [(b)] Marian Smoluchowski Institute of Physics, Jagiellonian University, Krakow; Poland
[85] Institute of Nuclear Physics Polish Academy of Sciences, Krakow; Poland
[86] Faculty of Science, Kyoto University, Kyoto; Japan
[87] Kyoto University of Education, Kyoto; Japan

JHEP06(2023)138

[88] Research Center for Advanced Particle Physics and Department of Physics, Kyushu University, Fukuoka; Japan
[89] Instituto de Física La Plata, Universidad Nacional de La Plata and CONICET, La Plata; Argentina
[90] Physics Department, Lancaster University, Lancaster; United Kingdom
[91] Oliver Lodge Laboratory, University of Liverpool, Liverpool; United Kingdom
[92] Department of Experimental Particle Physics, Jožef Stefan Institute and Department of Physics, University of Ljubljana, Ljubljana; Slovenia
[93] School of Physics and Astronomy, Queen Mary University of London, London; United Kingdom
[94] Department of Physics, Royal Holloway University of London, Egham; United Kingdom
[95] Department of Physics and Astronomy, University College London, London; United Kingdom
[96] Louisiana Tech University, Ruston LA; United States of America
[97] Fysiska institutionen, Lunds universitet, Lund; Sweden
[98] Departamento de Física Teorica C-15 and CIAFF, Universidad Autónoma de Madrid, Madrid; Spain
[99] Institut für Physik, Universität Mainz, Mainz; Germany
[100] School of Physics and Astronomy, University of Manchester, Manchester; United Kingdom
[101] CPPM, Aix-Marseille Université, CNRS/IN2P3, Marseille; France
[102] Department of Physics, University of Massachusetts, Amherst MA; United States of America
[103] Department of Physics, McGill University, Montreal QC; Canada
[104] School of Physics, University of Melbourne, Victoria; Australia
[105] Department of Physics, University of Michigan, Ann Arbor MI; United States of America
[106] Department of Physics and Astronomy, Michigan State University, East Lansing MI; United States of America
[107] Group of Particle Physics, University of Montreal, Montreal QC; Canada
[108] Fakultät für Physik, Ludwig-Maximilians-Universität München, München; Germany
[109] Max-Planck-Institut für Physik (Werner-Heisenberg-Institut), München; Germany
[110] Graduate School of Science and Kobayashi-Maskawa Institute, Nagoya University, Nagoya; Japan
[111] Department of Physics and Astronomy, University of New Mexico, Albuquerque NM; United States of America
[112] Institute for Mathematics, Astrophysics and Particle Physics, Radboud University/Nikhef, Nijmegen; Netherlands
[113] Nikhef National Institute for Subatomic Physics and University of Amsterdam, Amsterdam; Netherlands
[114] Department of Physics, Northern Illinois University, DeKalb IL; United States of America
[115] [(a)] New York University Abu Dhabi, Abu Dhabi; [(b)] United Arab Emirates University, Al Ain; [(c)] University of Sharjah, Sharjah; United Arab Emirates
[116] Department of Physics, New York University, New York NY; United States of America
[117] Ochanomizu University, Otsuka, Bunkyo-ku, Tokyo; Japan
[118] Ohio State University, Columbus OH; United States of America
[119] Homer L. Dodge Department of Physics and Astronomy, University of Oklahoma, Norman OK; United States of America
[120] Department of Physics, Oklahoma State University, Stillwater OK; United States of America
[121] Palacký University, Joint Laboratory of Optics, Olomouc; Czech Republic
[122] Institute for Fundamental Science, University of Oregon, Eugene, OR; United States of America
[123] Graduate School of Science, Osaka University, Osaka; Japan
[124] Department of Physics, University of Oslo, Oslo; Norway
[125] Department of Physics, Oxford University, Oxford; United Kingdom
[126] LPNHE, Sorbonne Université, Université Paris Cité, CNRS/IN2P3, Paris; France
[127] Department of Physics, University of Pennsylvania, Philadelphia PA; United States of America
[128] Department of Physics and Astronomy, University of Pittsburgh, Pittsburgh PA; United States of America
[129] [(a)] Laboratório de Instrumentação e Física Experimental de Partículas — LIP, Lisboa; [(b)] Departamento de Física, Faculdade de Ciências, Universidade de Lisboa, Lisboa; [(c)] Departamento

JHEP06(2023)138

de Física, Universidade de Coimbra, Coimbra; [(d)] *Centro de Física Nuclear da Universidade de Lisboa, Lisboa;* [(e)] *Departamento de Física, Universidade do Minho, Braga;* [(f)] *Departamento de Física Teórica y del Cosmos, Universidad de Granada, Granada (Spain);* [(g)] *Departamento de Física, Instituto Superior Técnico, Universidade de Lisboa, Lisboa; Portugal*

[130] *Institute of Physics of the Czech Academy of Sciences, Prague; Czech Republic*

[131] *Czech Technical University in Prague, Prague; Czech Republic*

[132] *Charles University, Faculty of Mathematics and Physics, Prague; Czech Republic*

[133] *Particle Physics Department, Rutherford Appleton Laboratory, Didcot; United Kingdom*

[134] *IRFU, CEA, Université Paris-Saclay, Gif-sur-Yvette; France*

[135] *Santa Cruz Institute for Particle Physics, University of California Santa Cruz, Santa Cruz CA; United States of America*

[136] [(a)] *Departamento de Física, Pontificia Universidad Católica de Chile, Santiago;* [(b)] *Millennium Institute for Subatomic physics at high energy frontier (SAPHIR), Santiago;* [(c)] *Instituto de Investigación Multidisciplinario en Ciencia y Tecnología, y Departamento de Física, Universidad de La Serena;* [(d)] *Universidad Andres Bello, Department of Physics, Santiago;* [(e)] *Instituto de Alta Investigación, Universidad de Tarapacá, Arica;* [(f)] *Departamento de Física, Universidad Técnica Federico Santa María, Valparaíso; Chile*

[137] *Department of Physics, University of Washington, Seattle WA; United States of America*

[138] *Department of Physics and Astronomy, University of Sheffield, Sheffield; United Kingdom*

[139] *Department of Physics, Shinshu University, Nagano; Japan*

[140] *Department Physik, Universität Siegen, Siegen; Germany*

[141] *Department of Physics, Simon Fraser University, Burnaby BC; Canada*

[142] *SLAC National Accelerator Laboratory, Stanford CA; United States of America*

[143] *Department of Physics, Royal Institute of Technology, Stockholm; Sweden*

[144] *Departments of Physics and Astronomy, Stony Brook University, Stony Brook NY; United States of America*

[145] *Department of Physics and Astronomy, University of Sussex, Brighton; United Kingdom*

[146] *School of Physics, University of Sydney, Sydney; Australia*

[147] *Institute of Physics, Academia Sinica, Taipei; Taiwan*

[148] [(a)] *E. Andronikashvili Institute of Physics, Iv. Javakhishvili Tbilisi State University, Tbilisi;* [(b)] *High Energy Physics Institute, Tbilisi State University, Tbilisi;* [(c)] *University of Georgia, Tbilisi; Georgia*

[149] *Department of Physics, Technion, Israel Institute of Technology, Haifa; Israel*

[150] *Raymond and Beverly Sackler School of Physics and Astronomy, Tel Aviv University, Tel Aviv; Israel*

[151] *Department of Physics, Aristotle University of Thessaloniki, Thessaloniki; Greece*

[152] *International Center for Elementary Particle Physics and Department of Physics, University of Tokyo, Tokyo; Japan*

[153] *Department of Physics, Tokyo Institute of Technology, Tokyo; Japan*

[154] *Department of Physics, University of Toronto, Toronto ON; Canada*

[155] [(a)] *TRIUMF, Vancouver BC;* [(b)] *Department of Physics and Astronomy, York University, Toronto ON; Canada*

[156] *Division of Physics and Tomonaga Center for the History of the Universe, Faculty of Pure and Applied Sciences, University of Tsukuba, Tsukuba; Japan*

[157] *Department of Physics and Astronomy, Tufts University, Medford MA; United States of America*

[158] *Department of Physics and Astronomy, University of California Irvine, Irvine CA; United States of America*

[159] *Department of Physics and Astronomy, University of Uppsala, Uppsala; Sweden*

[160] *Department of Physics, University of Illinois, Urbana IL; United States of America*

[161] *Instituto de Física Corpuscular (IFIC), Centro Mixto Universidad de Valencia — CSIC, Valencia; Spain*

[162] *Department of Physics, University of British Columbia, Vancouver BC; Canada*

[163] *Department of Physics and Astronomy, University of Victoria, Victoria BC; Canada*

[164] *Fakultät für Physik und Astronomie, Julius-Maximilians-Universität Würzburg, Würzburg; Germany*

JHEP06(2023)138

[165] Department of Physics, University of Warwick, Coventry; United Kingdom
[166] Waseda University, Tokyo; Japan
[167] Department of Particle Physics and Astrophysics, Weizmann Institute of Science, Rehovot; Israel
[168] Department of Physics, University of Wisconsin, Madison WI; United States of America
[169] Fakultät für Mathematik und Naturwissenschaften, Fachgruppe Physik, Bergische Universität Wuppertal, Wuppertal; Germany
[170] Department of Physics, Yale University, New Haven CT; United States of America

[a] Also Affiliated with an institute covered by a cooperation agreement with CERN
[b] Also at Borough of Manhattan Community College, City University of New York, New York NY; United States of America
[c] Also at Bruno Kessler Foundation, Trento; Italy
[d] Also at Center for High Energy Physics, Peking University; China
[e] Also at Centro Studi e Ricerche Enrico Fermi; Italy
[f] Also at CERN, Geneva; Switzerland
[g] Also at Département de Physique Nucléaire et Corpusculaire, Université de Genève, Genève; Switzerland
[h] Also at Departament de Fisica de la Universitat Autonoma de Barcelona, Barcelona; Spain
[i] Also at Department of Financial and Management Engineering, University of the Aegean, Chios; Greece
[j] Also at Department of Physics and Astronomy, Michigan State University, East Lansing MI; United States of America
[k] Also at Department of Physics and Astronomy, University of Louisville, Louisville, KY; United States of America
[l] Also at Department of Physics, Ben Gurion University of the Negev, Beer Sheva; Israel
[m] Also at Department of Physics, California State University, East Bay; United States of America
[n] Also at Department of Physics, California State University, Sacramento; United States of America
[o] Also at Department of Physics, King's College London, London; United Kingdom
[p] Also at Department of Physics, University of Fribourg, Fribourg; Switzerland
[q] Also at Department of Physics, University of Thessaly; Greece
[r] Also at Department of Physics, Westmont College, Santa Barbara; United States of America
[s] Also at Hellenic Open University, Patras; Greece
[t] Also at Institucio Catalana de Recerca i Estudis Avancats, ICREA, Barcelona; Spain
[u] Also at Institut für Experimentalphysik, Universität Hamburg, Hamburg; Germany
[v] Also at Institute of Particle Physics (IPP); Canada
[w] Also at Institute of Physics, Azerbaijan Academy of Sciences, Baku; Azerbaijan
[x] Also at Institute of Theoretical Physics, Ilia State University, Tbilisi; Georgia
[y] Also at Lawrence Livermore National Laboratory, Livermore; United States of America
[z] Also at The Collaborative Innovation Center of Quantum Matter (CICQM), Beijing; China
[aa] Also at TRIUMF, Vancouver BC; Canada
[ab] Also at Università di Napoli Parthenope, Napoli; Italy
[ac] Also at University of Chinese Academy of Sciences (UCAS), Beijing; China
[ad] Also at University of Colorado Boulder, Department of Physics, Colorado; United States of America
[ae] Also at Washington College, Maryland; United States of America
[af] Also at Yeditepe University, Physics Department, Istanbul; Türkiye
[ag] Also at Physics Department, An-Najah National University, Nablus, Palestine
[*] Deceased

JHEP06(2023)138